UNIVERSITY OF
LINCOLN

School of Pharmacy – College of Science

Hanna Cole BSc (Hons)

Thesis submitted to the University of Lincoln for the degree of Master of Science

Chitosan- Mediated Vaccine Delivery Through the Intestinal Epithelium

Abstract

Chitosan is one of the most widely studied materials in the field of drug delivery. Chitosan nanoparticles produced by ionic gelation can encapsulate macromolecular drug cargo. This work explores the potential of a specific chitosan molecule, ultrapure chitosan chloride, for oral vaccine delivery *in vitro* using polarised Caco-2 epithelial cells and *in vivo* using Balb/C mice.

The chosen antigen used in the chitosan nanoparticles was ovalbumin (OVA). Work revealed an optimum concentration of 1 mg/ml of chitosan and OVA (i.e. 1:1 mass ratio), with addition of tripolyphosphate (TPP), for production of nanoparticles with a size of 196.5 nm. The chitosan:OVA nanoparticles showed a zeta potential of +9.68 mv. SDS gel studies showed that OVA stability was not compromised following interaction with chitosan. Nanoparticle exposure to hydrochloric acid (HCl) and trypsin resulted in breakdown of OVA with HCl, while some protection was apparent with trypsin.

Chitosan:OVA nanoparticles at 1 mg/ml displayed a good toxicity profile, measured through 3-(4,5-dimethylthiazol-2-yl)-5-(3-carboxymethoxyphenyl)-2-(4-sulfophenyl)-2H- tetrazolium (MTS) and lactate dehydrogenase (LDH) assays. Transepithelial electrical resistance (TEER) data also support these findings, with TEER reversibility following application apparent. Application of chitosan:OVA nanoparticles to Caco-2 cell monolayers showed a reversible decrease in TEER, but a similar effect was seen with OVA solution and therefore a nanoparticle-specific effect could not be established in terms of tight junction opening. Chitosan:OVA nanoparticles however significantly and notably enhanced fluorescein isothiocyanate ovalbumin (FITC-OVA) permeability across Caco-2 monolayers when applied at 0.1 mg/ml (1:1 chitosan:OVA mass ratio).

Studies which used Balb/c mice whereby chitosan:OVA nanoparticles were administered orally, did not show a convincing immune response. Specifically, IgG1, IgG2a and IgA

showed no response, while total IgG showed a small response with and without cholera toxin.

This work therefore shows that a specific chitosan molecule is able to complex with OVA as a model antigen, producing sub 200 nm nanoparticles with a positive zeta potential. These systems showed clear effects *in vitro*, enhancing OVA permeability significantly, but *in vivo* response was not clear. This study illustrates that macromolecular absorption enhancement seen *in vitro* in intestinal models does not reliably predict *in vivo* immune response of vaccine delivery systems.

Acknowledgements

First and foremost I would like to show my extreme gratitude to my supervisors Dr's Driton Vllasaliu and Lorna Lancaster, for which without their patience, supervision and support I believe would not have succeeded or indeed it would have been harder. Although frustrated at times it was down to their support that I succeeded in my research; their training in formulation work and cell culture was essential.

I would like to thank Dr. Fatme Mawas and Dr. Donna Bryan at the National Institute for Biological Standards and Control (NIBSC) for their tireless efforts in assisting with *in vivo* studies. For which without a vital part of my research would not have been able to take place.

I would like to thank my boyfriend Mark Hodges for his patience, understanding and letting me vent my frustrations when not everything went to plan. Who has also been there as a shoulder to cry on when I needed it and there to celebrate when things succeeded. I also apologise if I was not the best girlfriend especially towards the end during the write up.

I would like to appreciate my family, who throughout my undergraduate and postgraduate degrees have only ever encouraged me to do well and be my absolute best; especially my Mum and Stepdad who without their help I would never have had the opportunity to undergo my Masters; I hope I have made them proud by doing so. To my Grandad Jack whose influence about education has always stayed with me throughout the years and has had a big impact on my life choices for my degrees, I hope he is very proud of me up in the clouds.

I would also like to thank my friends and colleagues Maria Pereira, Joanna Bird and Ria Peake for their support, patience and guidance throughout my project. To Maria assisting me when I first started cell culture and was still a little nervous on my own, as well as answering any questions I had or if I was unsure about something. To Joanna

who made for some interesting conversations about food and who made my time in the lab enjoyable. Lastly to Ria who, like Mark, let me vent my anger and who I will share many good memories with when science got too much and I needed a break.

I would like to thank Martyn Balmont for teaching me confocal microscopy and Dr. Enrique Ferrari for teaching me how to use Nanosight for which without would have made a significant difference to my thesis.

Table of Contents

List of Figures

Chapter 1

Chapter 2

Chapter 3

Chapter 4

Chapter 5

List of Tables

Abbreviations

>	Greater than
<	Less than
+	Positive
-	Negative
%	Percentage
°	Degree
°C	Degree celsius
$Al(OH)_3$	Aluminium hydroxide
APC	Antigen presenting cell
APS	Ammonium persulfate
BSA	Bovine serum albumin
C-2	Protein structural domain
C-3	Protein structural domain
C-6	Protein structural domain
CD4	Cluster of differentiation 4
Cl^-	Chloride ion
CLDN4	Claudin-4
cm^2	Centimetre squared
CMC	Carboxymethyl chitosan
CO_2	Carbon dioxide
CSK	CSKSSDYQC
Da	Dalton
dH_2O	Distilled water
DAPI	4',6-diamidino-2-phenylindole
DBS	Dried blood spot assay
DLS	Dynamic light scattering
DMEM	Dulbecco's modified eagle medium
DMSO	Dimethyl sulfoxide
DNA	Deoxyribonucleic acid
DTPA	Diethylene triamine pentaacetic acid
ECACC	European collection of cell cultures
EDTA	Ethylenediaminetetraacetic acid
ELISA	Enzyme linked immunosorbent assay

FAK	Focal adhesion kinase
FBS	Foetal bovine serum
FD4	Fluorescein isotheocyanate dextran 4
FD10	Fluorescein isotheocyanate dextran 10
FITC	Fluorescein isotheocyanate
fl	Fluid ounce
g	grams
g	G force
GI	Gastrointestinal
GIT	Gastrointestinaltract
GlcNAc	N-Acetylglucosamine
HBSS	Hanks balanced salt solution
HCl	Hydrochloric acid
HRP	Horseradish peroxidase
Ig	Immunoglobulin
IgG	Immunoglobulin G
IgG1	Immunoglobulin G1
IgG2a	Immunoglobulin G2a
IgA	Immunoglobulin A
kDa	kilodalton
L	Litre
LDH	Lactate dehydrogrenase
M	Molar
M cell	Microfold cells
MES	2-(*N*-morpholino)ethanesulfonic acid
mg	milligram
min	minute
mIU	milli- international unit
ml	millilitre
mM	millimolar
mm	millimetre
mQ	milli Q
MTS	3-(4.5-dimethylthiazol-2-yl)-5(3-carboxymethonyphen

mv	millivolts
Na^+	Sodium ion
Na_2CO_3	Sodium carbonate
NaCl	Sodium chloride
NAD	β- nicotinamide adenine dinucleotide
$NaHCO_3$	Sodium bicarbonate
NIBSC	National institute of biological standards and control
nm	nanometre
NTA	Nanoparticle tracking analysis
OD	Optical density
OPD	*o*-Phenylenediamine dihydrochloride
OVA	Ovalbumin
P_{app}	Apparent permeability coefficient
PBS	Phosphate buffered saline
PEG	Poly(ethyleneglycol)
pH	power of hydrogen
pKa	acid dissociation constant
PVA	Polyvinyl alcohol
rHBsAg	Hepatitis B antigen
rpm	revolutions per minute
S1	Sample 1
S2	Sample 2
S3	Sample 3
S4	Sample 4
S5	Sample 5
S6	Sample 6
SD	Standard deviation
SDS	Sodium dodecyl sulfate
Src	Sarcoma
PAGE	Polyacrylamide gel electrophoresis
TEER	Transepithelial electrical resistance

TEMED	Tetramethylethylenediamine
Th1	T helper 1 cell
Th2	T helper 2 cell
TM_{65}	
$TM_{56}Bz_{42}$	Methylated N-(4-
$TM_{65}CM_{50}$	Methylated N-(4-
$TM_{53}Py_{40}$	Methylated N-(4-
TMC	Trimethyl chitosan
TPP	Tripolyphosphate
UP CL	Ultra pure chloride
v/v	volume per volume
w/v	weight per volume
ZO-1	Zonula occludens-1
γPGA	poly(γ- glutamic acid)
µg	micrograms
µl	microlitres
µm	micrometres
$\alpha_V\beta_3$	Integrin
α	alpha
β	beta
Ω	omega
Ωcm^2	Ohms centrimetres squared

Chapter 1

Introduction

1.1 Oral vaccine delivery: possibilities and challenges

1.1.1 The possibilities

Infectious diseaseis the biggest threat for the human race and a cause of high morbidity rates. Up to 9.5 million people die because of infectious diseases per year (Kwon *et al*. 2013). Vaccinations have changed the face of medicine, causing the eradication of small pox and rinder-pest, and other diseases such as poliomyelitis to almost become extinct (Devriendt *et al*. 2012). Even though there are many oral vaccines currently on the market for diseases such as the oral polio vaccine, rota vaccine and an adenovirus vaccine; there are still disadvantages and problems that are not being addressed (Kwon *et al*. 2013).

Administration of vaccines by injections is associated with a number of disadvantages. Firstly, the formulations require sterile and cold storage. Secondly, patient safety is one of the biggest concerns. Administration of injections is associated with risks, including injection site injury and infections, as well as high administration costs (requirement of healthcare professionals to administer) and poor patient compliance due to uncomfortable and painful administrations of vaccines.

Oral delivery is the most desirable drug delivery method. Oral formulations used for vaccines may not need to be stored in cold stores which would be of benefit, especially in developing countries, this is due to the absense of an adjuvant e.g. a particular strain of virus (Devriendt *et al*. 2012). Patient compliance will also increase as patients will not have to be subjected to any pain or discomfort through invasive injections (Devriendt *et al*. 2012).

However, currently it is not possible to exploit the oral route for administration of vaccines. As protein-based actives, efficient oral delivery of vaccines requires specialist formulation solutions to overcome their poor stability in the gastrointestinal environment (e.g. presence of acid and proteolytic enzymes) and inability to interact with the mucosa in a way as to induce an immune response.

A key requirement for oral vaccine delivery is activation of the IgA immune response. This would create an immune response in all the mucosa throughout the body and the entry points where a pathogen may enter, for example the oesophagus, urogenital tract or the gastrointestinal tract. This would be a first line defence against certain pathogens such as influenza, chlamydia, gonorrhea and measles (Kim *et al*. 2011).

There are a few examples of mucosal vaccines to date which have been successful, increasing the motivation to make this for the majority of vaccines in the future. These include the *Sabin* polio vaccine, a vaccine against the rotavirus and vaccines against cholera and typhoid fever (Sharma *et al*. 2015). Due to most pathogens infecting humans at mucosal entries (nasal passages, oesophagus, trachea, gastrointestinal tract, etc.) the mucosa has been targeted as an effective site for immunity. The idea that if the mucosa is inoculated against certain pathogens there will then be systemic immunity throughout the body. The main route to combat pathogens infecting the gastrointestinal tract is to deliver the vaccine directly to the site. Delivering the vaccine to other mucosal sites would give a weaker response with less efficiency. However directing the vaccine towards the gut epithelium makes the response much more specific and robust (Kim *et al*. 2011).

1.1.2 The challenges

There are many challenges accompanying oral vaccine delivery. As briefly mentioned above, oral drug delivery requires that the drug molecule is able to withstand the environment of the digestive system. As the antigen is delivered via a mucosal route it is diluted due to the secretions (Sharma *et al*. 2015). Vaccines containing DNA, proteins and polysaccharides are prone to being degraded in the gastrointestinal

tract, resulting in a loss of bioactivity. The antigen used to activate the immune response also needs to be strong enough to create an IgA response throughout the body and in sufficient dose due to the large surface area of the gastrointestinal tract.

The current absence of effective oral vaccines on the market is down to, the lack of antigens causing immunogenicity and challenges related to delivery of vaccines in their active form to the required site in the gastrointestinal tract. Poor uptake by epithelial cells and antigen presenting cells (APC) in the gastrointestinal tract, coupled with degradation en route, are key barriers contributing to this (Devriendt *et al*. 2012). The antigen needs to be released at the right time to achieve the highest maximum immune response possible. The antigen used must not be unstable or toxic in any way to humans, and must be compatible with the delivery system used.

1.1.3 Oral drug delivery route

The oral route is by far the most preferred method of drug administration. This route has several advantages: it is safe, inexpensive and is associated with high patient compliance, especially compared to injections. However, this route also faces several challenges (Finlay, 2001). It can be unpredictable and many factors can affect the absorption of the drug, including food, as well as acid and enzymatic breakdown. Large drug molecules may be inactivated as drugs delivered via the oral route face a harsh environment, which is rich in enzymes such as pepsin and trypsin and changing pH from a highly acidic environment (pH 1.5-3.5) to mildly alkaline (7-8). The drug then has to be absorbed through the gastrointestinal tract, which is lined by a mucosal barrier, which has evolved to be a selective barrier to material entering the body (Finlay, 2001).

The mucosal surface is composed of the epithelium, covered by a mucus layer. Both the epithelium and the mucus layer present barriers to drug delivery. These barriers will be discussed below with respect to drug delivery in general and specifically vaccine delivery.

1.2 The digestive barrier

1.2.1 The digestive system

The physiological role of the digestive system is to convert food into nutrients, which are subsequently used by the body to obtain energy. The digestive system is made up of four main organs: the gastrointestinal tract, the liver, gallbladder and pancreas. The gastrointestinal tract is one long, hollow tube that runs from the mouth to the anus. It consists of the mouth, oesophagus, stomach, small intestine, large intestine, rectum and anus. The liver, gallbladder and pancreas are classed as the solid organs of the digestive system whilst the GI tract is classed as the hollow organ (Zhang *et al.* 2014). The role of the mouth is to chew food down into smaller and more managable pieces to ease with digestion. Saliva begins to breakdown food via a digestive enzyme amylase. The oesophagus transports the food broken down in the mouth to the stomach. Food is broken down further in the stomach via stomach acid and enzymes such as pepsin which degrades protein. The small intestine consisting of the duodenum, jejunum and ileum absorbs all of the nutrients needed from food into the bloodstream. The large intestine absorbs water and salts from the undigested food and produces a waste product (Yang *et al.* 2015). The liver and pancreas secrete hormones, whilst the gallbladder secretes bile used in the small intestine. The pH of the digestive tract varies from 1-7, with the stomach ranging from 1-3, the duodenum ranging between 6-6.5 and the large intestine ranging between 5-7 (Renukuntla *et al*. 2013).

1.2.1.1 The digestive system and oral vaccine delivery

Successful oral delivery of vaccines requires that the protein-based vaccine survives the harsh environment of the gastrointestinal tract, including low pH. Gastric acid is composed of many chemicals. HCl is secreted via the parietal gastric cells; these are the only exocrine cells within the body with such a function. A bicarbonate is also produced to help control the pH of the stomach and to act as a base (Dume *et al.* 2013).

The majority of drug absorption occurs within the small intestine, specifically across the villi which are responsible for absorbing food and protein (Renukuntla *et al*, 2013). This region of the gastrointestinal tract is rich in enzymes such as trypsin,

endopeptidases, chymotrypsin and exopeptidases, which also break down any foreign proteins they encounter (Choonara *et al*. 2014).

Both stomach acid and presence of enzymes within the gastrointestinal tract may cause loss of therapeutic activity by permanent denaturation or breakdown of the protein-based vaccine.

1.3 Chitosan

1.3.1 Source and physiochemical characteristics of chitosan

Chitosan is a polymer that is derived from chitin, which is the second most abundant compound on the Earth and is found in the exoskeletons of many insects, the shells and skeletons of crustaceans and even in the cell walls of some fungi and algae (Casettari *et al.* 2011). Chitosan was chosen for its four main poperties; it is non-toxic to cells, it is mucoadhesive and bioadhesive, lastly it is biodegradable. Structurally, chitin is described as a homoglycan, which is a polysaccharide with repeating units of the same monosaccharide. It is structurally similar to cellulose, there is one key difference, cellulose is a polymer of D-glucose, whereas chitin is a polymer of N-acetyl-D-glucosamine. It is composed of β- 1,4- linked N-Acetylglucosamine (GlcNAc) residues, each GlcNAc residue rotated 180° from the previous residue (Azevedo *et al*. 2011). The hydrogen bonds cause great tensile strength within the polymer. Chitosan is a popular derivative of chitin (Horton *et al*. 2006) and is derived by the process of alkaline deacetylation or by enzymatic degradation (Casettari *et al*. 2011). The molecule is composed much like cellulose with a sugar backbone with β-1,4- linked D- glucosamine, the one difference being the hydroxyl group on the C-2 position is substituted by an acetyl amino group (Sunilkumar *et al.* 2014). The structure of chitosan is shown below in Figure 1.1.

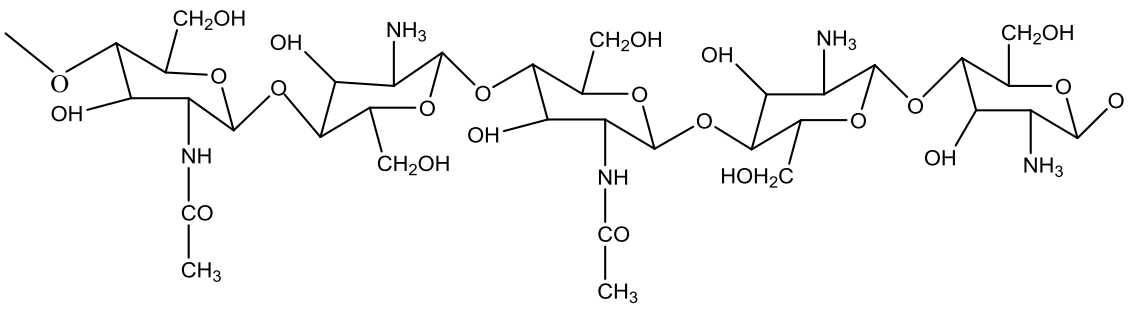

Figure 1.1: Chemical structure of polymer chitosan.

The main differences in physical properties of cellulose and chitosan are integral to their uses within the scientific community. Chitosan is hydrophillic and dissolves in water and solvents at a ph of 6. Cellulose does not dissolve in water or solvents. Chitosan can also form complexes with particular metal ions such as iron and copper. Cellulose is the main component in a plant cell wall due to its tensile strength, however chitosan is a more flexible molecule in terms of its rigidity which is discussed below.

The name chitosan itself actually covers a vast range of polysaccharides with different molecular weights, which ranges from 50-2000 kDa (Casettari *et al*. 2011). Chitosan also differs in the range of N-deacetylation, which ranges from 40-98%. Chitosan derivatives with a molecular weight of lower than 50 kDa are named oligochitosans (Casettari *et al*. 2011).

Chitosan has a polyelectrolyte nature, with the repeated amino groups rendering the polymer with a positive charge at pH below its pKa (6.3). This provides chitosan with a strong electrostatic attraction to sialic acids e.g. in mucus, or a charge-mediated attraction towards epithelial cells, which have a negative membrane charge. This attraction of chitosan to mucus and epithelial surfaces is termed mucoadhesion and bioadhesion, respectively. Both muco- and bioadhesion properties of chitosan contribute to its biomedical applications, especially in drug delivery (Casettari *et al*. 2011).

1.3.2 Chitosan variability

There are many varieties of chitosan on the market due to the fact that many variations of chitosan can be obtained depending on the way the chitosan was derived from chitin and the quality of the original chitin (Casettari *et al*. 2011). There are two types of chitin, alpha and beta. Alpha chitin has hydrogen bonds connecting the alternating polysaccharide chain in its structure; beta chitin does not have these hydrogen bonds. Alpha chitin is the more stable of the two and because of this it is less susceptible to de- acetylation than beta chitin. These produce a chain reaction

to the chitosan that is produced and therefore beta chitosan is considered more reactive, less rigid and has an increased solubility. The beta chitosan as a result is preferred to the alpha chitosan even if the molecular weights are similar. This is one of the main reasons why chitosan deacetylated from chitin will not be identical to perhaps another chitosan molecule from the same chitin derivative (Jung and Zhao, 2012).

These factors discussed above induce variations within the physiochemical and biomedical properties of chitosan, such as their ability to enhance the mucosal absorption of drugs (Casettari *et al*. 2011). Modifying the structure of chitosan is what causes the alteration in the properties of the molecule. There are three main groups that are altered; an amino group placed at C-2, a primary hydroxyl group at C-6 and a secondary hydroxyl group at C-3. Changing these major groups alters the molecules properties for biomedical applications. Therefore, the way the chitosan is processed chemically has a major impact upon the polymer. There are several ways chitosan is characterised depending on the property, including purity, physical appearance, molecular weight, viscosity and the degree of deacetylation. The different varieties of chitosan (e.g. CMC, TMC and PEG modified chitosan) have different intrinsic properties (such as an increased water solubility, increased biodegradability, absorption enhancement and increasing movement into the mucosa) causing them to be used in many applications in biomedical science (Sunilkumar *et al*. 2014). The variability of chitosan can be controlled via modification of the chitosan polymer to consistantly reproduce reliable nanosystems for drug delivery. These modifications are made to chitosans structure and once the 'ideal' formulation has been modified. It is repeated reproducing a reliable nanosystem as a result.

1.3.3 Chitosan derivatives

One of the most commonly researched derivatives of chitosan is carboxymethyl chitosan (CMC). CMC has been studied in many areas including bio-imaging, wound healing, theranostics, *in vitro* diagnostics and gene therapy, as well the staple areas of drug delivery and tissue engineering (Upadhyaya *et al*. 2014). This is the most

popular and most widely used derivative of chitosan as it improves some of the characteristics of the parent molecule, chitosan.

The advantages of CMC are; increased water solubility, increased biocompatibility, an increased moisture retention, increased biodegradability, increased antimicrobial and antifungal activity (Upadhyaya *et al*. 2014). CMC has shown to be more bioactive, e.g. increasing osteogenesis (Hsu *et al*. 2012). There are many different CMC formulations currently in research, including: microspheres, nanoparticles, aggregates, hydrogels, films and membranes (Upadhyaya *et al*. 2014).

CMC shows potential for vaccine and protein delivery, including diphtheria toxoid and tetanus toxoid delivery, as well as insulin and bovine serum albumin delivery (Janes *et al.* 2001). One pitfall of using chitosan is the molecule's insolubility at a pH higher than its own pKa which is estimated at 5.5-6.5 (Deng *et al*. 2013). If it is being used for mucosal delivery in the lower intestine, chitosan will therefore not be soluble due to pH > 7. CMC has increased water solubility and is therefore more useful for mucosal drug delivery and tissue engineering (Upadhyaya *et al.* 2014).

There are many different drug delivery formulations of CMCs. One is a hydrogel, which is a network of chitosan polymer chains that are hydrophillic and which can hold water up to five hundred times its own weight (Moghassemi *et al.* 2013). It is formed through the occurrence of cross linkages that are irreversible leading to the formation of the hydrogel (Upadhyaya *et al*. 2014). This gel permits the absorbance of water and related biocompounds and it also allows the drug it is carrying to be released via diffusion (Upadhyaya *et al*. 2014). Other formulations are in the form of microspheres, micelles or aggregates and nanoparticles. The latter are the most common and widely used formulation of CMCs (Moghassemi *et al.* 2013), with the ability to prolong the drugs half life which enhances the drugs therapeutic effect, increase the solubility of hydrophobic drugs and providing stimuli-responsive drug release potentially allowing minimisation of side effects (Upadhyaya *et al*. 2014).

Another chitosan derivative is poly (ethyleneglycol) (PEG)-modified chitosan. PEG-chitosan nanoparticles have been found to reduce the overall positive charge of the

nanoparticles and increase the biocompatibility (Janes *et al*. 2001). Furthermore, PEG chains on the nanoparticle surface cause extravasation of the particles and movement into the mucosa (Sharma *et al*. 2015) hence, potentially increasing the immune response.

Trimethyl Chitosan (TMC) is another common, partially quarternised derivative of chitosan. The advantage and difference of TMC is that it has enhanced mucoadhesive effects and provides absorption enhancement at a neutral pH (Zhang *et al*. 2014). This is because the polymer has a permanent cationic charge and is more soluble in water with a wide pH range. This enables it to survive better in the harsh environment of the gastro intestinal tract and digestive system (Moghassemi *et al*. 2015). Other benefits are higher antibody production when the antigen or adjuvant is attached to this chitosan derivative (Kwon *et al.* 2014),it is also tolerable in mice and less toxic than other polymers on the market, in addition to being biodegradable (Scheers *et al.* 2014).

1.4 Potential biomedical applications of chitosan

Chitosan has three ideal properties that have attracted the attention of researchers within the drug delivery field. These are: low toxicity, biodegradability and biocompatibility. These are very important properties of the molecule and give an advantage and versatility for potential use in a broad range of biomedical applications, from wound healing to antimicrobial activity (Vllasaliu *et al.* 2010). However, the predominantly researched applications of chitosan include drug delivery, gene delivery and tissue engineering.

1.4.1 Use of chitosan in drug delivery

In terms of drug delivery chitosan has shown potential when used in solution or in the form of nano-sized delivery systems with the ability to deliver various drug cargoes, including nucleic acids (Upadhyaya *et al*. 2014), small molecules such as anticancer drugs (Fan *et al*. 2012) and protein drugs (Upadhyaya *et al*. 2014). Furthermore, these systems have been investigated for systemic delivery and for their ability to enhance drug delivery across mucosal surfaces. The capacity of

chitosan to facilitate drug delivery across mucosal membranes is attributed to its mucoadhesive properties and its ability to open the epithelial tight junctions.

Tight junctions are structures that keep adjacent epithelial cells in close proximity with one another, hence creating a barrier to the movement of material, including drugs, between the cells (Vllasaliu *et al*. 2010). Tight junctions also act as an immune defence mechanism as it prevents bacterial toxins and particles from entering a cell (Wu *et al*. 2014). Tight junctions are composed of many integral proteins such as occludin, claudin and regulate proteins responsible for securing the proteins to the cytoskeleton (Yeh *et al*. 2011). The protein group claudin are known to hold the cells together between the tight junctions (Hsu *et al*. 2012). They also regulate the signal transductions entailing the tight junction permeability and cell differentiation (Yeh *et al*. 2011). Epithelial tight junctions are depicted in Figure 1.2.

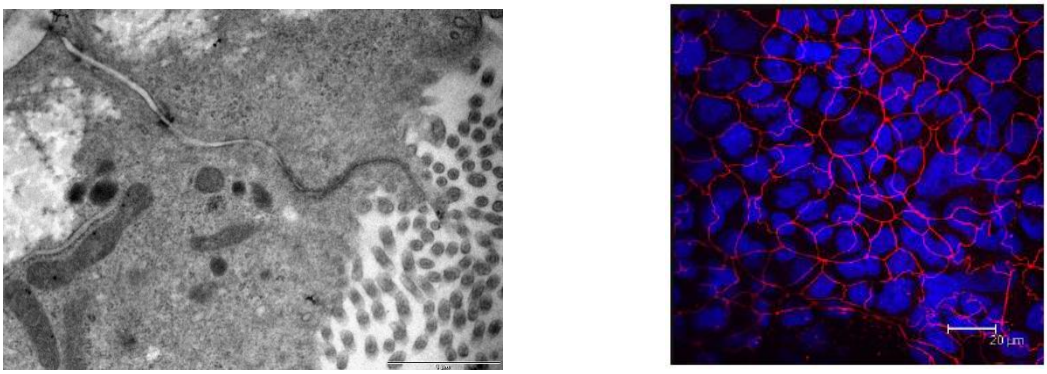

Figure 1.2: Epithelial tight junctions of Caco-2 cells. a) Transmission electron micrograph and b) confocal micrograph of Caco-2 monolayers immunostained for tight junction protein, Zonula Occludens-1 (ZO-1). a) Taken from Vllasaliu et al, 2011 and b) taken from Fowler, 2012.

Both mucoadhesiveness and tight junction opening properties of chitosan are a result of the positive charge of the polymer (Vllasaliu *et al.* 2010). Positively charged amine groups on the backbone of the chitosan molecule interact with negatively charged integrins on the surface of the epithelial cell and the tight junctions (Hsu *et al*. 2013). Chitosan's positive charge disrupts the integrin $\alpha_V\beta_3$ which has a negative charge causing the receptors to cluster on the membrane; this subsequently causes phosphorylation of Focal adhesion Kinase (FAK) and Src tyrosine kinases leading to the reaction with protein claudin-4 (CLDN4), which is integral in the permeability of

the tight junctions (Hsu *et al*. 2013). Chitosan redistributes the protein from the cell membrane to the cytosol, causing a disruption in the tight junctions ability to moderate permeability allowing macromolecules to enter the epithelial cells (Hsu *et al*. 2013). This process also causes a decrease in transepithelial electrical resistance (TEER) – a sign of tight junction opening (Yeh *et al*. 2011).

Another method also discovered and thought to be a mechanism of tight junction opening is the activation of protein kinase C. The protein kinase C pathway is activated by phorbol myristate acetate, causing movement of some protein kinase C from the cytosol to the membrane. This disrupts the monolayer membrane permeability in the epithelial cells and therefore leads to the breakdown of the tight junctions (Smith *et al*. 2005). With the application of chitosan nanoparticles to cells, protein kinase C α was moved from the cytosol to the membrane, which leads to the disruption of tight junctions (Smith *et al.* 2005).

The ability of chitosan to promote mucosal drug absorption is particularly important when considering macromolecules such as peptides and proteins, as well as oligonucleotides, which are not capable of crossing the epithelial surfaces due to their unfavourable physicochemical characteristics. Specifically, hydrophilic molecules larger than 1 kDa (which include most peptides, proteins and oligonucleotides) are poorly absorbed across the epithelial surfaces and are prone to degradation (e.g. from acid or enzymes) in some biological environments (e.g. stomach and duodenum). Researchers have therefore extensively looked into chitosan as a drug delivery molecule to aid the mucosal absorption of macromolecules (Zhang *et al.* 2014).

1.5 Strategies for oral delivery of vaccines

There are many delivery strategies for vaccines, including oral, nasal and intramuscular. This thesis is primarily focusing on oral drug delivery. Drug delivery strategies to enable oral delivery of vaccines have mainly centred around nanoparticles thus far this is due to several reasons; a reduction in toxicity, reduction in side effects of the drugs, prolongation of the antigen used, higher specificity and easy modification of the size and surface charge characteristics. Nanoparticles can

be synthesised using many different materials; however, researchers have taken a keen interest in chitosan, which is biodegradable and non-toxic material with mucoadhesive and tight junction opening properties (Hsu *et al*. 2012). Chitosan can be modified and altered, for e.g. PEG, TMC, and CMC, allowing the polymer to exhibit enhanced characteristics compared to the original polymer.

There are a number of different cells lining the gastrointestinal mucosa. From oral vaccine delivery point of view, M cells are of particular interest. M cells are located within the Peyer's patches of the GI tract and represent only 5% of the human follicle-associated epithelium. M cells can deliver proteins and peptides from the lumen of GI tract to the lymphoid tissues, which results in an immune response. A high endocytic ability of M cells enables them to potentially absorb peptide drugs via oral delivery. They also have a high transcytotic ability which enables them to transport a wide variety of material including, macromolecules and drug delivery systems (e.g. nanoparticles and microparticles) (Renukuntla *et al*. 2013).

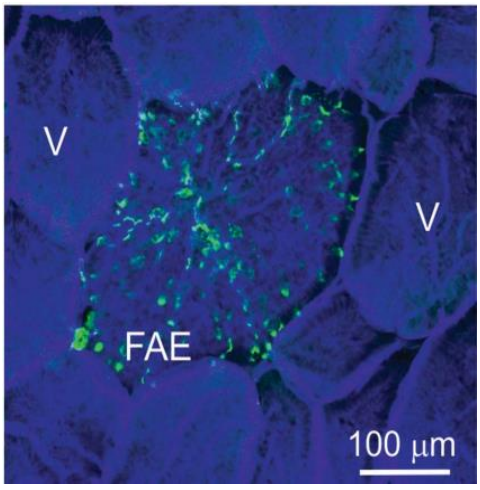

Figure 1.3 Whole-mount immunohistochemical analysis of glycoprotein 2 (GP2) mature M cells (green) in the follicle-associated epithelia (FAE) of a mouse Peyer's patch. Where V is villi. Taken from Mabbott et al. 2013.

The commonly researched strategies to improve oral delivery of vaccines are similar to those employed for increasing the oral bioavailability of other classes of macromolecule-based drugs (e.g. peptides, antibodies and DNA). These typically make use of absorption enhancers, with a number of different such systems being researched.

Absorption enhancers work in several ways; they can temporarily disrupt the intestinal epithelial integrity (Wei *et* al. 2012), decrease mucus viscosity (Dünnhaupt *et al.* 2015), temporarily open epithelial tight junctions (Kondoh *et al.* 2012), increase epithelial membrane fluidity (Wei *et* al. 2012), prolong contact with the mucosal surface (Benektsdóttir *et al.* 2014) and inhibit drug degrading enzymes (Pereira de Sousa and Bernkop- Schnürch, 2014). There are several example systems within each of these categories. The use of one method over the other depends on the characteristics of the drug used (e.g. physicochemical properties), the chosen mucosal route and the therapeutics of the drug entailed. Absorption enhancers may also be used together, producing an enhancing effect on drug absorption. The many types of enhancer classes that have been researched so far are; chelating agents (Bishnu *et al,* 2014), surfactants (Daful, and Mackie 2014), fatty acids and their derivatives (Mori *et* al, 2004), bile salts (Holm *et al.* 2013) and polymers (Abramov *et al*. 2015).

Chelators disrupt the epithelial intercellular tight junctions and decrease transepithelial electrical resistance (TEER) through a decrease in calcium levels. Surfactants affect the intracellular bilayers (order, fluidity and orientation) and may inhibit efflux mechanisms (Schrøder *et al.* 2014). Fatty acids and their derivatives increase the fluidity of the phospholipid membranes, with opening of tight junctions (Vllasaliu *et al*. 2010). Polymers may be mucoadhesive and may open the epithelial tight junctions (Renukuntla *et al*. 2013). An example of an absorption enhancer is the polymer chitosan, which is the subject of this thesis.

1.5.1 Nanoparticles used for oral vaccine delivery

For the purpose of drug delivery, nanoparticles are drug carriers in the nano-scale dimension, between 1-1000nm, but more typically 50-200nm. The properties of the nanoparticles vary with the materials used to formulate them and the method of formulation (Abramov *et al*. 2015). Nanoparticles are employed in drug delivery to enable or enhance the therapeutic effect of drugs. For example, nanoparticles can be employed to selectively target certain tissues, protect the encapsulated drug and control the rate of drug release (Renukuntla *et al*. 2013). However there are several

challenges. There is difficulty in synthesising non- aggregated nanoparticles with constistantly desirable characterisitcs, the ambiguity of the distribution and targeting of nanoparticles and how nanoparticle characteristics influence the interactions with cells in the body.

From oral drug delivery perspective nanoparticles are interesting as they provide potential advantages such as enhancement of drug stability, prolongation of the residence time in the GI tract, mucoadhesion, site specific drug delivery and enhanced cell uptake of the drug.

Nanoparticles exploiting the changes in the pH across the GI tract are particularly attractive in nanoparticle-mediated oral drug delivery. These are based on nanoparticles that release the encapsulated drug depending on pH (SchrØder *et al*. 2014). One example of this is poly (ɣ- glutamic acid) (ɣPGA)-chitosan nanoparticles, incorporating diethylene triamine pentaacetic acid (DTPA) as an agent known to disrupt the tight junctions in cells and inhibit intestinal proteases. These systems have been used in an attempt to improve oral delivery of insulin (Renukuntla *et al*. 2013). DTPA was attached to poly (ɣ- glutamic acid) (ɣPGA) and nanoparticles were formed by mixing the ɣPGA-DTPA with a cationic chitosan. The nanoparticles formed were pH dependent and degraded above a pH of 7.0. When given to rats and viewed via confocal microscopy and scintigraphy (Daful and Mackie 2014), results showed that nanoparticles accumulated in the kidneys and bladder and the delivered insulin significantly reduced blood glucose levels for up to 4 hours after administration (Renukuntla *et al*. 2013).

Another study used nanoparticles to target goblet cells to enhance oral absorption of insulin. Trimethyl chitosan chloride was combined with CSKSSDYQC (CSK) cell targeting peptide. This peptide improved the uptake of the nanoparticles across the GIT membrane; these modified nanoparticles showed a 1.5-fold increase in the oral bioavailability of insulin and an increased hypoglycaemic effect (Renukuntla *et al*. 2013).

1.5.2 Chitosan nanoparticles in drug and vaccine delivery

Chitosan nanoparticles are more stable in the gastrointestinal tract compared to other carriers such as liposomes (Deng *et* al. 2013), providing better protection of the drug or antigen that is encapsulated in the polymer. Liposomes are composed of a phospholid bilayer vesicle enclosing the chosen drug and an aqueous volume. It is negatively charged and cannot bind as easily to the intergrins on the epithelial gut surface. As it is composed of a phospholipid vesicle it decreases the availability of the drugs or antigen used. This makes chitosan a popular drug delivery polymer as exemplified by high research activity in the area.

Chitosan also has the ability to gel when coming into contact with polyanions such as tripolyphosphate, which is caused by many intermolecular cross-linkages. The ionic gelation (also called ionotropic gelation) technique has been developed to create chitosan nanoparticles using tripolyphosphate (TPP). Upon mixing, chitosan and TPP interact through electrostatic interactions to create nanoparticles (Janes *et al*. 2001). The electrostatic interactions themselves occur between the positively charged amino groups of chitosan with the negatively charged groups of TPP. TPP is mainly used due to its non-toxic nature. Sometimes these nanoparticles are created with the drug, antigen or additional polymers added to the mix to create the system of interest (Calvo *et al.* 1997).

The size of the chitosan nanoparticles produced by TPP ionic gelation method depends on the type of chitosan used (e.g. its molecular weight), chitosan:TPP ratio and the pH of the solution (Kang *et al*. 2015). Maintaining an overall positive charge on the surface of nanoparticles is thought to be important in order to preserve the chitosans ability to interact with negatively charged mucus and epithelial surfaces, as well as its ability to open the tight junctions (Chao *et al.* 2015). The TPP-mediated ionic gelation method produces chitosan nanoparticles under mild conditions - temperature and pH. This is important with protein-based therapeutics (e.g. vaccines), preventing damage to the therapeutic during the formulation process. The negative side to this however is that ionic gelation is associated with a wide particle distribution size and low stability, though, as mentioned above, the type of

chitosan used often dictates this, with a low molecular weight chitosan seemingly producing smaller nanoparticles (Fan *et al*. 2012).

Chitosan nanoparticles promote oral drug and vaccine delivery in a number of ways. Before considering ways in which chitosan nanoparticles may improve oral delivery, it is worth mentioning that materials in general cross the gastrointestinal epithelium via the paracellular route, which is the space between adjacent epithelial cells whereby tight junctions form 'kissing points' between cells, or through the transcellular pathway. The latter takes place through epithelial cells and may be due to passive absorption, active transport and endocytosis. Passive transport is the facilitated movement of material from an area of high concentration to low concentration. This relies strongly on the ability of the molecules to diffuse through the membrane. Active transport is the opposite of passive transport: it transports a material against a concentration or electrical gradient and requires energy to take place. Finally, endocytosis requires energy and involves the molecule being engulfed by cells and transported through the membrane, which may or may not be released on the other side (in a process known as transcytosis) (Choonara *et al*. 2014).

In the paracellular pathway, material crosses the aqueous channels within epithelial tight junctions ('paracellular corridor'). These channels are selective to small molecules (<100- 200 kDa) (Choonara *et al*. 2014) and with molecules over 700 Da bioavailability starts to decrease significantly (Renukuntla *et al*. 2013). Macromolecules, including vaccine antigens, therefore cannot utilise this route to traverse the intestinal epithelium. The paracellular space equates to 0.01-0.1 cm^2 surface area of the intestine therefore in reality does not normally contribute significantly in intestinal absorption of orally administered drugs.

Nanoparticles are probably likely to cross the GIT via the transcellular pathway. It is the more common method of drug absorption than the paracellular route. This is due to properties of the nanoparticles and the size of the antigen chosen. There are a number of ways in which nanoparticles in general are internalised into cells. These are: phagocytosis, pinocytosis and receptor-mediated endocytosis (Choonara *et al*. 2014). Phagocytosis involves the engulfment of nanoparticles up to 10µm in

diameter by macrophages and neutrophils. Pinocytosis is a type of cellular uptake mechanism this is caused by the absorption of nanoparticles alone and in solution. This happens within all cell types and with smaller nanoparticles (Renukuntla *et al*. 2013). During endocytosis the nanoparticles associate with the cell membrane, e.g. via receptors. The nanoparticles are then internalised into vesicles into the cell cytoplasm. The nanoparticles subsequently may be degraded by lysosomes or escape the degradative route and travel to other organelles and/or released by exocytosis. In epithelial cells such as enterocytes nanoparticles may travel from the intestinal lumen into systemic circulation via transcytosis (Choonara *et al*. 2014).

1.6 Project aims

The introduction suggests the polymer chitosan can intergrated into vaccine delivery due to its popular physical and chemical properties. The aim of this project is to investigate the potential of a specific chitosan product, namely ultrapure chitosan chloride which previously has shown significant absorption-enhancing potential *in vitro*, to deliver vaccines across the intestinal epithelium. The initial work of this project will focus on formulation and characterisation of chitosan nanoparticles before studies commence *in vitro* using a Caco-2 epithelial cell line. Following physiochemical characterisation, formulations will be tested for their toxicity. Concentrations with an acceptable toxicity profile will be further tested for their ability to: 1) open epithelial tight junctions *in vitro*, 2) enhance the permeability of OVA *in vitro* and 3) elicit a systemic immune response *in vivo* following oral gavage immunisations using Balb/C mice.

1.7 References

1. Abramov, E., Cassiola, F., Schwob, O., Karsh- Bluman, A., Shapero, M., Ellis, J., Luyindula, D., Adini, I., D' Amato, R., J. and Benny, O. (2015). *Cellular Mechanism of Oral Absorption of Solidified Polymer Micelles*, Nanomedicine: Nanotechnology, Biology and Medicine, 11 (3): 795- 823.

2. Azevedo, J., R., Sizilio, R., H., Brito, M., B., Costa, A., M., B., Serafini, M., R., Araújo, A., A., S., Santos, M., R., V., Lira, A., A., M. and Nunes, R., S. (2011). *Physical and Chemical Characterization Insulin- Loaded Chitosan- TPP Nanoparticles*, Journal of Thermal Analysis and Calorimetry, 106: 685-689.
3. Benediktsdóttir, B., E., Baldursson, O. and Másson, M. (2014). *Challenges in Evaluation of Chitosan and Trimethylated Chitosan (TMC) as Mucosal Permeation Enhancers: From Synthesis to In Vitro Application*, Journal of Controlled Release, 173: 18-31.
4. Bishnu, C., D., Aparajeya, P., Pramod, K., S., Somanath J. and Payodhar, P. (2014). *Effect of Chromium (VI) on Wheat Seedlings and the Role of Chelating Agents*, Current Science, 106(10): 1387-1393.
5. Calvo, P., Remuñán-López, C., Vila-Jato, J., L. and Alonso, M., J. (1997). *Development of Positively Charged Colloidal Drug Carriers: Chitosan- Coated Polyester Nanocapsules and Submicron-emulsions*, Colloid and Polymer Science, 1: 46-53.
6. Casettari, L., Vllasaliu, D., Castagnino, E., Stolnik, S., Howdle, S. and Illum, L. (2011). *PEGylated Chitosan Derivatives: Synthesis, Characterisations and Pharmaceutical Applications*, Progress in Polymer Science: 1-27.
7. Choonara, B., F., Choonara, Y., E., Kumar, P., Bijukumar, D., du Toit, L., C. and Pillay, V. (2014). *A Review of Advanced Oral Drug Delivery Technologies Facilitating the Protection and Absorption of Protein and Peptide Molecules*, Biotechnology Advances, 32(7): 1269-1282.
8. Daful, A., G. and Mackie, A., D. (2014). *Micellular Morphological Transformations for a Series of Linear Diblock Model Surfactants*, The Journal of Chemical Physics, 140(9): 1049051- 1049058.
9. Deng, X., Zhang, G., Shen, C., Yin, J. and Meng, Q. (2013). *Hollow Fiber Culture Accelerates Differentiation of Caco-2 Cells*, Applied Microbiology and Biotechnology, 97: 6943-6955.
10. Devriendt, B., De Geest, B., G., Goddeeris, B., M. and Cox, E. (2012). *Crossing the Barrier: Targeting Epithelial Receptors for Enhanced Oral Vaccine Delivery*, Journal of Controlled Release, 160: 431-439.
11. Dume, C., A., Puscas, I. and Coltau, M. (2013). *Evolution of Gastric and Duodenal Ulcers at Patients with Helicobacter pylori Infection, after Treatment with Proton*

Pump Inhibitors and an Associated Treatment, Studia Universitatis Vasile Goldis Seria Stiintele Vietii (Life Science Series), 23(1): 39-43.

12. Dünnhaupt, S., Barthelmes J., Köllner, S., Sakloetsakun, D., Shahnaz, G., Düregger, A. and Bernkop- Schnürch, A. (2015). Thiolated Nanocarriers for Oral Delivery of Hydrophilic Macromolecular Drugs, 117: 577-584.
13. Fan, W., Yan, W., Xu, Z. and Ni, H. (2012). *Formation Mechanism of Monodisperse, Low Molecular Weight Chitosan Nanoparticles by Ionic Gelation Technique*, Colloids and Surfaces B: Biointerfaces, 90: 21-27.
14. Chao, F., Li, J., Kong, M., Liu, Y., Cheng, X., J., Li, Y., Park, H., J. and Chen, X., G. (2015). *Surface Charge Effect on Mucoadhesion of Chitosan Based Nanogels for Local Anti-Colorectal Cancer Drug Delivery*, Colloids and Surfaces B: Biointerfaces, 128: 439-447.
15. Dumitriu, S. (2004). *Polysaccharides: Structural Diversity and Functional Versatility,* 2nd ed. New York: Marcel Dekker, p 625.
16. Finlay, W., H. (2001). *The Mechanic of Inhaled Pharmaceutical Aerosols*, London: Academic Press, p 2.
17. Fowler, R. (2012). *Crossing Mucosal Barriers for Non- Invasive Protein Delivery: a Vitamin B_{12} - Mediated Approach*, (thesis), University of Nottingham.
18. Holm, R., Müllertz, A. and Mu, H. (2013). *Review: Bile Salts and their Importance for Drug Absorption*, International Journal of Pharmaceutics, 453(1): 44-55.
19. Horton, H., R., Moran, L., A., Scrimgeour, K., G., Perry, M., D. and Rawn, J., D. (2006). *Principles of Biochemistry*, 4th ed. New Jersey: Pearson Education, p 241.
20. Hsu, L-W., Lee, P-L., Chen, C-T., Mi, F-L., Juang, J-H., Hwang, S-M., Ho, Y-C. and Sung, H-W. (2012). *Elucidating the Signaling Mechanism of an Epithelial Tight- Junction Opening Induced by Chitosan*, Biomaterials, 33(26): 6254- 6263.
21. Hsu, L-W., Ho, Y-C., Chuang, E-Y., Chen, C-T., Juang, J-H., Su. F-Y., Hwang, S-M. and Sung, H-W. (2013). *Effects of pH on Molecular Mechanisms of Chitosan- Integrin Interactions and Resulting Tight- Junction Disruptions*, Biomaterials, 34(3): 784- 793.
22. Janes, K., A., Calvo, P. and Alonso, M., J. (2001). *Polysaccharide Colloidal Particles as Delivery Systems for Macromolecules*, Advanced Drug Delivery Reviews, 47: 83-97.
23. Jung, J. and Zhao, Y. (2012). *Comparison in Antioxidant Action Between α- Chitosan and β- Chitosan at a Wide Range of Molecular Weight and Chitosan Concentration*, Bioorganic and Medicinal Chemistry, 20(9): 2905-2911.

24. Kang, B., S., Lee, S., E., Ng, C., L., Kim, J., K. and Park, J., S. (2015). *Exploring the Preparation of Albendazole- Loaded Chitosan- Tripolyphosphate Nanoparticles*, Materials, 8: 486-498.
25. Kim, S., H., Jung, D., I., Yang, I., Y., Jang, S., H., Kim, J., Truong, T., T., Van Pham, T., Truong, N., U., Lee, K., Y. and Jang, Y., S. (2011). *Application of M Cell Targeting Ligand for Oral Vaccination to Induce Efficient Systemic and Mucosal Immune Responses Against Viral Antigens*, Immunology, 216(11): 1164-1171.
26. Kondoh, M., Takahashi, A. and Yagi, K. (2012). *Spiral Progression in the Development of Absorption Enhancers Based on the Biology of Tight Junctions*, Advanced Drug Delivery, 64(6): 515-522.
27. Kwon, K., C., Verma, D., Singh, N., D., Herzog, R. and Daniell, H. (2013). *Oral Delivery of Human Biopharmaceuticals, Autoantigens and Vaccine Antigens Bioencapsulated in Plant Cells*, Advanced Drug Delivery Reviews, 65(6): 782-799.
28. Moghassemi, S., Parnian, E., Hakamivala, A., Darzianiazizi, M., Vardanjani, M., M., Kashanian, S., Larijani, B., Omidfar, K. (2015). *Uptake and Transport of Insulin Across Intestinal Membrane Model Using TriMethyl Chitosan Coated Insulin Niosomes*, Materials Science and Engineering: C, 46: 333-340.
29. Mori, S., Matsuura, A., Rama Prasad, Y., V. and Takada, K. (2004). *Studies on the Absorption of Low Molecular Weight Heparin Using Saturated Fatty Acids and their Derivatives as an Absorption Enhancer in Rats*, Biological and Pharmaceutical Bulletin, 27(3): 418- 421.
30. Pereira de Sousa, I. and Bernkop- Schnürch, A. (2014). *Pre- Systemic Metabolism of Orally Administered Drugs and Strategies to Overcome it*. Journal of Controlled Release, 192: 301-309.
31. Renukuntla, J., Vadlapudi, A., D., Patel, A., Boddu, S., H., S. and Mitra, A., K. (2013). *Approaches for Enhancing Oral Bioavailablity of Peptides and Proteins*, International Journal of Pharmaceutics, 447(1-2): 75-93.
32. Scheers, N., M., Almgren, A., B. and Sandberg, A., S. (2014). *Proposing a Caco-2/ HepG2 Cell Model for In Vitro Iron Absorption Studies*, Journal of Nutritional Biochemistry, 25: 710-715.
33. Sharma, R., Agrawal, U., Mody, N. and Vyas, S., P. (2015). *Polymer Nanotechnology Based Approaches in Mucosal Vaccine Delivery: Challenges and Opportunities*, Biotechnology Advances, 33(1): 64-79.

34. Schrøder, T., D., Long, Y. and Olsen, L., F. (2014). *Experimental and Model Study of the Formation of Chitosan- Tripolyphosphate- siRNA Nanoparticles*, Colloid and Polymer Science, 292(11): 2869- 2880.
35. Smith, J., M., Dornish, M. and Wood, E., J. (2005). *Involvement of Protein Kinase C in Chitosan Glutamate- Mediated Tight Junction Disruption*, Biomaterials, 26(16): 3269-3276.
36. Sunilkumar, M., Ummu Habeeba, A., A., Prejina, P., P. and Sujith, A. (2014). *Chitosan Nanoparticles: A Systematic Study Based on Degree of De- Acetylation and Molecular Weight*, Polymers from renewable sources, 5(4): 167-184.
37. Upadhyaya, L., Singh, J., Agarwal, V. and Tewari, R., P. (2014). *The Implications of Recent Advances in Carboxymethyl Chitosan Based Targeted Drug Delivery and Tissue Engineering Applications*, The Journal of Controlled Release, 186: 54-87.
38. Vllasaliu, D., Fowler, R., Garnett, M., Eaton, M. and Stolnik, S. (2011). *Barrier Characteristics of Epithelial Cultures Modelling the Airway and Intestinal Mucosa: a Comparison*, Biochemical and Biophysical Research Communications, 415(4): 579-589.
39. Vllasaliu, D., Exposito- Harris, R., Heras, A., Casatteri, L., Garnett, M., Illum, L. and Stolnik, S. (2010). *Tight Junction Modulation by Chitosan Nanoparticles: Comparison with Chitosan Solution*, International Journal of Pharmaceutics, 400: 183-193.
40. Wei, Z., Kun, M., Q., Jin , J., S., Wen, Z., J., Shi, J., L., Bao, C., C. and Liu, Q., D. (2012). *Improvement of Intestinal Absorption of Forsythoside A in Weeping Forsythia Extract by Various Absorption Enhancers Based on Tight Junctions*, Phytomedicine, 20(1): 47-58.
41. Wu, S., J., Don, T., M., Lin, C., W. and Mi., F., L. (2014). *Delivery of Berberine Using Chitosan/ Fucoidan- Taurine Conjugate Nanoparticles for Treatment of Defective Intestinal Epithelial Tight Junction Barrier*, Marine Drugs, 12(11): 5677- 5697.
42. Yang, B., Zhang, M., Li, L., Pu, F., You, W. and Ke, C. (2015). *Molecular Analysis of Atypical Family 18 Chitinase from Fujian Oyster Crassostrea Angulata and its Physiological Role in the Digestive System*, PLoS ONE, 10(6): 1-13.
43. Yeh, T-H., Hsu., L-W., Tseng., M., T., Lee, P-L., Sonjae., K., Ho., Y-C. and Sung., H-W. (2011). *Mechanism and Consequence of Chitosan- Mediated Reversible Epithelial Tight Junction Opening*, Biomaterials, 32(26): 6164- 6173.

44. Zhang, B., Ye, H., Zhu, X., M., Hu, J., N., Li, H., Y., Tsao, R., Deng, Z., Y., Zheng, Y., N. and Li, W. (2014). *Esterification Enhanced Intestinal Absorption of Ginsenoside Rh2 in Caco-2 Cells Without Impacts on its Protective Effects Against H2O2- Induced Cell Injury in Human Umbilical Vein Endothelial Cells (HUVCs)*, Journal of Agricultural and Food Chemistry, 62: 2096- 2103.

45. Zhang, J., Zhu, X., Jin, Y., Shan, W. and Huang, Y. (2014). *Mechanism Study of Cellular Uptake and Tight Junction Opening Mediated by Goblet Cell- Specific Trimethyl Chitosan Nanoparticles*, Molecular Pharmaceutics, 11(5): 1520-1532.

Chapter 2

Materials and General Methods

2.1 Materials

2.1.1 Cells, culture media, media components and cell solutions

Caco-2 cells were obtained from the European Collection of Cell Cultures (ECACC) and used from passages 57-88 (passage used in terms of the level of cell differentiation). All of the following was purchased from Sigma Aldrich (UK); the medium used during the culture of this cell line was dulbeco's modified eagle's medium (DMEM) (with added 110mg sodium pyruvate, 4500mg glucose and L- glutamine), other media components used were antibiotic and antimycotic solution (which contains 10,000 units of penicillin, 10 mg of steptomycin and 25 µg amphotericin) and foetal bovine serum (FBS). Hank's balanced salt solution (HBSS) (with sodium bicarbonate, without phenol red), was used as a solution for cell uptake, transepithelial electrical resistance (TEER) and permeability studies. Phosphate buffered saline (PBS), trypsin (EDTA added, 0.25% w/v) and dimethyl sulfoxide (DMSO) were used in the process of cell rinsing, detachment from flask surface (during cell 'passaging') and cryopreservation of the cells, as referred to in section 2.2.1.2.

A standard bottle of DMEM (500 ml) was supplemented with 55 ml of FBS and 5 ml of antibiotic/antimycotic solution; containing penicillin, streptomycin and amphotericin, before being applied to the cells. This was developed in the university labs and from this point onwards the supplemented DMEM will be referred to as cell media.

2.1.2 Plasticware and glassware

Transwell permeable supports (also referred to as filters) of 12 mm diameter and 0.4 µm pore size and sterile, clear and black 96 well polystyrene microplates (tissue culture treated) were both obtained from Costar (USA). Cell culture flasks (75 cm^2, canted neck with vented caps) were obtained from Nunclon (Denmark) and sterile pipettes which were used for general use whilst maintaining Caco-2 cells were from Sarstedt (Germany). Sterile centrifuge tubes were from Sigma Aldrich (UK). Small glass cylinders

(50 ml) and small 20 ml disposable scintillation glass vials were obtained from Fisherbrand (UK). A metal set of different sized spatulas were purchased from RSG Solingen (Germany). Duran bottles (varying in size from 100 ml to 1000 ml) used for making up stock solutions were purchased from SCHOTT. Vivaspin™ sample concentrators (molecular weight cut of 1,000,000 Da) were from Sartorius (Germany).

2.1.3 Cell toxicity assay reagents

3-(4,5-dimethylthiazol-2-yl)-5(3-carboxymethonyphenol)-2-(4-sulfophenyl)-2H-tetrazolium (MTS) reagent, which is commercially known as 'CellTiter 96 AQueous One Solution Cell Proliferation Assay' was obtained from Promega (USA). For the LDH (lactate dehydrogenase) assay, the 'pierce LDH cytotoxicity assay kit' (Thermo Scientific, USA) commercial kit was used according to the manufacturer's instructions.

2.1.4 Chemicals

Different types of Ovalbumin (OVA) were used: Fluorescein isothiocyanate (FITC)-labelled ovalbumin (OVA) (FITC-OVA, 3 moles dye/mole), purchased from Molecular Probes (USA); non- labelled OVA was purchased from Sigma Aldrich (UK) and endotoxin-free OVA (EndoGrade® was purchased from Cambridge Bioscience (UK). Ultrapure chitosan chloride of 213 kDa average molecular weight ('Protasan UP CL 213') was obtained from Novamatrix (Denmark). Other reagents used were; tripolyphosphate (TPP), Triton X-100, 2-(N-morpholino)ethanesulfonic acid (MES), paraformaldehyde and fluoroshield with DAPI. These were all purchased from Sigma-Aldrich (UK).

Tween surfactant and hydrochloric acid (HCl) were bought from Fisher Scientific (USA). Bovine serum albumin (BSA), sodium carbonate (Na_2CO_3), sodium bicarbonate ($NaHCO_3$), heparin and ammonium persulfate (APS) were all obtained from Sigma Aldrich (UK). Acrylamide was obtained from BIORAD (USA) and glycine, tris, sodium dodecyl sulfate (SDS) and tetramethylethylenediamine (TEMED) were all obtained from Melford (UK).

2.1.5 Antibodies

Goat anti-mouse IgG H & L horseradish peroxidase (HRP) pre-absorbed was purchased from Abcam (UK), goat anti- mouse IgA-HRP was obtained from Invitrogen and goat anti-mouse IgG1- HRP was purchased from Southern Biotech (USA).

2.2 Methods

2.2.1 Maintenance of the cells

2.2.1.1 Maintenance of Caco-2 cells in culture flasks

Caco-2 cells were routinely maintained in 75 cm^2 flasks placed in incubators with 5 % CO_2, 95 % relative humidity, with a temperature of 37 °C until 70-80 % confluency. Cell medium was replaced every 2-3 days in the culture flasks, which was done by aspirating out the old media and replacing it with 12 ml of fresh medium. All cell culture buffers (PBS and HBSS) were also pre-warmed to 37 °C prior to contact with the cells and all protocols involved with handling Caco-2 cells in culture were performed aseptically. When at least 70-80 % confluent, cells were 'passaged' or seeded into a 75 cm^2 flask as detailed below.

The following protocol was used for cell passaging (or subculturing); old medium was aspirated out and the cells were washed with 5 ml of PBS twice, making sure to remove all of the old medium and any dead cells there may be, using a gentle swirling motion. Washing the cells is an important step in the process as left over FBS present in DMEM inactivates trypsin, making it less efficient for cell detachment. Once the cells had been washed, the PBS was aspirated out and 3 ml of trypsin was added and gently swirled ensuring the trypsin covered all the cells; the flask was then incubated although the time length is dependent on the cell line and the confluency within the flask. For Caco-2 at 75 % confluency this is approximately 10-15 minutes. After incubation the cells were completely detached from the bottom of the flask, at which point 9 ml of fresh medium was added to inactivate the trypsin. After giving the flask another gentle swirl, 1.5 ml of cell suspension was added to a new flask, corresponding to 1:6 'split ratio'. 10.5 ml of fresh media was then added to the newly created flask and the flask clearly labelled with the cell line, passage number, user name and date. The flask was then placed back in

the incubator for further culture. The medium used for culturing Caco-2 cells was DMEM; for supplements added to the medium refer to section 2.1.1.

2.2.1.2. Frozen storage of cells

Cells were cultured until they were confluent and then detached from the bottom of the flask using the method previously described in section 2.2.1.1. However, after the fresh medium was added to the flask to deactivate the trypsin, the cell suspension was centrifuged at 2500g for 5 minutes to create a pellet at the bottom of the centrifuge tube. The supernatant was then aspirated out and the cell pellet re-suspended in 1 ml of fresh medium containing 100 µl of DMSO (i.e. DMSO was used at 10 % v/v). The suspension was then added to a sterile cryovial, which was clearly labelled with the relevant details (name, date, cell line and passage number). This process was repeated for each confluent flask, creating one cryovial from one flask. These were then placed into a freezing container, 'Mr Frosty' in a -80 °C freezer. The cells were stored at -80 °C for up to 3 weeks. After 3 weeks the cells were then transferred into the liquid nitrogen storage tank; the cells were stored in liquid nitrogen for as long as required.

2.2.1.3. Cell revival

The relevant cryovials were removed from the liquid nitrogen storage tank and placed in an incubator to thaw for 2-5 minutes at 37 °C. The cell suspension was then transferred to a flask with 16 ml of fresh cell medium in. Note, one cryovial was transferred into one cell culture flask for cell growth.

2.2.1.4. Culture of cells on transwells

Caco-2 cells were cultured until they were confluent (75-95 %) and kept at 37 °C with 5 % CO_2 levels. It is standard practice to culture cells on transwell filters when performing studies *in vitro* in drug absorption studies. Cells were detached from flasks using the previously described method in section 2.2.1.1. While the cells were incubating with trypsin, medium was added to the transwell filters. 0.5 ml was added to the apical chamber and 1.5 ml was added to the basolateral chamber. This was done so when the cells were added to the apical chamber they had a more stable environment and were more likely to adhere to the plastic membrane. A volume of cell suspension corresponding to $1x10^5$-$2x10^5$ cells (usually 20 µl) was added to the apical transwell

compartment. The cells were then cultured in normal cell culture conditions until they formed a polarised/differentiated monolayer, which was approximately 21 days with regular replacement of cell medium (every 2-3 days).

2.2.2. Measurement of transepithelial electrical resistance (TEER)

Measuring the TEER is a very important technique in epithelial cell culture, this gives an indication of cell monolayer integrity, cell polarity and epithelial tight junction function. TEER was measured using an epithelial voltohmmeter with 'chopstick' electrodes (World Precision Instruments, USA). One electrode is longer than the other to account for the depth of basolateral and apical transwell compartments. The electrodes measure the electrical resistance to the ion flux (e.g. Ca^{2+}, K^{-}, Na^{+} and Cl^{-}) across the epithelial cell monolayer. This method has become the universal method within epithelial *in vitro* research to measure the formation and function of tight junctions, as well as cell membrane integrity, it is convenient, reliable and does not damage the cells used.

Figure 2.1 demonstrates how to use the equipment. Before the cells were measured the probes were placed in 70 % ethanol to sterilise them. This was for approximately 20-25 minutes. The longer probe was placed in the basolateral transwell compartment and the shorter probe was placed in the top, apical compartment. Note that TEER was measured before any replacement of medium or cell passaging took place; this was because we noticed that the TEER temporarily changes when the cell medium is replaced from the transwell filter. TEER was measured before any studies with polarised Caco-2 monolayers took place to establish the integrity, confluence of the cells and the formation and function of tight junctions.

TEER values reported in this research have taken into account the area of the cell layer, which is assumed the same as the area of the transwell membrane. These values are expressed as Ωcm^2. Background resistance was also measured on all cell-free transwell filters (typically 100 Ωcm^2): this was subtracted from the TEER values taken for cells throughout this thesis.

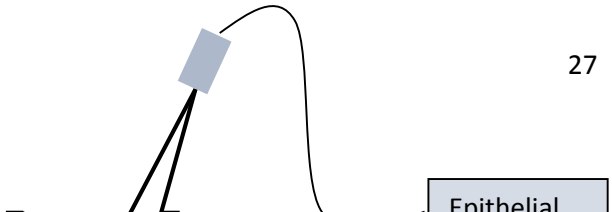

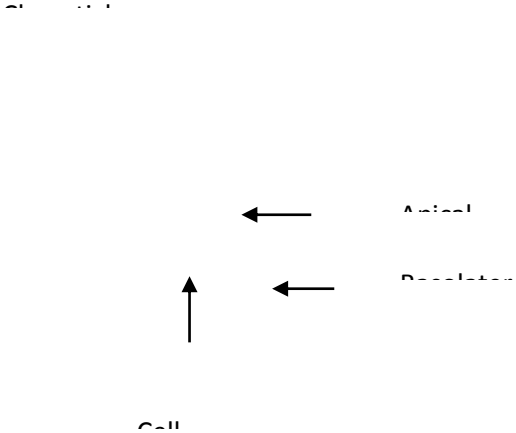

Figure 2.1 Representation of the equipment used to measure the TEER of the cell layers.

2.2.3. Preparation of chemicals

2.2.3.1. Tripolyphosphate

10 mg of tripolyphosphate (TPP) was weighed out and mixed with 10 ml of hank's balanced salt solution (HBSS) and mixed until TPP dissolved.

2.2.3.2. 2-(N-Morpholino)ethanesulfonic acid hydrate (MES hydrate)

195 mg of 2-(N-Morpholino)ethanesulfonic acid hydrate (MES hydrate) was added to 100 ml of HBSS and mixed until the MES hydrate had dissolved in the solution. This created 10 mM HBSS with a pH of 6.0.

2.2.3.3. Wash buffer (PBSx20/0.05 % tween surfactant)

2.5 ml of tween surfactant was added to 250 ml phosphate buffered saline at a concentration of x20. These were then added to 5 litres of distilled water.

2.2.3.4. Assay diluent

10 g of bovine serum albumin (BSA) was added to 1 litre of water with 5 PBS tablets. These were mixed and dissolved before 3 ml of tween surfactant was added. Lastly, 3.7 g of EDTA was added to the solution.

2.2.3.5. Preparation of pH 9.6 carbonate buffer

16 ml of 0.2 M stock solution of sodium carbonate was added to 34 ml of sodium bicarbonate stock solution. 150 ml of distilled water was then added to dilute to a pH of 9.6.

2.2.3.6. Resolving buffer

Resolving gel buffer consisted of 1.5 M tris pH 8.8 and 0.4 % SDS.

2.2.3.7. Preparation of Stacking buffer

Stacking gel buffer consisted of 0.5 M tris pH 6.8 and 0.4 % SDS.

2.2.3.8.resolving gel (12%)

The resolving gel was made up as follows: 4.1 ml of autoclaved mQ water, 3 ml of resolving buffer (see 2.2.3.6), 4.8 ml of 30 % acrylamide/bis.

2.2.3.9. Stacking gel (4%)

The stacking gel was made up as follows: 3 ml of autoclaved mQ water, 1.3 ml of stacking buffer (see 2.2.3.7), 0.67 ml of 30 % acrylamide/bis and 5 µl of bromophenol blue to visually see the wells.

2.2.3.10. Running buffer

Running buffer consisted of 115.2 g glycine, 24 g tris and 2 L of deionised water.

2.2.4. Cell toxicity studies

2.2.4.1. MTS cell metabolic activity assay

The MTS assay measures the metabolic activity of the cell once the sample has been applied. The cell viability is measured at the end of the assay. Tetrazolium in the MTS reagent is reduced to a coloured formazan product via the presence of the electron acceptor phenazine ethyl sulphate in metabolically active cells. This dye is visible once the assay has finished. Cells were seeded onto a 96-well, clear multiwell plate (cell culture treated) and were left to incubate with DMEM at 37 °C 5 % CO_2 for 24 hours for the cells to establish attachment on the bottom of the plate and grow. The cell medium

was aspirated out, making sure the pipette tip did not touch the bottom of the 96 well plate so not to damage the cells. The samples tested were then applied at differing concentrations (0.1 mg/ml, 0.05 mg/ml, 0.025 mg/ml and 0.0125 mg/ml) in HBSS. A 10 % v/v solution of triton X-100 in HBSS was prepared as a positive control and finally HBSS alone was used as a negative control. 100 µl of each sample was placed into 6 wells for repeats (i.e. n=6) and placed into an incubator at 37 °C/5 % CO_2 for 3 hours. After 3 hours the samples were aspirated from the wells and 100 µl of cell medium was applied to each well. 20 µl of MTS reagent was then added to all the wells. The 96-well plate was placed in an incubator at 37 °C/5 % CO_2 for 2 hours, according to the manufacturer's protocol. When the plate had finished incubating, the absorbance at 490 nm was measured using tecan.

The relative cell metabolic activity (%) was calculated using the following equation:

$$\text{Relative metabolic activity} = \frac{S-T}{H-T}\ X100$$

Key:

- S is the absorbance of cells incubated with tested samples
- T is the absorbance of cells incubated with triton X-100
- H is the absorbance of cells incubated with HBSS

2.2.4.2. Lactate dehydrogenase (LDH) assay

The LDH assay measures cell membrane integrity by measuring the release of the enzyme lactate dehydrogenase, this is only released when cell membranes are compromised via toxicity. This differs from the MTS assay by measuring different aspects of the cells. Cells were seeded onto a clear, flat-bottomed 96 well plate 48 hours before the assay. Cell medium was aspirated from the 96 well-plate and samples differing in concentrations and dissolved in HBSS were then applied to each well. A 10 % solution of triton X-100 in HBSS was prepared as a positive control and finally HBSS alone was used as a negative control. 100 µl of the required samples were applied to the cells with repeats of 6 and left to incubate at 37 °C/5 % CO_2 for 3 hours. 50 µl of each sample was then transferred to another clear flat-bottomed 96-well plate. The assay was conducted

according to manufacturer's instructions. 50 µl of the LDH reaction mixture was then added to each sample and mixed using a pipette. The plate was then left at room temperature for 30 minutes and covered with foil. 50 µl of stop solution (1 M acetic acid) was then applied to each well and mixed by gentle tapping. The absorbance was measured at 490 nm by tecan.

The LDH release was calculated as the percentage relative to the controls using the following equation:

$$\text{Relative LDH release} = \frac{S-H}{T-H} X100$$

Key:

- S is the absorbance of cells incubated with the tested samples
- H is the absorbance of cells incubated with HBSS
- T is the absorbance of cells incubated with triton X-100

2.2.5. TEER studies

All TEER studies were conducted on cells that were cultured on transwell inserts for at least 21 days. Cell medium was aspirated out of each well and HBSS was applied to each well (warmed to 37 °C) and the TEER was measured (method described in section 2.2.2.) The transwell plate was then placed in an incubator for 40-45 minutes for the cells to adjust to the change in environment (replacement of medium with HBSS). The samples tested were dissolved in HBSS. The HBSS from the apical side was aspirated out and 0.5 ml of each sample was applied to the wells. Three wells were used per sample and HBSS was used as a negative control. TEER was measured, as described in section 2.2.2., at time 0 and then every 30 minutes for 3 hours (30, 60, 90, 120, 150 and 180 min).

2.2.6. Nanoparticle permeability study

Transwell-cultured cells with a minimum TEER of 900 Ωcm^2 (Chen *et al*. 2015) were deemed suitable for cell permeability studies. TEER measurements were taken before permeability studies took place as a reassurance of the cellular tight junctions formation and the integrity of the Caco-2 cell monolayers. HBSS was warmed in a water-bath to 37

°C. The cell medium was aspirated out and replaced with HBSS (1.5 ml in the basolateral side and 0.5 ml in the apical chamber); the transwell plate was placed in an incubator at 37 °C/5 % CO_2 for 40-45 minutes. When the cells had adjusted, tested via TEER, the HBSS was aspirated from the apical side and replaced with 0.5 ml of the test sample at differing concentrations (0.1 mg/ml, 0.05 mg/ml, 0.025 mg/ml and 0.0125 mg/ml). At time 0, 100 µl of the sample was taken from the basolateral chamber and placed in a 96-well black plate. The sampled solutions were replaced with equal volumes of HBSS and the transwell was placed back in the incubator at 37 °C 5 % CO_2. Basolateral samples were further taken every 30 minutes for 3 hours, repeating the method just described. Translocation of the tested sample was quantified by fluorescence using tecan (488 nm excitation and 520 nm emission).

These measurements were analysed by converting the fluorescence into concentrations and then into amounts (micrograms). This was done through the calibration curves (0.1-0.000195 mg/ml).

Permeability is expressed as the apparent permeability coefficient (P_{app}), which was calculated using the following equation:

$$P_{app} = \frac{dQ}{dt} \times \frac{1}{A \times C_0}$$

Key:

- P_{app} is the apparent permeability
- dQ is the amount of drug
- dt is the drug transport transported by time
- A is the membrane surface area
- C_0 is the donor concentration at time 0

2.2.7. Cell fixation for microscopy

Cells were fixed after the completion of permeability studies. The sample was aspirated from the apical and basolateral membranes and cells washed twice with PBS. 100 µl of paraformaldehyde was then applied to the apical membrane chamber and left for 5

minutes. After the cells had been fixed the paraformaldehyde was removed and PBS was placed into the apical and basolateral chambers. The transwell plate was then covered with foil and placed into the fridge until needed for imaging.

2.2.8 Sodium dodecyl sulphate polyacrylamide gel electrophoresis (SDS- PAGE)

To make the electrophoresis gels, the following method was used: a glass plate and a white plate were put together with a spacer of 1 mm in between the plates. It was made sure that the plates were levelled off to prevent any leaks from occurring. The plates were bolted into the gel caster and dH_2O was poured between the plates to ensure there were no leaks. The gel caster was tipped upside down to remove all of the dH_2O.

Next, 12 % gels were made. Two sterilins were used; one labelled resolving gel, one labelled stacking gel. Stacking gel concentrates all of the samples into one band so all of the samples run at the same time once they pass into the running buffer. The resolving gel seperates the samples based on their molecular weight. Once the resolving gel (see section 2.2.3.8.) and the stacking gel (2.2.3.9.) was prepared, 100 µl of ammonium persulphate (APS) and 16 µl of tetramethylethylenediamine (TEMED) was added to the resolving gel. APS and TEMED are used to catalise the polymerisation of acrylamide/ bisacrylamide. This forms a mesh which ultimately forms the gels that are used. 10 % APS solution was made fresh that day by adding dH_2O to APS powder. Once APS and TEMED were added to the gel, the gel started to set. The dH_2O was removed from the gel casters and the resolving gel was applied first; a small amount of residue was left at the bottom of the sterilin so it was clear when the gel polarised. Resolving gel was poured between the clear and white plates, 2/3 of the way up. A small amount of dH_2O was added on top of the resolving gel to make sure the resolving gel was level. After the resolving gel had set, 50 µl APS and 16 µl of TEMED was added to the stacking gel. The stacking gel was then added to the gel casters. The stacking gel was filled to the top of the plates and a well caster was placed between the plates to create the wells. This took 10-15 minutes to set.

The gels were then clipped in place in a tank and running buffer was then added to the plates. Once samples were applied to the wells, the gels were wired up to an electric current and run at 150 mv for 1 hour. One reference ladder was added per gel.

2.2.9. Polyacrylamide gel staining and imaging

When the gels finished running, the stacking gel was cut off and placed in a pot. Coomassie blue stain was applied for 10-15 minutes. The excess stain was poured back into the bottle and the gel was then immersed in dH_2O. Destain (already made up) was then applied for 10-15 minutes. The gel was rinsed in dH_2O and DE Stain was applied again and left overnight. The next day the gel was compared to the reference ladder.

2.2.10 Nanosight

The equipment used a technique called nanoparticle tracking analysis (NTA) this is a combination of both dynamic light scattering (DLS) and brownian motion to get a true result of the particle size and concentration in liquid suspension. The laser is shone through the sample chamber and the particles in the path of this beam scatter light for the person using the equipment to visualise the particles. There is a video camera attached to capture the particles move in brownian motion.

Following formulation, chitosan:OVA nanoparticles were diluted 1:100-1:200 in dH_2O or HBSS before size measurement in Nanosight. The sample was then inserted into the Nanosight top plate using a small syringe. Size analysis was carried out using the in-built Nanosight control user interface software. A range of concentrations (1 mg/ml, 0.5 mg/ml, 0.25 mg/ml and 0.125 mg/ml) were used to find the ideal size (200nm).

2.2.11 Confocal Microscopy

Caco-2 cells were first fixed using the above method in section 2.2.7. A slide with transwell filter was then prepared using the following method; a scalpel was placed in absolute ethanol for approximately 30 minutes to sterilise it before use. This was then used to carefully cut the transwell membrane, which was then carefully removed with tweezers and placed on a slide, cell side up. DAPI nuclei stain was then applied to the cells. The cell-populated transwell membrane was covered with a coverslip before confocal imaging. A Leica SP8 confocal microscope was used for imaging.

Image analysis was carried out using the in-built confocal control user interface software (Leica SP8) and digital imaging system.

2.2.11 Statistical Analysis

Statistical comparisons were performed by ANOVA in multiple group comparisons. Values of $p<0.05$ were considered statistically different.

2.3 References

1. Chen, S., Einspanier, R. and Schoen J. (2015). *Transepithelial Electrical Resistance (TEER): a Functional Parameter to Monitor the Quality of Oviduct Epithelial Cells Cultured on Filter Supports*. Histochemistry and Cell Biology, 144(5): 509-15.

Chapter 3

Formulation and Characterisation of Chitosan:OVA Nanoparticles

3.1 Introduction

Chitosan is an organic biomaterial derived from the exoskeleton of many crustaceans. It has shown many potential applications in biomedicine, including use in formulation drug delivery systems such as microparticles and nanoparticles with the ability to cross mucosal membranes (Raftery *et al*. 2015). The capacity of chitosan to facilitate drug delivery across mucosal membranes is attributed to its mucoadhesive properties and its ability to open the epithelial tight junctions in cells. Tight junctions are structures that keep adjacent epithelial cells in close proximity with one another, hence creating a barrier to the movement of material between the cells (Vllasaliu *et al*, 2010). Tight junctions also act as an immune defence mechanism as it prevents bacterial toxins and particles from entering the body (Wu *et al*. 2014).

Chitosan nanoparticles are often researched and used within the drug delivery sector to facilitate drug delivery across mucosal membranes, including those of the gastrointestinal tract (Kheradmand *et al*. 2015). There are several advantages to chitosan nanoparticles, for example: low toxicity, high drug loading efficiency, simple preparation, prolonged circulation in the blood, amenability to controlled release (chemical stimulus such as pH) and targeted and controlled delivery (Zhang *et al*. 2015). Nanoparticles are an effective way to improve drug delivery and prevent the degradation of the therapeutic agent (Madureira *et al*. 2015).

Although chitosan has been previously researched for its potential for mucosal vaccine delivery, this work set out to determine the potential of nanoparticles formulated from ultrapure chitosan chloride specifically, as a chitosan salt which has previously shown significant potential for mucosal protein delivery *in vitro* (Vllasaliu *et al*. 2010). The work

further investigates the action of chitosan nanoparticles *in vivo*, as well as the mechanisms by which chitosan nanoparticles facilitate transepithelial delivery of ovalbumin (OVA) as a model antigen.

This chapter will detail the formulation and characterisation of chitosan:OVA nanoparticles, which were initially formulated by the ionic gelation method, followed by characterisation studies. Characterisation of nanoparticles was conducted with respect to size and charge of nanoparticles, their ability to complex and release the payload (OVA) on contact with a negatively charged macromolecule (heparin) and capability to protect OVA from acidic and enzymatic degradation.

3.2 Methods

3.2.1 Preparation of nanoparticles

3.2.1.1 Preparation of chitosan:OVA nanoparticles

Chitosan ('Protasan UP CL 213') nanoparticles were prepared in different concentrations and chitosan:OVA ratios in order to identify an optimal formulation 'recipe' producing nanoparticles of desirable characteristics to be used in further studies. Chitosan was used in different concentrations: 1 mg/ml, 0.5 mg/ml, 0.25 mg/ml and 0.125 mg/ml, whilst OVA was kept constant at 1 mg/ml. First, stock solutions of 2 mg/ml of chitosan in dH_2O and 2 mg/ml OVA in dH_2O were prepared. As a chloride salt, the specific chitosan used in this project ('Protasan UP CL 213') dissolves in dH_2O with continuous stirring in approximately 20 minutes. Once dissolved chitosan was mixed with OVA creating a 1 mg/ml concentration (1:1 ratio).

Following mixing of chitosan and OVA solutions, TPP solution (1 mg/ml) (see section 2.2.3.1) was then added via a syringe and needle and added to the chitosan:OVA solution in a slow, drop-wise manner. TPP was added until the solution started to look opalescent which indicated the formation of nanoparticles (nanoparticle solution should look between figures 3.1 b and c). Care was taken to avoid adding TPP in excess as this resulted in formation of visible particulate matter, probably as a result of excessive nanoparticle aggregation and/or precipitation (if this was encountered, the samples were discarded (see figure 3.1 d for reference). Samples were diluted in dH_2O as appropriate to the following ratios: 1:2, 1:4 and 1:8.

a) b) c) d)

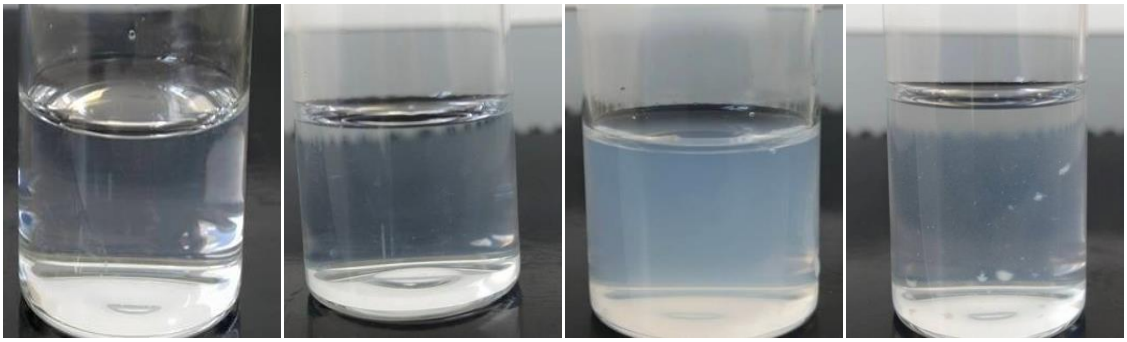

Figure 3.1 a) Chitosan and OVA mixed solution with no TPP, b) Chitosan:OVA nanoparticles with a few drops of TPP, c) Opalescent chitosan:OVA nanoparticle solution, d) Aggregated particulate matter due to too much TPP.

Three different types of OVA were used in this project. For TEER, cytotoxicity and nanoparticle characterisation studies, unlabelled OVA was used. For permeability studies, OVA release and confocal microscopy, fluorescently labelled, FITC-OVA, was purchased and employed to enable OVA permeability quantitation through fluorescence measurement and visualisation with confocal microscopy. *In vivo* studies utilised unlabelled, endotoxin-free OVA.

3.2.1.2 Preparation of chitosan nanoparticles

Chitosan ('Protasan UP CL 213') nanoparticles were used in the same concentrations and ratios as chitosan:OVA nanoparticles for comparison in future studies (1 mg/ml, 0.5 mg/ml, 0.25 mg/ml and 0.125 mg/ml). First a stock solution of 2 mg/ml of chitosan in dH_2O was prepared. TPP solution (1 mg/ml) was then added via a syringe and needle and added to the chitosan solution in a slow, drop-wise manner.

3.2.2 Nanoparticle size characterisation using Nanoparticle Tracking Analysis ('Nanosight')

Nanoparticle size characterisation was conducted using Nanoparticle Tracking Analysis by Nanosight LM10 HS instrument (Malvern, UK). This was an essential part of the nanoparticle formulation, establishing optimal ratio of chitosan and OVA.

3.2.3 Nanoparticle surface charge characterisation using Zetasizer

Nanoparticle surface charge characterisation was conducted using Dynamic Light Scattering (DLS) by a Zetasizer Nano ZS (Malvern, UK). Particles suspended in a liquid will move in accordance with brownian motion. The light scatters off particles in the liquid reflecting onto other particles. The velocity in which the particles move is measured by the zetasizer calculating the surface charge of the suspension. This is explained by the Stokes-Einstein equation: $D = \frac{kT}{6\pi R\eta}$

Key:

- D is diffusion coefficient
- K is the Boltzmann constant
- T is the temperature
- η is the viscosity of the solution
- R is the hydrodynamic radius of the particle

Chitosan and chitosan:OVA nanoparticles were formulated as described previously (section 3.2.1.2 and 3.2.1.1) and diluted in dH_2O or HBSS/MES (pH 6.0) to compare the difference in surface charge. Four measurements were taken and the average zeta potential was calculated by the instrument.

3.2.4 Characterisation of OVA release from chitosan:OVA nanoparticles

1 mg/ml samples of chitosan:OVA nanoparticles (1:1 mass ratio) were prepared, as per section 3.2.1.1, using FITC-OVA. This particular formulation was used as a comparison for permeability studies *in vitro*. 100 µl of chitosan:OVA nanoparticles were placed into 6 wells in a 96 well flat bottomed plate and the fluorescence was read using a Tecan Infinite M200 Pro plate reader (Tecan Group ltd, Switzerland). The excitation wavelength at 488 nm and the emission wavelength at 520 nm. These were covered with foil until further needed. 1 ml of heparin was applied to one scintillation vial of chitosan:FITC-OVA nanoparticles previously prepared and left for 30 minutes at room temperature (approximately 22 °C). After 30 minutes 1 ml of chitosan:FITC-OVA nanoparticles exposed to heparin and control chitosan:FITC-OVA nanoparticles were processed for membrane unltrafiltration by using vivaspin centrifugal concentrator tubes (MWCO 1,000,000 Da) and centrifuging for 20 minutes at 3000 rpm. Following

centrifugation 100 µl of the filtrate was transferred to a 96 well flat bottomed plates. The fluorescence was then read by Tecan and the results recorded.

3.2.5 Characterisation of OVA stability in chitosan:OVA nanoparticles

Stability of OVA within chitosan:OVA nanoparticles was tested following exposure to hydrochloric acid (HCl) and trypsin 10x is a 2.5% solution of 1:250 trypsin. Comparison of OVA solution and chitosan:OVA nanoparticles after exposure to HCl or trypsin was made. HCl and trypsin play a key part within the digestion of food. Trypsin is one of the digestive enzymes which assists in food breakdown within the stomach. This study was designed to test the stability of OVA to two of the materials found within the digestive system which would present a great barrier to protein stability. Chitosan:OVA samples were exposed to HCl or trypsin, followed by exposure to heparin in order to release OVA before analysis of OVA stability by SDS PAGE. All samples were prepared at 1 mg/ml, samples were prepared as follows;

Sample	Formulation
1.	1ml Chitosan:OVA nanoparticles after exposure to heparin.
2.	1ml Chitosan:OVA nanoparticles after exposure to HCl and heparin.
3.	1ml Chitosan:OVA nanoparticles after exposure to trypsin (concentration 10x) and heparin.
4.	1ml OVA in HBSS at pH7 (control).
5.	1ml OVA after exposure to HCl at pH1-2.
6.	1ml OVA after exposure to trypsin (concentration 10x).

Table 3.1 Samples prepared for OVA stability characterisation study.

Chitosan:OVA nanoparticles were prepared (see section 3.2.1.1) for samples 1, 2 and 3. OVA solution, using HBSS/MES, was prepared for samples 4, 5 and 6. 100 µl of 70 % HCl was added to 900 µl of chitosan:OVA nanoparticle solution in sample 2 and OVA solution in sample 5. 10 µl of trypsin (concentration 10x) was added to 990 µl of chitosan:OVA nanoparticles in sample 3 and OVA solution in sample 6. These samples were incubated for one hour at room temperature. Note that sample 2 and sample 3 were exposed to

HCl (sample 2) and trypsin (concentration 10x) (sample 3) first. After 30 minutes samples 5 and 6 were also exposed to HCl (sample 5) and trypsin (concentration 10x) (sample 6), all samples were left for a further 30 minutes at room temperature. Room temperature was used because the HCl was not stable enough to heat. While the samples were incubating, a 5 mg/ml solution of heparin was prepared in dH_2O. When samples 2 and 3 had finished incubating (HCl and trypsin, respectively), 1 ml of 5 mg/ml heparin solution was applied (1:1 heparin:chitosan mass ratio) to samples 1, 2 and 3 for 30 minutes. Note, samples 2 and 3 finished incubating 30 minutes before samples 5 and 6, this was so samples would all finish incubating at the same time.

After incubation samples 1, 2 and 3 (exposed to heparin) were filtered using Vivaspin membrane ultrafiltration tubes with centrifugation at 3000rpm for 15 minutes. The filtrate was collected and placed in a labelled Eppendorf tube. All samples were analysed by SDS-PAGE (see section 2.2.8).

3.3 Results

3.3.1 Chitosan:OVA and chitosan nanoparticle characterisation

3.3.1.1. Nanoparticle sizing using DLS (dynamic light scattering)

A preliminary dynamic light scattering study using a 1 mg/ml chitosan solution (in HBSS/MES, ph 6.0) alone was performed. The data showed no peaks suggesting that there is no nanoparticle formation without the addition of TPP.

Figure 3.2 is a control study, in this instance that of 1 mg/ml OVA solution alone in HBSS/MES. The figure shows positive signal suggesting presence of particulates of 75

and 135 nm (mode = 77.4 nm). It is unclear where this signal originates from in the sample, as OVA protein in solution is significantly smaller (6 nm). However, it could be due to aggregation of OVA, there is a high aggregation of OVA to increase OVA to 77.4nm in size.

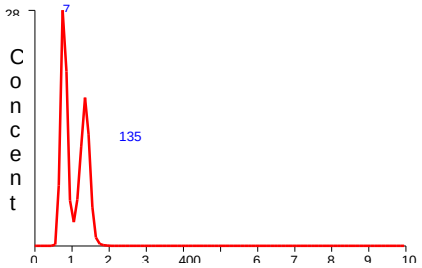

Mean	100.5nm
Mode	77.4nm
SD	29.8nm

Figure 3.2 Control experiment: 1 mg/ml OVA solution. 3 repeat samples were formulated for repeats.

Figure 3.3 is another control experiment of 1 mg/ml chitosan and OVA solution (no TPP) to determine the size in suspension of a mixture of chitosan and OVA without the addition of TPP. The figure shows the presence of a number of particle population sizes, resulting in an overall mode of 292.5 nm. Figure 3.2 and 3.3 demonstrates there are no particles without the addition of TPP to the chitosan:OVA complex and therefore TPP is needed for nanoparticles to form.

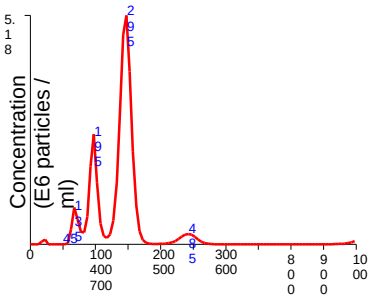

Mean	381.2nm
Mode	292.5nm
SD	295.6nm

Figure 3.3 Control experiment: diameter of 1 mg/ml solution of chitosan and OVA (no TPP). 3 repeat samples were formulated for repeats.

Figure 3.4 shows 1 mg/ml solution of chitosan:OVA nanoparticles, 1:1 mass ratio. Data shows a dominant peak of particle species with 195 nm diameter, with smaller particle

populations of larger size, producing an overall mode of 196.5 nm. It is worth noting that chitosan:OVA nanoparticles display a smaller size and particles where a large proportion is of a narrow size range compared to physical mixture of OVA and chitosan without TPP (above). This could be explained by TPP-induced ionic gelation creating smaller and more compact particles.

Note that the 1:1 chitosan:OVA mass ratio of nanoparticles was used in subsequent experiments, *in vitro* and *in vivo* due to optimal nanoparticle size (196.5 nm).

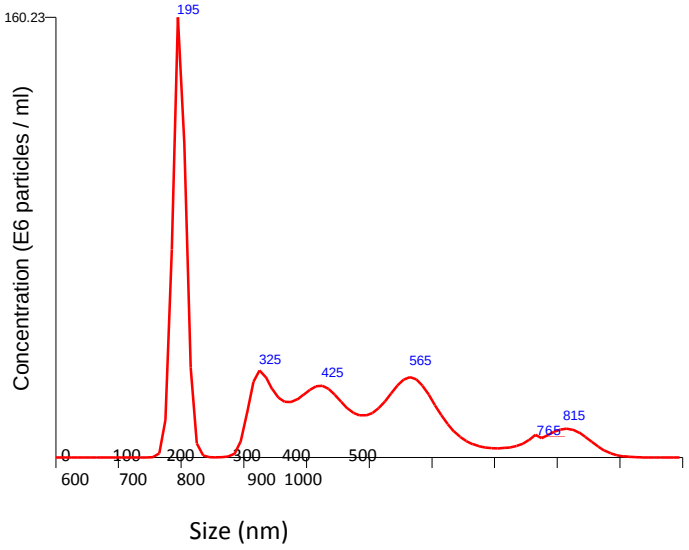

Mean	411.3nm
Mode	196.5nm
SD	195.7nm

Figure 3.4 Size analysis of 1 mg/ml chitosan:OVA nanoparticles (1:1 mass ratio) in dH_2O. 3 repeat samples were formulated for repeats.

Figure 3.5 shows nanoparticles of 1:2 chitosan:OVA mass ratio. The graph has a broad peak suggesting polydisperse nanoparticle sample with a mode of 301.5 nm. Figure 3.5

shows multiple peaks of high concentration in the sample rather than one concentration predominating, this was also shown infigure 3.4, as well as a higher mode. Lower content of chitosan therefore leads to higher polydispersity. There is less chitosan to interact ionically with TPP, therefore there are more free TPP molecules and free OVA in the solution.

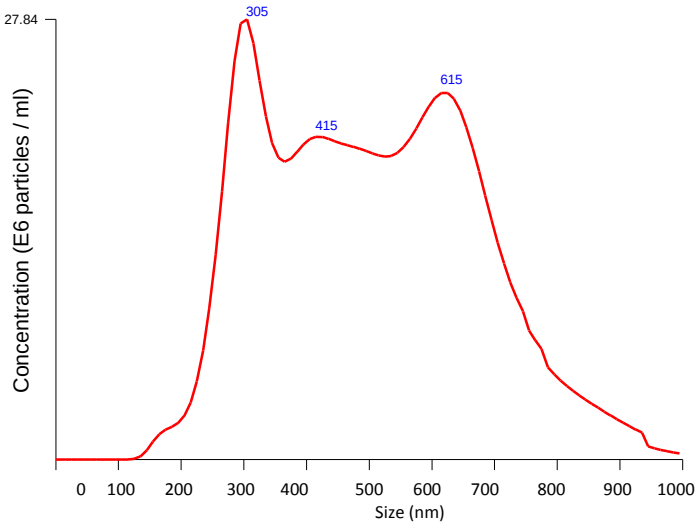

Mean	499.0nm
Mode	301.5nm
SD	170.4nm

Figure 3.5 Size analysis of 1:2 mass ratio chitosan:OVA nanoparticles in dH_2O. 3 repeat samples were formulated for repeats.

Figure 3.6 shows nanoparticles of 1:4 chitosan:OVA mass ratio. Data again suggests a polydisperse sample with multiple peaks of high concentration as opposed to one concentration predominating (as in figure 3.4). Mode is higher at 329.7 nm.

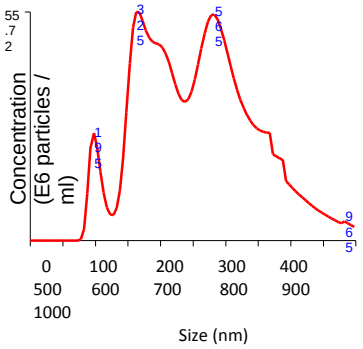

Mean	519.0nm
Mode	329.7nm
SD	192.2nm

Figure 3.6 Size analysis of 1:4 mass ratio chitosan:OVA nanoparticles in dH_2O. 3 repeat samples were formulated for repeats.

Figure 3.7 shows nanoparticles of 1:8 chitosan:OVA mass ratio. The mode is 380.9 nm and multiple peaks also contribute to a large proportion (y axis shows high concentration) in the sample rather than one concentration predominating, as in Figure 3.4.

We can conclude from Figures 3.4-3.7 that the optimal chitosan:OVA mass ratio for further studies is 1:1, which is why we took this ratio forward for future experiments.

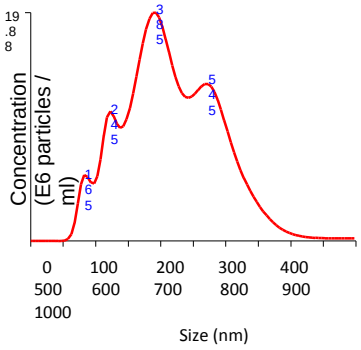

Mean	427.7nm
Mode	380.9nm
SD	151.3nm

Figure 3.7 Size analysis of 1:8 mass ratio chitosan:OVA nanoparticles in dH_2O. 3 repeat samples were formulated for repeats.

Figure 3.8 shows 1 mg/ml, 1:1 ratio of chitosan:OVA nanoparticles in HBSS/MES (pH 6.0). This figure was studied to show the size in the biological cell solution used for *in vitro* studies. The data in fact shows a smaller mode of 126.1 nm in HBSS/MES than in dH_2O which has a pH of 7.0. This factor could be a contributing cause to the displayed monodispersity. The data also shows that a single particle population with 125 nm diameter dominates in the sample, i.e. even though the sample is polydisperse (other peaks are apparent), a single population size is dominant. The standard deviation is also relatively small at 35.2 nm.

Note only a 1:1 ratio of chitosan:OVA nanoparticles were tested in HBSS. Once the ideal size was found in dH_2O, the nanoparticles were tested in HBSS.

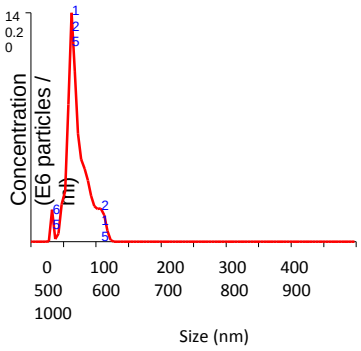

Mean	138.1nm
Mode	126.1nm
SD	35.2nm

Figure 3.8 Diameter of 1 mg/ml chitosan:OVA nanoparticles in HBSS. 3 repeat samples were formulated for repeats.

3.3.1.2. Surface Charge

Table 3.2 compares the surface charge of chitosan:OVA nanoparticles against chitosan nanoparticles (without OVA) in HBSS and dH_2O. It is apparent that samples have a lower surface charge in HBSS compared to dH_2O. Chitosan:OVA nanoparticles in HBSS had a surface charge at +9.68 mv in comparison to chitosan:OVA nanoparticles in dH_2O (+37.9mv). HBSS acts as a buffer and neutralises the surface charge with negatively charged counter ions in the solution which surround the nanoparticles lowering the positive charge. The zeta potential is lower in chitosan:OVA systems, with chitosan

nanoparticles (no OVA) having a zeta potential of +13.1. This is again expected as OVA has a slightly negative charge, decreasing chitosan's positive surface charge. In table 3.2 the most stable sample is chitosan nanoparticles in dH_2O with a surface charge of +41.9 mv. The least stable sample is chitosan:OVA nanoparticles in HBSS with a surface charge of +9.68 mv. However OVA and HBSS needed to be within the nanoparticle complex, as the antigen used and the cell solution used for *in vitro* studies.

Sample (0.5 mg/ml)	**Zeta potential (mv)**
Chitosan:OVA nanoparticles in HBSS	+9.68 mv
Chitosan nanoparticles in HBSS	+13.1 mv
Chitosan:OVA nanoparticles in dH_2O	+37.9mv
Chitosan nanoparticles in dH_2O	+41.9mv

Table 3.2 Zeta potential comparison of chitosan:OVA nanoparticles against chitosan nanoparticles in HBSS and dH_2O.

3.3.1.3 Characterisation of OVA release from chitosan:OVA nanoparticles

The release of OVA from chitosan:OVA nanoparticles was tested by the addition of a highly negatively charged molecule, heparin. It was envisaged that with heparin having a significantly higher negative charge than OVA, it would interact electrostatically with the positively charged chitosan and 'release' OVA from the nanoparticles. Figure 3.9 shows data related to OVA release from formulated chitosan:OVA nanoparticles. The stoichiometry of dye:protein used within this study is 3:1. The fluorescence of 1:1 mass ratio of chitosan:FITC-OVA nanoparticles (1 mg/ml each) was measured before and after OVA release, which was triggered by exposure to heparin and membrane ultrafiltration. Control chitosan:OVA NP and chitosan:OVA NP bars indicate the sample before vivaspin-mediated filtration, without exposure to heparin. There is not a significant decrease between the two bars. The average fluorescence intensity for control chitosan:OVA nanoparticles alone is 6904 and the average for chitosan:OVA nanoparticles before exposure to heparin is 7175. The filtrate and chitosan:OVA NP + heparin filtrate bars represent the samples after membrane ultrafiltration. The fluorescence intensity of the filtrate bar of chitosan:OVA nanoparticles without heparin treatment is dramatically lower – 499 – compared to 6904 before filtration. This suggests that 499 of OVA is lost following filtration of chitosan:OVA nanoparticles, most likely excess unincorporated OVA, but the majority remains incorporated in chitosan:OVA nanoparticles, which are not able to pass through membrane pores of vivaspin. With chitosan:OVA nanoparticles

exposed to heparin and then filtered through vivaspin membranes, the fluorescence intensity decreases following filtration, but this decrease, from 7175 to 6232.16 is not as notable as with control samples not exposed to heparin. The high fluorescence intensity of the filtrate of the sample treated with heparin suggest successful release of OVA from chitosan:OVA nanoparticles, which is then able to cross vivaspin membrane pores in the ultrafiltration process. If this study expressed FITC-OVA:chitosan complexation efficiency from fluorescence/membrane ultrafiltration study (Figure 3.9), then a high efficiency of 93 % is obtained (fluorescence after filtration/fluorescence before filtration assuming a linear fluorescence versus concentration). The concentration of OVA in figure 3.10 for control chitosan:OVA NP is 0.85, after centrfugation and filtration it is -0.29. This has a decrease of -0.56 in concentration. When heparin is added there is an increase in OVA concentration. Chitosan:OVA NP was 0.90 the concentration after was 0.73. There was a relatively small decrease of 0.17.

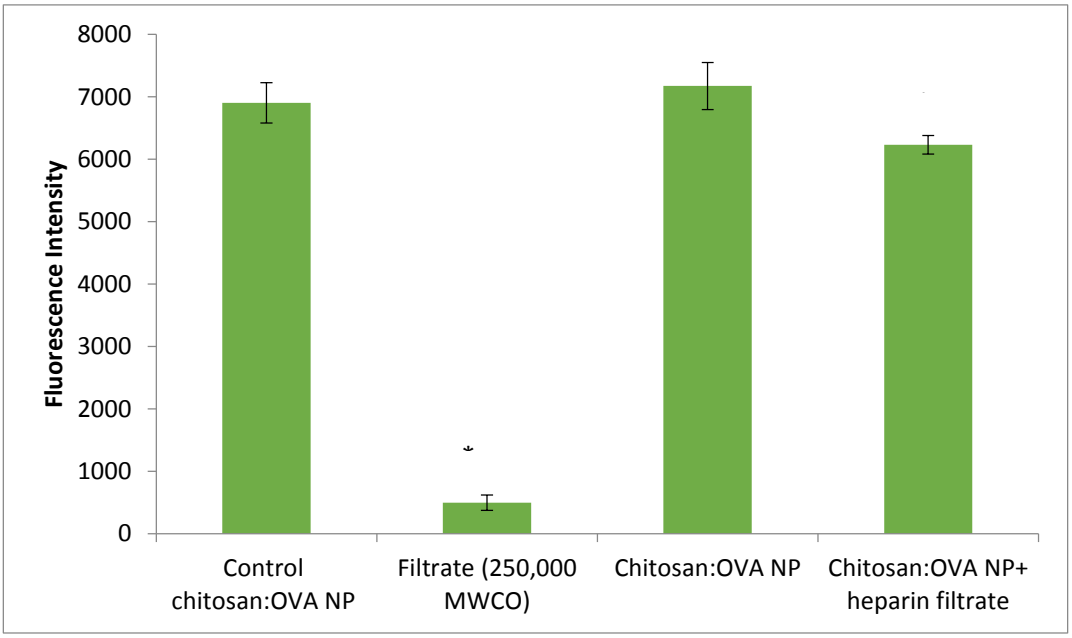

Figure 3.9 Release of OVA from chitosan:OVA nanoparticles, tested following exposure to heparin and membrane ultrafiltration (using vivaspin tubes). The statistical test ANOVA was used in this figure *** signifies P=0.0002; * signifies P= 0.0356.

3.3.1.4 Stability of OVA to acid and enzymatic exposure analysed by SDS PAGE

OVA has a molecular weight of 45kDa. Figure 3.10 shows that samples (with the exception of S2 and S5) have a band between 55kDa and 40kDa on the SDS gel.Therefore these bands belong to OVA. Sample 1 - chitosan:OVA nanoparticles exposed to heparin,

shows a 45 KDa band of medium size. Sample 2 - chitosan:OVA nanoparticles exposed to HCl and heparin shows no band due to degradation by HCl. Sample 3 - chitosan:OVA nanoparticles exposed to trypsin (concentration x10) and heparin shows a thin 45KDa band, this demonstrates some degration by trypsin although not as much as samples 2 and 5. Bands below the main 45KDa band are visible, although faint showing further breakdown of OVA. Sample 4 - OVA alone (positive control) is the thickest band on the gel (45KDa). Sample 5 - OVA exposed to HCl shows there is no band. The HCl breaks down the OVA leaving no protein visible. Sample 6 - OVA exposed to trypsin (concentration x10), shows a moderately sized 45KDa band. Smaller bands below the main band are visible showing the continuous breakdown of OVA. The bands are more pronounced (more visible) in comparison to sample 3.

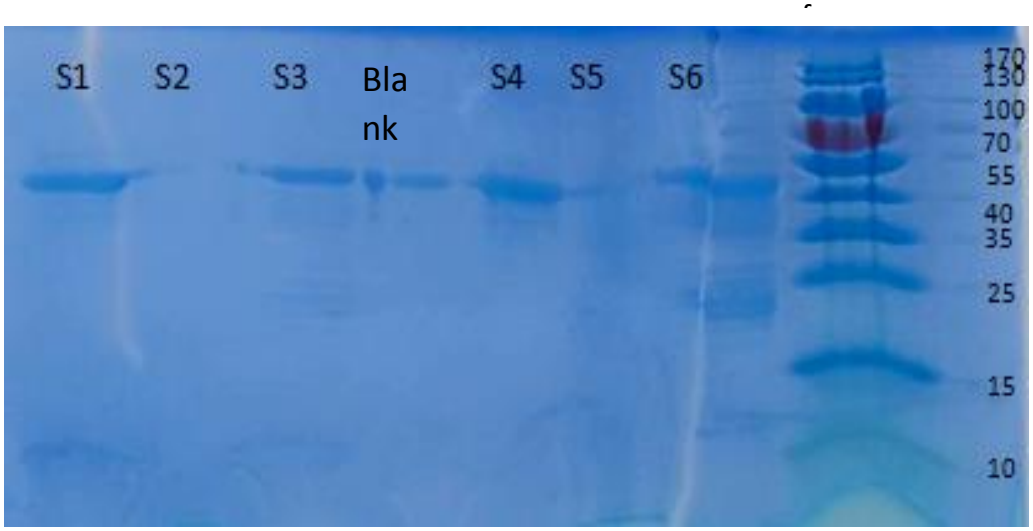

Figure 3.10 SDS Gel showing the stability of OVA when exposed to hydrochloric acid or trypsin in solution or in chitosan:OVA nanoparticles. S1 - chitosan:OVA nanoparticles exposed to heparin, S2 - chitosan:OVA nanoparticles exposed to HCl and heparin, S3 - chitosan:OVA nanoparticles exposed to trypsin (concentration x10) and heparin, S4 - OVA alone (positive control), S5 - OVA exposed to HCl and S6 - OVA exposed to trypsin (concentration x10).

3.4 Discussion

This chapter describes the formulation and characterisation of chitosan:OVA nanoparticles. Since OVA was used in this research as a model antigen, it was important to characterise the formulation, including the size of the nanosystem produced, surface charge, the ability of OVA to be released from the system and the ability of nanoparticles to protect OVA from acid and enzymatic degradation. The latter is crucial if oral delivery of vaccines is to become a viable approach.

Nanoparticle size is a very important factor, it determines cell uptake (Schrøder *et al*. 2014). Nanoparticles of several chitosan to ovalbumin ratios were formulated producing different systems, which were tested to determine optimal nanoparticle formulation via nanoparticle tracking analysis. We considered an optimal system to be one which produces nanoparticles in the size range 100-300 nm and low polydispersity.

It was found the chitosan:OVA ratio is an important determinant of nanoparticle size. Even though the ratio of chitosan:TPP is also critical in terms of size control, we found it was the chitosan:OVA ratio which exerted a larger control on size. A decrease in chitosan left OVA and TPP in excess instead of binding to chitosans positive amine groups which decreased the formation of the compact, stable nanoparticle complexes. This caused aggregation of OVA causing an increase in polydispersity. Therefore these parameters were focused on. We noted the TPP requirement in the system was minimal in order to produce nanoparticles. This is in agreement with previous research, which found that low TPP content can lead to production of smaller nanoparticles (Schrøder *et al*. 2014). The more TPP that was added to the solution, the more cloudy the solution became due to the nanoparticles aggregating. TPP can bind up to five particles of chitosan creating larger particles and aggregates within the solution (Antoniuo *et al*. 2015).

The chitosan:OVA nanoparticles formulated in this work had a relatively low polydispersity. It has been reported that the higher the molecular weight of the chitosan the higher the increase in polydispersity, explained by the higher molecular weight chitosan agglomerating more quickly than the lower molecular weight chitosan and thus increasing the polydispersity within the solution (Antoniuo *et al*. 2015).

The 1:1 mass ratio of chitosan:OVA nanoparticles produced a size of 196.5 nm in diameter. As this ratio decreased, the size of the nanoparticles, as well as polydispersity, increased. The size of nanoparticles produced in this study is similar to a study reporting systems of 210 nm (Nallamuthu *et al.* 2015). In dH_2O different nanoparticle ratios had a larger polydispersity than in HBSS. A 1:1 ratio of chitosan:OVA nanoparticles were tested for size in HBSS and producing monodispersity. This is because there are negatively charged counter ions within the solution making the nanoparticles much more compact and therefore more monodisperse.

The measurement of the zeta potential is also important with nanosystems, especially considering a link between the nature of the surface charge, toxicity and biological effects of the systems. Surface charge also is a good predictor of the colloidal stability of the system, meaning there is no aggregation at a significant rate from the nanoparticles. Chitosan has a positive charge of around + 35 to + 40 mv (Gan *et al*. 2005) for a high molecular weight chitosan, which is why it is bioadhesive and mucoadhesive to epithelial and mucosal cells. The surface charge of the chitosan:OVA nanoparticles prepared in this work is lower compared to values typically reported for two reasons. One being that OVA lowers the surface charge of the nanoparticles as itself has a slight natural negative charge. Ovalbumin holds a positive charge from pH 1.0-4.5 however as the pH increases the zeta potential decreases. From a pH 6.0-6.7 OVA has a charge of -20 to -25 mv (Niu *et al*. 2014). The biological medium, HBSS, also lowers surface charge, this being due to the negatively charged counter ions within it. As demonstrated from table 3.2 the chitosan:OVA nanoparticles in HBSS have a surface charge of + 9.68 mv, and chitosan:OVA nanoparticles in dH_2O have a surface charge of + 37.9 mv. This is comparable to other studies: chitosan:OVA nanoparticles ranged between +18- +25 mv (SchrØder *et al.* 2014). Alprazolam-loaded chitosan-egg albumin nanoparticles had a zeta potential of + 7.88 mv (Jana *et al*. 2013). This is comparable to this data and again shows a protein such as OVA decreases the zeta potential of chitosan nanoparticles. Overall this has an impact upon the colloidal stability of the nanoparticles, decreasing it.

Heparin was used to 'release' OVA from the chitosan:OVA nanoparticle complex in figure 3.9. This was shown, membrane ultrafiltration prevented FITC-OVA within chitosan:FITC-OVA nanoparticles from passing through filter pores, while, following

incubation with heparin, this was no longer the case (filtrate showed high fluorescence intensity). It was important to test the ability of chitosan to release the payload as to achieve a therapeutic effect. The incorporated cargo has to be released in the ileum on the M cells to induce the desired immune response.

A study where FITC-OVA was used in the preparation of nanoparticles, went through similar methodology as ours (Amidi *et al*. 2006). Nanoparticles were centrifuged at 18,000g for 20 minutes and the fluorescence of the supernatant was read before and after centrifugation, to measure how much uncomplexed OVA is present in the system. Their results showed a high nanoparticle loading capacity, as suggested by a low free OVA value in the supernatant and this was attributed to the negative charge of OVA bonding to the positive charge of the chitosan nanoparticles. The study also found the highest loading capacity and loading efficiency concentration was 0.5 mg/ml, a loading capacity of 55 % and a loading efficiency of 45 % (used in this work) was found at a concentration of 1 mg/ml (Amidi *et al*. 2006).

The stability of OVA within chitosan:OVA nanoparticles was also tested using SDS gels to analyse whether the stability of OVA is compromised when 1) complexed into chitosan:OVA nanoparticles, and 2) when chitosan:OVA nanoparticles are exposed to harsh chemical conditions such as those of the gastrointestinal tract. Figure 3.10 sample 1 shows chitosan:OVA nanoparticles where OVA was released with heparin treatment, demonstrates a clear band attributed to OVA. This suggests that the complexation of OVA to chitosan and subsequent release does not compromise OVA stability, which is a key requirement of the delivery system. Samples 2 and 5, treated with HCl however showed no bands on the gel, pointing to complete breakdown of OVA. The data therefore implies that chitosan:OVA nanoparticles at 1:1 mass ratio are not capable of protecting OVA upon HCl exposure. in sample 3, the presence of a clear band, which seems more prominent than that of free OVA, with chitosan:OVA nanoparticles exposed to trypsin suggests that OVA within nanoparticles demonstrates somewhat higher stability towards trypsin digestion, although the data is not quantitative. In a similar study SDS PAGE was used to measure protein integrity of OVA, which was destabilised by NaCl and the nanoparticles were placed in a 7.5 % polyacrylamide gel (Amidi *et al*. 2006). The results found that the integrity of OVA was not compromised when bound to the chitosan nanoparticles, which is in agreement with our data. There was no evidence

of previously published studies that tested the stability of chitosan:OVA nanoparticles to HCl and trypsin, therefore a comparison with literature in this respect cannot be made.

The stability of OVA is very important within the nanoparticle complex as the antigen needs to be released from the system in an intact form in order to exert the desired immune-inducing effect *in vivo*. For oral vaccine delivery, ability of the system to provide protection from the acidic environment of the GI tract is crucial. However, this could be achieved by modulating the formulation, e.g. through encapsulation of nanoparticles within an enteric-coated delivery system. This particular system works by coating the nanoparticles with the chosen enteric coating (e.g. sodium alginate), protecting the nanoparticle in the stomach and dissolving at an alkaline pH, e.g. the small intestine (Biswas *et al*. 2015).

3.5 Conclusion

Overall the data within this chapter demonstrated that chitosan:OVA nanoparticles formulated via the ionic gelation method at 1:1 mass ratio displayed optimal characteristics, including a diameter below 200 nm and a positive zeta potential, which was reduced compared to chitosan nanoparticles, in the biological solution, HBSS. This ratio was taken forward for cell and animal studies. Chitosan was demonstrated to complex with OVA at high efficiency into chitosan:OVA nanoparticles, which were subsequently able to release the OVA payload on exposure to the highly negatively charged heparin. This was clearly demonstrated by membrane ultrafiltration/fluorescence measurement studies. Complexation of OVA into chitosan nanoparticles did not compromise OVA stability (shows by SDS page). While there is some evidence of a degree of OVA protection to trypsin offered by chitosan nanoparticles, this protection is not obvious with exposure to HCl.

3.6 References

1. Abdulkarim, M., Agulló, N., Cattoz, B., Griffith, P., Bernkop-Schnürch, A., Gómez Borros, S. and Gumbleton, M. (2014). *Nanoparticle Diffusion within Intestinal Mucus: Three Dimensional Response Analysis Dissecting the Impact of Particle Surface Charge, Size and Heterogeneity across Polyelectrolyte, Pegylated and Viral Particles*, European Journal of Pharmaceutics and Biopharmaceutics.
2. Amidi, M., Romeijn, S., G., Borchard, G., Junginger, H., E., Hennink, W., E. and Jiskoot, W. (2006). *Preparation and Characterisation of Protein- Loaded N- Trimethyl Chitosan Nanoparticles as Nasal Delivery System*, Journal of Controlled Release, 111(1-2): 107-116.
3. Antoniuo, J., Liu, F., Majeed, H., Qi, J., Yokoyama, W. and Zhong, F. (2015). *Physicochemical and Morphological Properties of Size- Controlled Chitosan-Tripolyphosphate Nano- particles*, Colloids and Surfaces A: Physicochemical and Engineering Aspects, 465: 137-146.
4. Gan, Q., Wang, T., Cochrane, C. and McCarron, P. (2005). *Modulation of Surface Charge, Particle Size, and Morphological Properties of Chitosan- TPP Nanoparticles Intended for Gene Delivery*, Colloids and Surfaces B: Biointerfaces, 44 (2-3): 65- 73.
5. Hassani, S., Laouini, A., Fessi, H. and Charcosset, C. (2014). *Preparation of Chitosan-TPP Nanoparticles Using Microengineered Membranes- Effect on Parameters and Encapsulation of Tacrine*, Colloids and Surfaces A: Physicochemical and Engineering Aspects, 482: 34-43.
6. Jain, A., Thakur, K., Kush, P. and Jain, U., K. (2014). *Docetaxel Loaded Chitosan Nanoparticles: Formulation, Characterisation and Cytotoxicity Studies*, International Journal of Macromolecules, 69: 546- 553.
7. Jana, S., Maji, N., Nayak, A., K., Sen, K., K. and Basu, S., K. (2013). *Development of Chitosan Based Nanoparticles Through Inter-polymeric Complexation for Oral Drug Delivery*, Carbohydrate Polymers, 98(1): 870-876.
8. Kheradmud, E., Anvaripour, B., Motavassel, M. and Jadidi, N. (2015). *Optimising the Essential Parameters in Production of Chitosan Nanoparticles by Calvo Method*, Science International, 27(3): 2139-2142.
9. Madureira, A., R., Pereira, A. and Pintado, M. (2015). *Current State on the Development of Nanoparticles for use Against Bacterial Gastrointestinal Pathogens.*

Focus on Chitosan Nanoparticles Loaded with Phenolic Compounds, Carbohydrate Polymers, 130: 129-139.

10. Nallamuthu, I., Devi, A. and Khanum, F. (2015). *Chlorogenic Acid Loaded Chitosan Nanoparticles with Sustained Release Property, Retained Antioxidant Activity and Enhanced Bioavailability*, Asian Journal of Pharmaceutical Sciences, 10: 203-211.
11. Niu, F., Su, Y., Liu, y., Wang, G., Zhang, Y. and Yang, Y. (2014). *Ovalbumin- Gum Arabic Interactions: Effect of pH, Temperature, Salt, Biopolymers Ratio and Total Concentration*, Colloids and Surfaces B: Biointerfaces, 113: 407- 482.
12. Raftery, R., M., Tierney, E., G., Curtin, C., M., Cryan, S., A. and O' Brien, F., J. (2015). *Development of a Gene- Activated Scaffold Platform for Tissue Engineering Applications using Chitosan- pDNA Nanoparticles on Collagen- Based Scaffolds*, Journal of Controlled Release, 210: 84-94.
13. SchrØder, T., D., Long, Y. and Olsen, L., F. (2014). *Experimental and Model Study of the Formation of Chitosan- Tripolyphosphate- siRNA Nanoparticles*, Colloid and Polymer Science, 292(11): 2869- 2880.
14. Slütter, B. and Jiskoot, W. (2010). *Dual Role of CpG as Immune Modulator and Physical Crosslinker in Ovalbumin Loaded N-Trimethyl Chitosan (TMC) Nanoparticles for Nasal Vaccination,* Journal of Controlled Release, 148(1): 117-121.
15. Vllasaliu, D., Exposito- Harris, R., Heras, A., Casatteri, L., Garnett, M., Illum, L. and Stolnik, S. (2010). *Tight Junction Modulation by Chitosan Nanoparticles: Comparison with Chitosan Solution*, International Journal of Pharmaceutics, 400: 183-193.
16. Wu, S., J., Don, T., M., Lin, C., W. and Mi., F., L. (2014). *Delivery of Berberine Using Chitosan/ Fucoidan- Taurine Conjugate Nanoparticles for Treatment of Defective Intestinal Epithelial Tight Junction Barrier*, Marine Drugs, 12(11): 5677- 5697.
17. Zhang, L., Wang, J., Ni, C., Zhang, Y. and Shi, G. (2015). *Preparation of Polyelectrolyte Complex Nanoparticles of Chitosan and Poly(2- Acry1amido-2-methylpropanesulfonic acid) for Doxorubicin Release*, Materials Science and Engineering: C, 58: 724-729.

Chapter 4

Study of Chitosan:OVA Nanoparticles in the Caco-2 *In Vitro* Intestinal Model

4.1 Introduction

Following the formulation and characterisation of chitosan:OVA nanoparticles in the previous chapter, this work investigates their effects on an intestinal cell model. Caco-2 cells were used as a model for the intestinal barrier owing to their track record of being the most commonly used intestinal cell-based model. Despite their common use, there are several limitations associated with the Caco-2 model and these must be kept in mind. The model is homogenous and does not represent cell types other than epithelial cells, which also include Microfold cells (M cells) and mucus producing goblet cells. These are both important from the point of view of oral drug delivery as mucus presents a barrier especially to particulates. M cells are crucial in vaccine delivery owing to their role in antigen presenting and stimulation of mucosal immunity. Caco-2 cells typically take 21 days to differentiate, form tight junctions and require culture on specialist microporous tissue culture plates (transwell system was used in this work).

This chapter outlines studies into the interaction of chitosan:OVA nanoparticles with Caco-2 epithelial cells. Initially, nanoparticle toxicity was tested using the MTS and LDH assays in order to test and make sure a non-toxic concentration was selected for future *in vitro* and *in vivo* studies. Thereafter, effect of nanoparticles on epithelial tight junctions was assessed by TEER measurements. The ability of nanoparticles to promote epithelial absorption of a model antigen (fluorescently labelled, FITC-OVA) was finally determined in permeability studys.

4.2 Methods

4.2.1. MTS cell metabolic activity assay

The MTS assay or 3-(4,5-dimethylthiazol-2-yl)-5(3-carboxymethonyphenol)-2-(4-sulfophenyl)-2H-tetrazolium reagent is reduced to a red coloured formazan product by the intermediate electron acceptor phenazine ethyl sulphate transferring an electron from NADH in the cytoplasm to MTS in the cell media. Caco-2 epithelial cells were seeded onto a 96 well, clear plate (cell culture treated) and were left to incubate for 24 hours. This was for the cells to establish attachment on the bottom of the plate and proliferate. Nanoparticles were prepared using the described method in section 3.2.1.1. 1 ml of the nanoparticle suspension was diluted with 9 ml of HBSS creating a nanoparticle suspension of 0.1 mg/ml (1:1 mass ratio). Other concentrations were also prepared (0.05 mg/ml, 0.025 mg/ml and 0.0125 mg/ml, all at 1:1 mass ratio). In addition to the nanoparticles, chitosan solution (in HBSS:MES, pH 6.0) and HBSS:MES (pH 6.0) were used to compare toxicity against the chitosan:OVA nanoparticles.

For toxicity studies, a 10% v/v solution of triton X-100 (a surfactant known to lyse cells) in HBSS was prepared as a positive control and finally HBSS alone was used as a negative control. For toxicity studies, each concentration was applied in 6 repeats. 100 µl of each sample was applied to the cells into the wells, the plate placed into the incubator at 37°C/5% CO_2 for 3-hour incubation. After 3 hours, samples were removed and 100 µl of cell medium applied. Thereafter 20 µl of MTS reagent was applied to all the wells and the 96 well plate placed in an incubator at 37 °C/ 5% CO_2 for 2 hours. Absorbance at 490 nm was measured using a Tecan Infinite m200 Pro plate reader.

4.2.2. Lactate Dehydrogenase Assay

The enzyme lactate dehydrogenase is present in all cells. It is released from the cytoplasm when the membrane integrity is compromised. LDH interconverts lacate and pyruvate. Caco-2 cells were seeded onto a clear, flat-bottomed 96 well plate 48 hours before the assay. Cell media was aspirated from the wells and samples differing in concentrations (0.1, 0.05, 0.025 and 0.0125 mg/ml) and dissolved in HBSS were then applied to each well. 100 µl of each concentration of the sample was applied to 6 wells for repeats. A 10% v/v solution of triton X-100 and HBSS was prepared as a positive control (1 ml of triton X-100 in 9 ml of HBSS) and finally HBSS alone was also used as a

negative control. Chitosan:OVA nanoparticles were prepared using the method previously described in section 3.2.1.1. The cell media was aspirated out and replaced with 100 µl of the required samples and controls (n=6). Cells were incubated with samples at 37°C/5% CO_2 for 3 hours. The LDH assay reagents were prepared according to manufacturer's instructions whilst the cells were incubating. Following 3 hours incubation of cells with the samples, 50 µl of each sample and the controls were transferred to another clear flat bottomed 96 well plate. 50 µl of the reaction mixture prepared earlier was added to each sample and control and mixed. The plate was then left at room temperature for 30 minutes and covered with foil. 50 µl of stop solution was added to each well, mixing by gentle tapping. The absorbance of lactate dehydrogenase was measured at 490 nm using Tecan Infinite m200 Pro plate reader.

4.2.3. TEER study

HBSS was warmed in a water bath at 37 °C and applied to Caco-2 monolayers for 40-45 mins for the cells to adjust to the change in environment before sample application. The TEER was measured (method described in section 2.2.2.) in HBSS (1.5 ml in the basolateral side and 0.5 ml in the apical chamber). Chitosan:OVA nanoparticles were prepared using the method described in section 3.2.1.1 at concentrations of 0.1 mg/ml, 0.05 mg/ml and 0.025 mg/ml, (1:1 chitosan/OVA mass ratio). HBSS was used as a negative control. When the nanoparticles were ready, the HBSS was removed from the apical chamber and replaced with the required samples. 3 wells (n=3) were used for each sample for triplet repeats for validity and reliability. The TEER was measured (see section 2.2.2.) at time 0 and then every 30 minutes for 3 hours (30, 60, 90, 120, 150, 180 min). A mean was taken of the samples over the given time period.

This study was repeated with a 0.1 mg/ml concentration of chitosan:OVA nanoparticles, a solution of chitosan and ovalbumin (i.e. no TPP) at 0.1 mg/ml concentration, a 0.1 mg/ml concentration of chitosan solution in HBSS and lastly a 0.1 mg/ml concentration of OVA solution in HBSS. These were used as controls or for comparison of any TEER effects resulting from chitosan/OVA.

4.2.4. Permeability study

Caco-2 cell monolayers were cultured for 21 days. Cell monolayers with a TEER of at least 900 Ωcm^2 were deemed suitable for cell permeability studies. TEER measurements were taken before permeability studies as a reassurance of the integrity of the cells. HBSS was warmed in a water bath to 37 °C. The cell media was aspirated out and replaced with HBSS; the transwell was then placed in an incubator at 37°C/5% CO_2 for 40-45 minutes. The chitosan:OVA nanoparticles and chitosan nanoparticles were prepared using the methods described in section 3.2.1.1 and 3.2.1.2. Fluorescein isothiocyanate-labelled ovalbumin (FITC-OVA) was used for these studies instead of the standard non-labelled ovalbumin in order to enable quantitation by fluorescence measurements. Measuring fluorescence is the best method to visualise permeability during confocal microscopy. Nanoparticles were prepared at 1 mg/ml solution (1:1 chitosan:FITC-OVA mass ratio) then diluted with HBSS to 0.1 mg/ml, 0.05 mg/ml, 0.025 mg/ml and 0.0125 mg/ml.

Permeability study was started by replacing HBSS with the samples at different concentrations (0.1 mg/ml, 0.05 mg/ml, 0.025 mg/ml and 0.0125 mg/ml). A 0 time sample was taken from the basolateral chamber (100 µl of sample was taken from the basolateral membrane chamber and placed in a 96-well black plate). A sample was then taken every 30 minutes for 3 hours, with replacement of the sampled basolateral solution with fresh HBSS. Samples were quantified by measuring the fluorescence with the Tecan plate reader using an excitation wavelength of 488 nm and emission wavelength of 520 nm.

4.3 Results

4.3.1 MTS Assay

Figure 4.1 shows chitosan:OVA nanoparticle toxicity against Caco-2 cells, as determined via the MTS assay. The data shows concentration 0.1 mg/ml chitosan:OVA nanoparticles resulted in a reduction of relative cell viability to approximately 62% (negative control, HBSS = 100% viability and positive control, triton X-100 = 0%). As chitosan:OVA nanoparticle concentrations decreased, the effect on relative cell viability diminished. Chitosan:OVA nanoparticle concentration 0.05 mg/ml w/v displayed a reduction of

relative cell viability to 85% and the 0.025 and 0.0125 mg/ml were associated with a small reduction of relative cell viability to 94-95%. Figure 4.1 shows a concentration dependant correlation. 0.1 mg/ml concentration showed the lowest cell viability at 62%, this is because although chitosan is not toxic to cells, OVA has a slight toxicity decreasing cell viability. 0.1 mg/ml is also the strongest concentration and it was expected to have the largest decrease. However it is still over the cell viability threshold (60%).

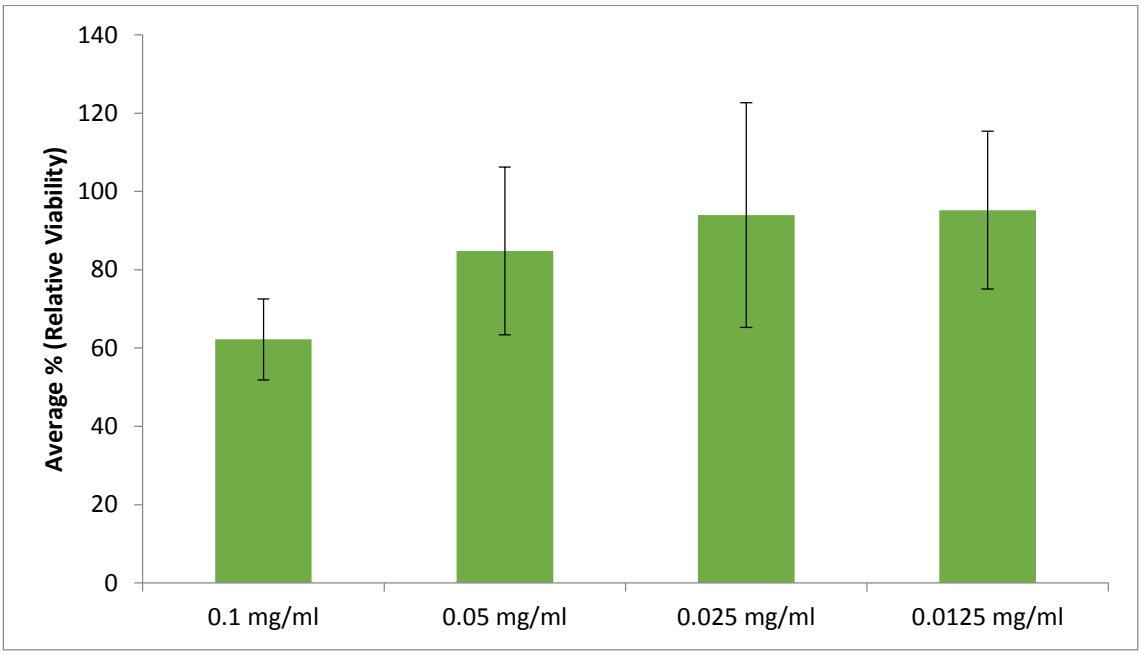

Figure 4.1 Effect of different concentrations of chitosan:OVA nanoparticles on Caco-2 relative viability, as determined by the MTS assay. Data shows the mean ± SD (n = 6).Cell viability relative to HBSS negative control. ANOVA performed, no statistical significance shown (P=0.413).

Figure 4.2 shows a study of chitosan solution (no TPP) effect on relative cell viability, tested by the MTS assay. OVA was added to this study as a control. In this study, all tested chitosan samples showed relative cell viability higher than 100%. OVA had a negligible effect on cell viability.

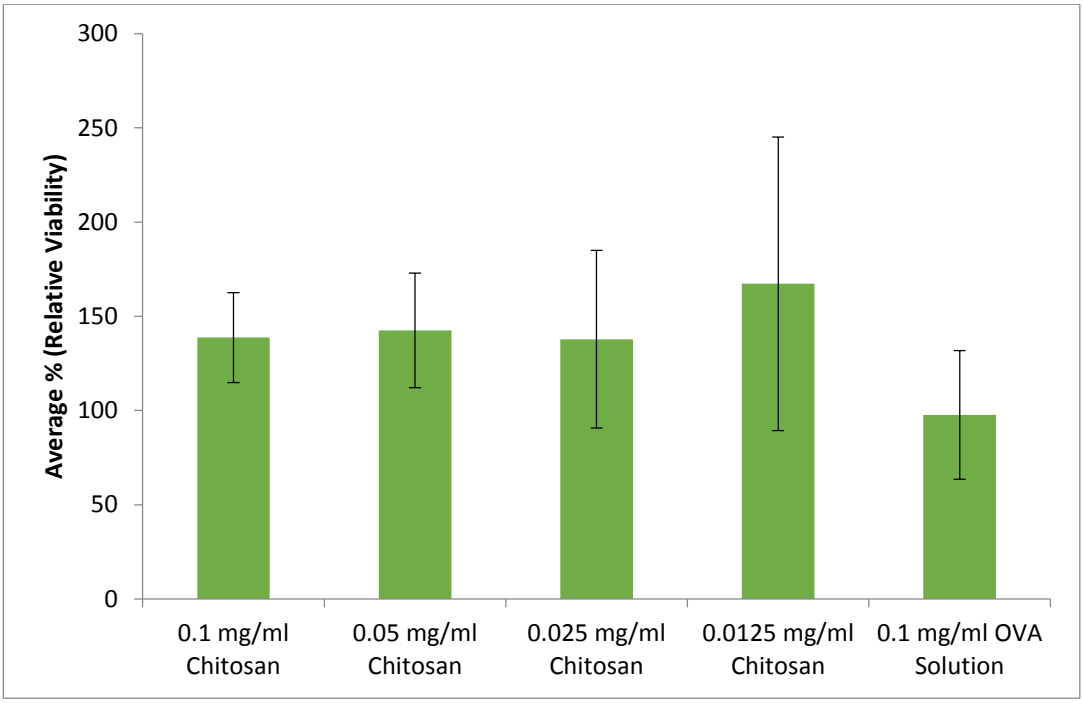

Figure 4.2 Effect of different chitosan solutions (no addition of TPP) and OVA (used as the control), on Caco-2 relative viability as determined by the MTS assay. Data shows the mean ± SD (n = 6). Cell viability relative to HBSS negative control. ANOVA performed, no statistical significance shown (P=0.179).

Figure 4.3 shows the comparison of chitosan:OVA nanoparticles against chitosan solution at 0.1 mg/ml. This data is in agreement with figure 4.2 in that chitosan:OVA nanoparticles did not decrease cell viability (in fact values are very similar). Figure 4.3 also shows that chitosan solution at 0.1 mg/ml is associated with an increase rather than decrease in Caco-2 cell viability. It is not known why an increase in cell viability was apparent in figure 4.2 and 4.3, but studies do vary (e.g. due to potential user error in dosage application, cell seeding density, incubation time, etc.). Although the standard deviation is particularly high for 0.1 mg/ml chitosan solution the results are still valid for a normal distribution of data.The MTS assay revealed that all of the tested samples were over the designated cell viability threshold (60%) for toxicity and could be taken forward in future experimentswithin this chapter.

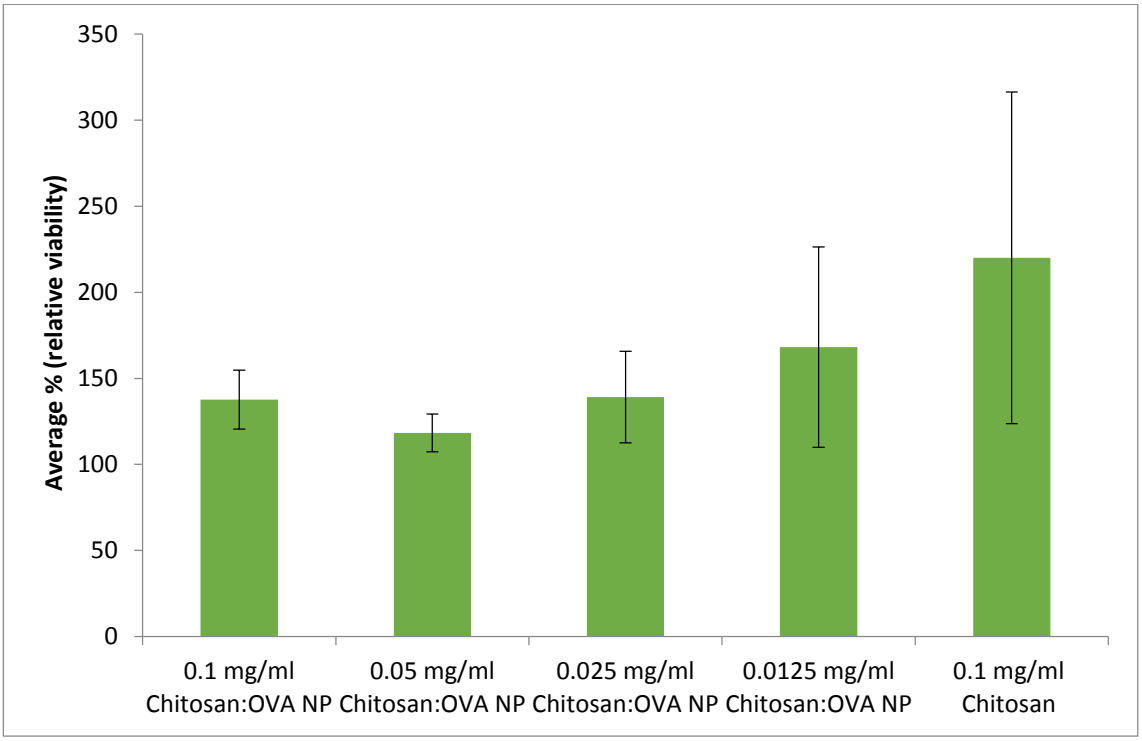

Figure 4.3 Comparison of different concentrations of chitosan:OVA nanoparticles against 0.1 mg/ml chitosan solution in terms of Caco-2 relative viability, as determined by the MTS assay. Data shows the mean ± SD (n = 6). Cell viability relative to HBSS negative control. ANOVA performed, no statistical significance shown (P=0.426).

4.3.2 Lactate Dehydrogenase Assay

Figure 4.4 shows the LDH assay, membrane toxicity study of chitosan:OVA nanoparticles. This assay measures the leakage of an intracellular enzyme, lactate dehydrogenase (LDH), which occurs when the cell membrane is damaged. LDH assay is therefore a measure of the integrity of the cell membranes, which is important to study for positively charged systems such as chitosan. The data below clearly shows that the chitosan:OVA samples are very close to the negative control, HBSS, and dramatically below the triton X-100 (positive control), indicating that minimal LDH was released from cells upon exposure to chitosan:OVA nanoparticles. The absorbance reading for triton X-100 was 1.029 and HBSS 0.139; chitosan:OVA nanoparticle samples ranged between 0.144 and 0.1612 which closely resembled values of the negative control, HBSS. Triton X-100 error bars are particularly large in comparison to the other samples. An improvement would be to normalise the cell number, SD would increase in accuracy and reliability. This would be an improvement for all *in vitro* cell studies used within this research.

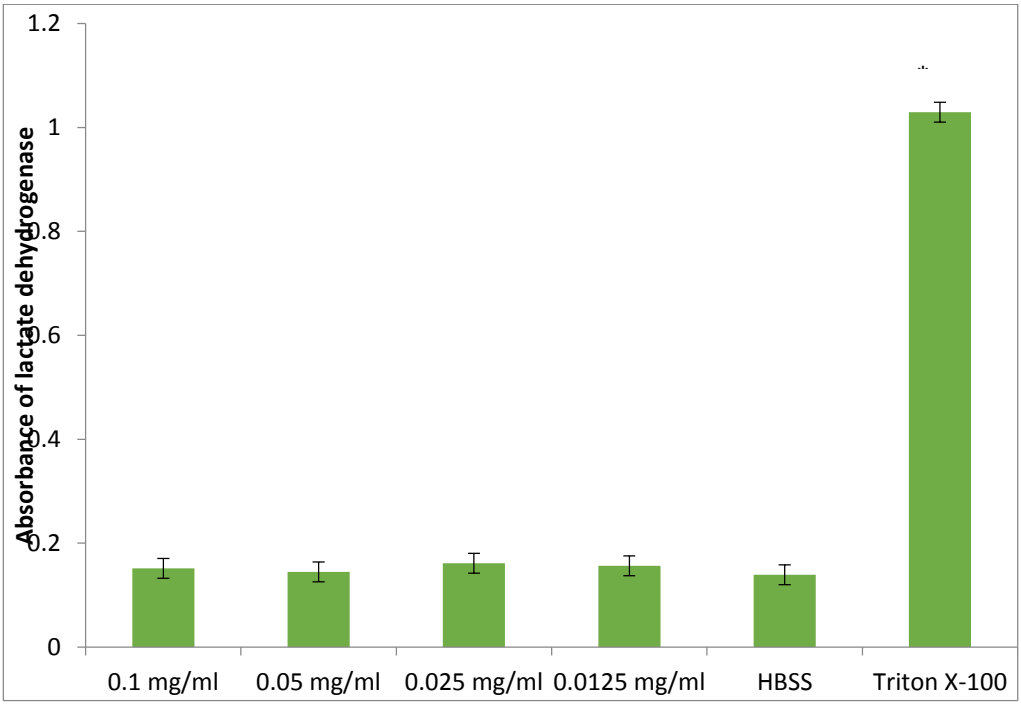

Figure 4.4 Effect of different concentrations of chitosan:OVA nanoparticles on LDH release. HBSS used as a negative control and triton X-100 as a positive control. **Data shows the mean ± SD (n = 6). ANOVA was performed, this graph is statistically significant (***=P=0.00).**

4.3.3 TEER studies

Figure 4.5 shows Caco-2 cell TEER measured from days 1-23 on transwell culture. The data shows a typical increase in TEER over time, which can be attributed to cell growth and tight junction formation. Towards the end of the culture and measurement period, the TEER plateaus. After approximately 21 days cells form a monolayer on the apical membrane. Caco-2 cells produce signals named contact inhibitions which tell the cells when there is no longer a need for an increase in resistance due to the formation of the monolayer.

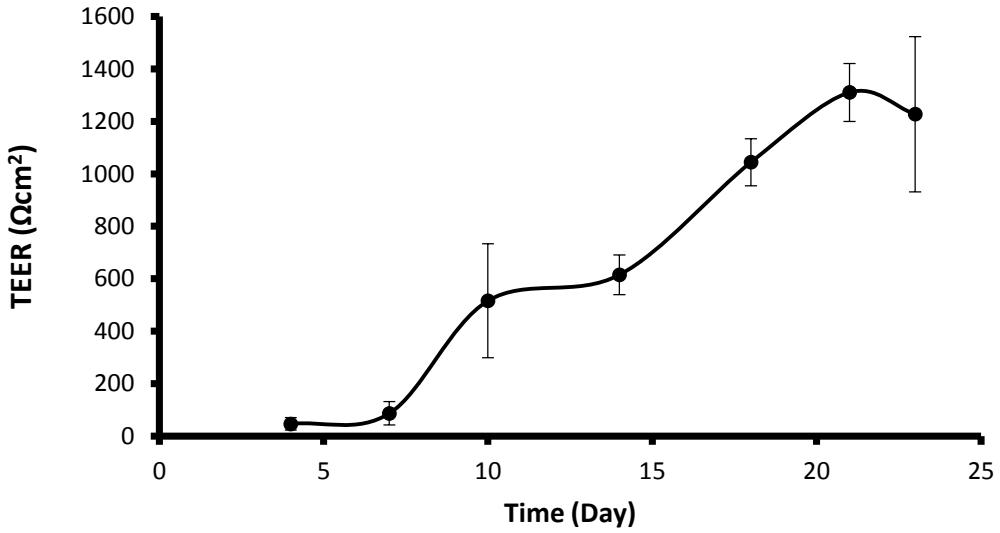

Figure 4.5 Caco-2 cell TEER measured over 23 days when cultured on transwell inserts. Data shows the mean ± SD (n = 12).

Figure 4.6 shows Caco-2 cell TEER with different concentrations of chitosan:OVA nanoparticles (0.1 mg/ml, 0.05 mg/ml, 0.025 mg/ml and 0.0125 mg/ml), as well as 0.1 mg/ml OVA solution as a comparison. OVA solution caused a decrease in TEER to 584.33 Ωcm^2 after 60 min and continued to decrease. After 48 hours OVA solution-treated cells were back to original TEER values. Chitosan:OVA nanoparticle samples caused a steeper (faster) reduction in TEER compared to OVA solution after 30 min, although, interestingly, the minimum TEER values with chitosan:OVA nanoparticle samples were higher than those with OVA solution. With all samples, TEER values returned to the baseline value after 48 hours.

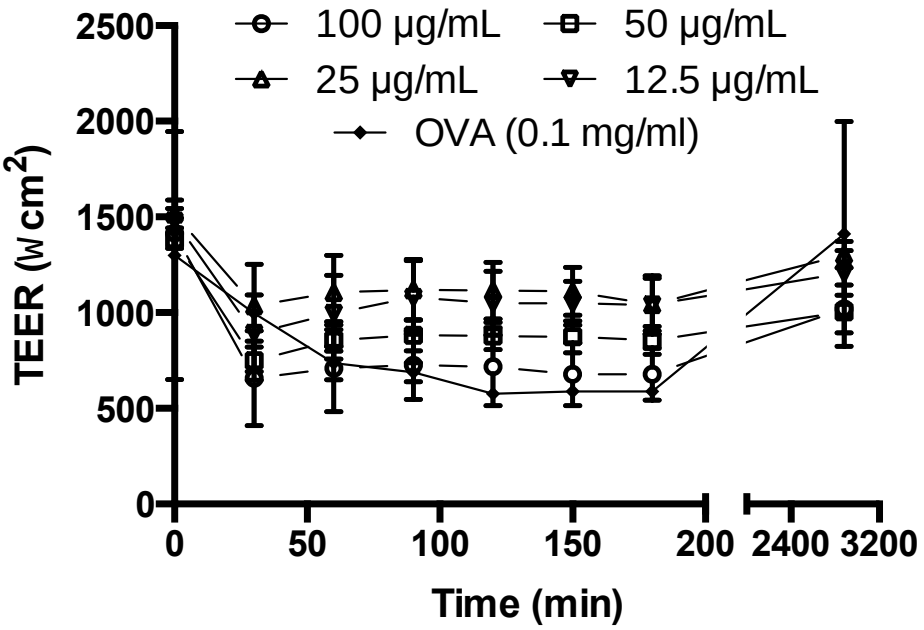

Figure 4.6 Effect of different concentrations of chitosan:OVA nanoparticles (0.1 mg/ml, 0.05 mg/ml, 0.025 mg/ml and 0.0125 mg/ml) and OVA solution at 0.1 mg/ml on Caco-2 monolayer TEER. Data shows the mean ± SD (n =3).

Figure 4.7 shows Caco-2 TEER values for different conditions. Chitosan:OVA nanoparticles were tested against chitosan solution, OVA solution and chitosan and OVA solution (no TPP). The values are lower than figure 4.6 although this could be due to a number of reasons for example each cell study will vary slightly as all cells vary after differentiation, the tight junctions may not have formed properly. At 24 hours the TEER values are higher compared with time 0 measurement. The TEER was between 400-600 Ωcm^2 to start, the cells could have continued differentiating and forming tight junctions increasing the cells TEER. If this was the case the samples will have had a lower effect on the cells.

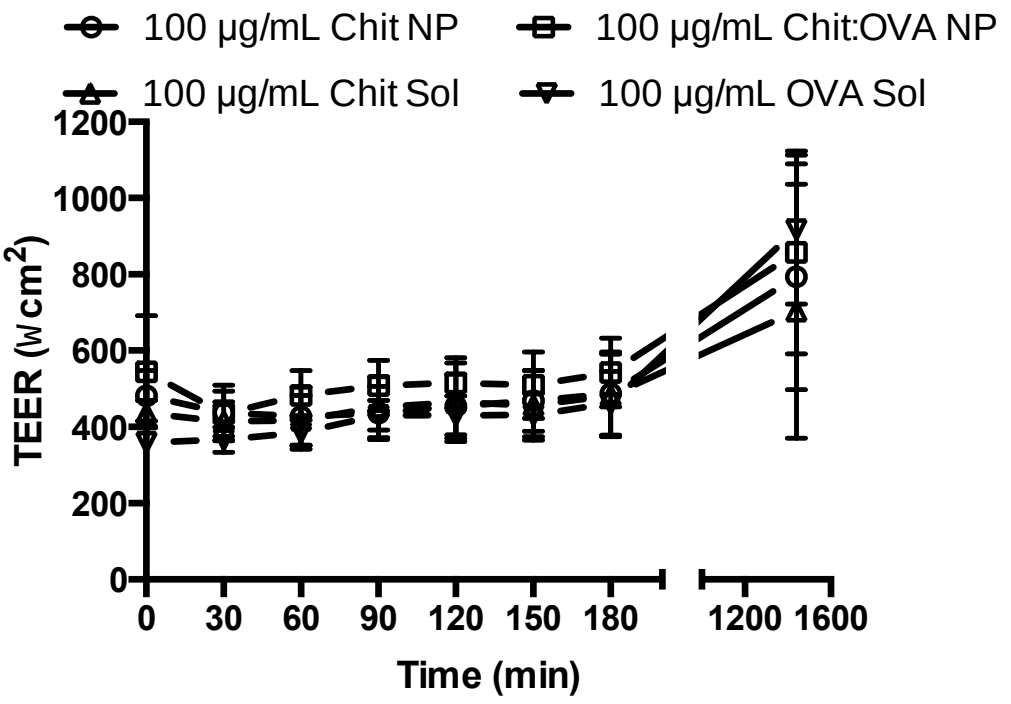

Figure 4.7 Comparison of the effect on TEER between chitosan:OVA nanoparticles, chitosan solution, OVA solution and chitosan and OVA solution (no TPP). Data shows the mean ± SD (n = 3).

4.3.4 Permeability studies

Permeability studies are calculated using the equation described earlier in chapter 2 section 2.2.6. Figure 4.8 shows apical-to-basolateral permeation of FITC-OVA, following application of chitosan:FITC-OVA nanoparticles to Caco-2 monolayers at different concentrations. Note that FITC-OVA was quantified in these studies through fluorescence measurement and it is not possible to state whether FITC-OVA crossed the cells complexed in chitosan nanoparticles or whether it was released en route. The concentration which showed the highest permeation was 0.1 mg/ml, i.e. the highest applied concentration of chitosan:OVA nanoparticles. This concentration had the lowest cell viability in figures 4.1 (62%) and 4.3 (137%). Apart from the lowest concentration, other samples displayed a concentration-dependent effect with permeability being proportional to applied chitosan:OVA nanoparticle concentration. There is no clear reason why concentration 0.0125 mg/ml increased however it could be due to background noise or seeding density errors.

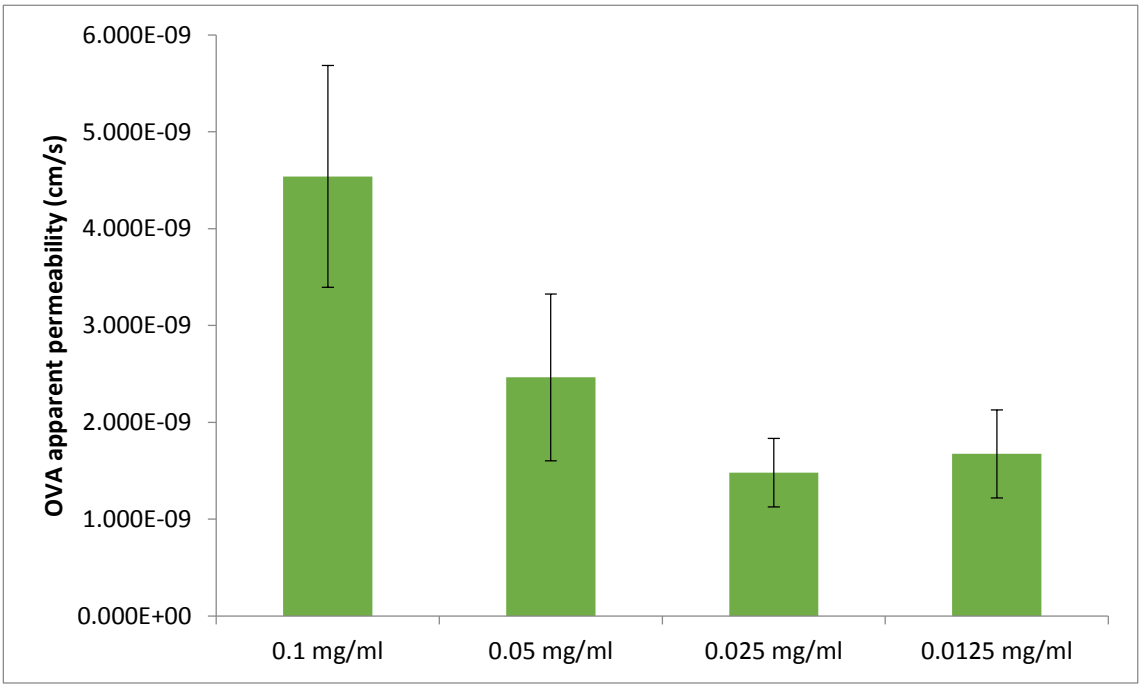

Figure 4.8 FITC-OVA permeability following application of chitosan:FITC-OVA nanoparticles at different concentrations. Data shows the mean ± SD (n = 3). ANOVA test was performed, no statistical significance shown (P=0.303).

Figure 4.9 shows another permeability experiment, comparing FITC-OVA permeability following the application of chitosan:OVA nanoparticles at a concentration of 0.1 mg/ml (1:1 mass ratio) and 0.1 mg/ml of FITC-OVA solution. The graph shows that FITC-OVA permeability across Caco-2 monolayers was significantly higher than OVA in solution with all chitosan:OVA nanoparticle concentrations.

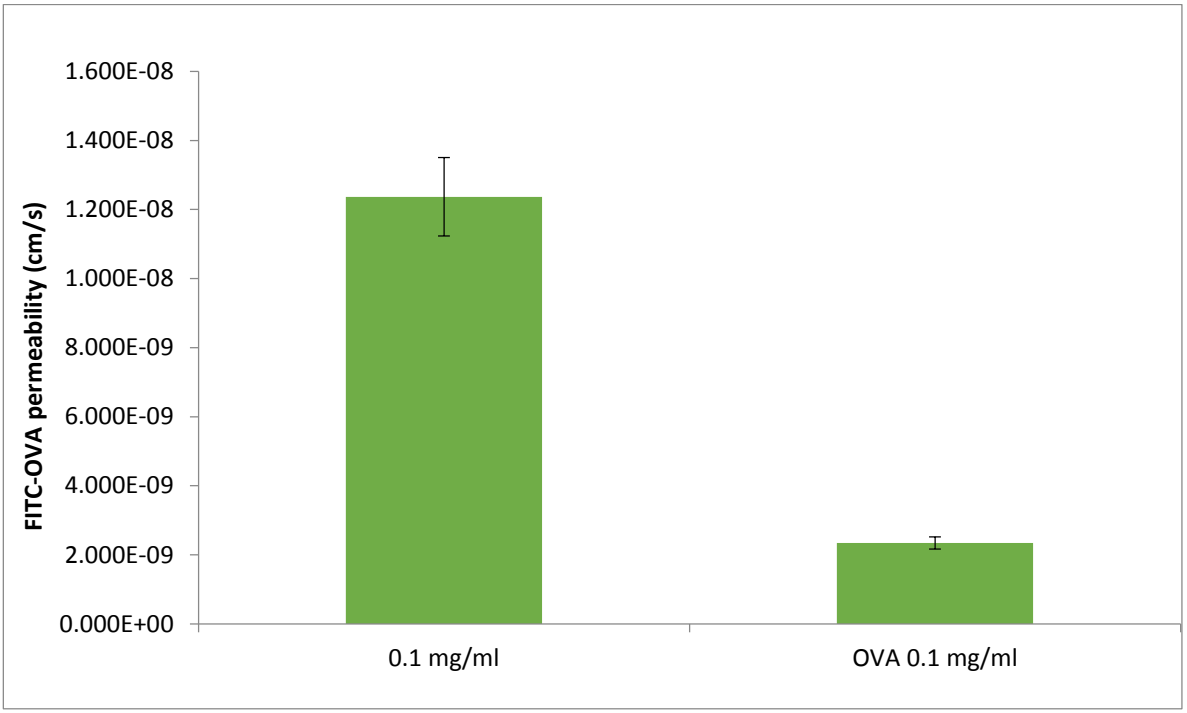

Figure 4.9 FITC-OVA permeability following application of chitosan:FITC-OVA nanoparticles at 0.1 mg/ml and comparison with OVA in solution, applied at 0.1 mg/ml. ** = P=0.0036.

4.3.5 Confocal imaging

Following the permeability study with chitosan:FITC-OVA nanoparticles at 0.1 mg/ml, cells were imaged using confocal microscopy in order to ascertain information on the cell uptake of the nanoparticles.

Figure 4.10 shows the presence of fluorescence due to FITC-OVA within the cells. However, with this information available, it is not clear on whether FITC-OVA remains complexed with chitosan in the cell interior or if it is released before entering the cells. Unfortunately there is no negative cntrol for comparison.

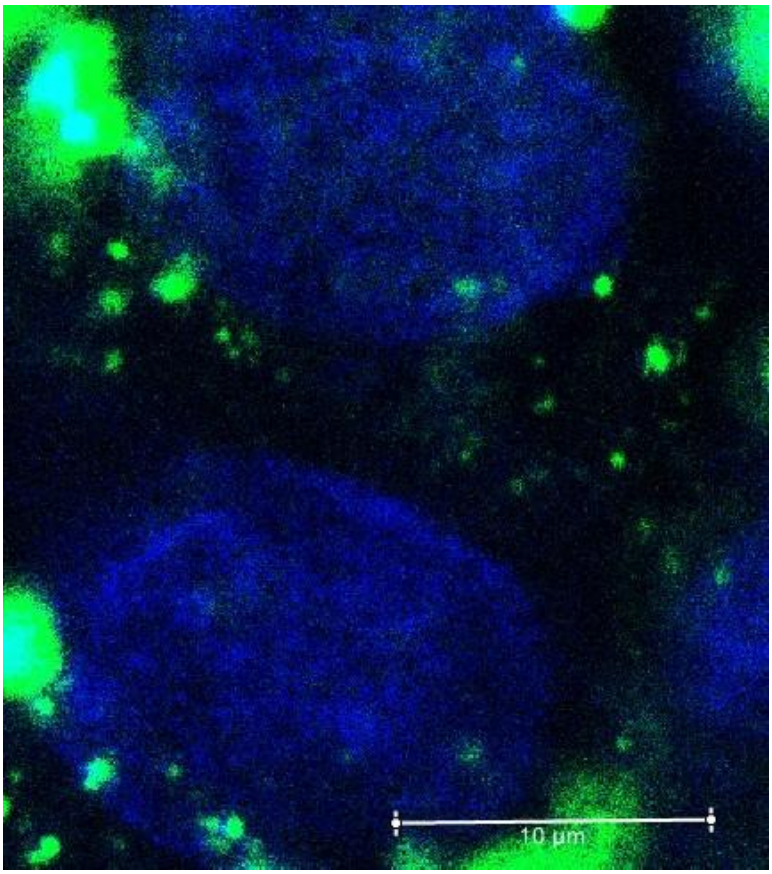

Figure 4.10 Magnified confocal imaging following the application of chitosan:FITC- OVA nanoparticles on Caco-2 cells, applied at 0.1 mg/ml There is no negative control.

Figure 4.11 shows the cell depth of a section of Caco-2 monolayers following application of 0.1 mg/ml chitosan:FITC-OVA nanoparticles. This micrograph demonstrates the presence of fluorescence, most likely attributed to chitosan:FITC-OVA nanoparticles, in cells. Figure 4.11 shows the uptake of chitosan:FITC-OVA nanoparticles in Caco-2 epithelial cells. The figure shows the chitosan:FITC-OVA nanoparticles passing through the cells, concluding the transcellular pathway is most likely used.

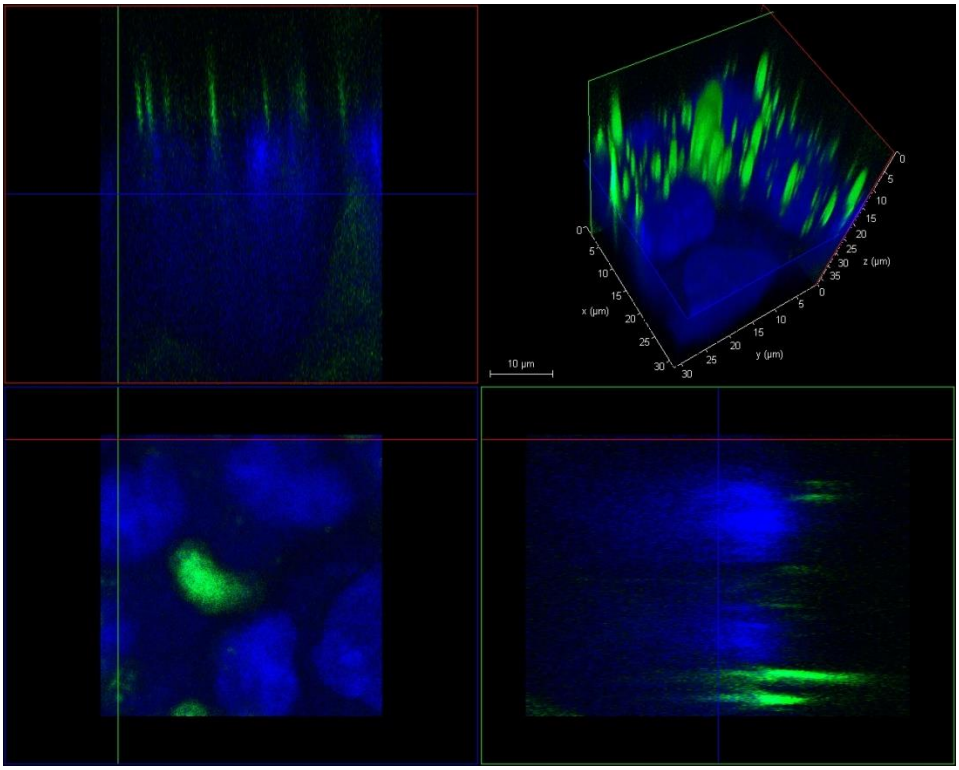

Figure 4.11 Confocal imaging of cell depth when treated with 0.1 mg/ml chitosan:FITC-OVA nanoparticles. Chitosan:FITC-OVA nanoparticles stained green and Caco-2 cells stained blue with DAPI.

4.5 Discussion

The aim of the work in this chapter was to test the toxicity and antigen (OVA, used as a model antigen) delivery potential of chitosan nanoparticles. The toxicity was tested through the MTS assay to test cell viability and LDH assay to test the effect the chitosan:OVA nanoparticles had on the integrity of the cell membranes. Effect on epithelial tight junctions was assessed via TEER studies and permeability studies were employed to determine whether OVA translocates across Caco-2 monolayers.

Figure 4.3 shows that chitosan:OVA nanoparticles did not reduce Caco-2 cell viability at tested concentrations. In a similar study chitosan nanoparticles via ionic gelation, used the MTS assay to show a concentration-dependent effect on Caco-2 cells, with 0.025 mg/ml concentration showing the greatest reduction in cell viability. Chitosan solution of comparable concentration showed a similar effect on Caco-2 cells (Vllasaliu *et al*. 2010). It is interesting to note that application of chitosan solution to Caco-2 cells at 0.1 mg/ml w/v resulted in a dramatic reduction in cell viability, to 26% (Vllasaliu *et al*. 2010), whereas in the present work chitosan:OVA nanoparticles at the same concentration of chitosan did not decrease cell viability. This may be related to the presence of OVA in the system, possibly due to a reduction in the positive surface charge of nanoparticles, as demonstrated by zeta potential measurements (Chapter 3).

Lactate dehydrogenase (LDH) is a soluble cytoplasmic enzyme which is released when the cells are lysed or damaged; this is used as a measurement of membrane toxicity to cells. LDH catalyses the following reaction; NADH+ pyruvate ↔ NAD+ Lactate (Chen *et al*. 2015). NADH is reduced to β- nicotinamide adenine dinucleotide when pyruvate is oxidised to lactate, a tetrazolium salt is then produced into a coloured formazan product using synthesised NADH in the presence of an electron acceptor. The formazan product is then measured by spectroscopy at 490 nm (Chan *et al*. 2013).

Chitosan:OVA nanoparticles at all tested concentrations did not significantly increase LDH release and displayed values similar to HBSS (negative control). A similar study demonstrated that there was no cytotoxicity observed in the chitosan nanoparticles, compared to metal or metal oxides encapsulated in nanoparticles, which is known to be cytotoxic to cells (Yang *et al*. 2015). Another study demonstrated an LDH assay conducted with chitosan nanoparticles formulated by ionic gelation, although this was on airway Calu-3 cells. This study described a concentration-dependent increase in LDH release and Calu-3 cells were significantly more sensitive to chitosan application compared to the present study with chitosan:OVA system in Caco-2 cells (Vllasaliu *et al*. 2010).

Transepithelial electrical resistance (TEER) was studied to establish if the nanoparticles caused tight junction modulation. TEER is a strong indicator of the integrity of the epithelial barriers, including tight junction function and modulation.

TEER reduction was observed in this work, although the same observation was also apparent for OVA solution at concentration equivalent to that present in nanoparticles (0.1 mg/ml). It is interesting to note that the pattern of TEER reduction was different in chitosan:OVA nanoparticles to OVA solution (control), with the latter associated with a delayed effect (maximum TEER reduction at 120 min compared to 30 min with chitosan:OVA nanoparticles).All the concentrations of chitosan:OVA nanoparticle samples at the 24 hour and 48 hour measurement, the TEER always returned back to its original value suggesting reversibility. This is another indication of no toxicity exerted by nanoparticles to Caco-2 cells. This suggests that the chitosan:OVA nanoparticles do not cause irreversible damage to Caco-2 cells, but is not clear whether a tight junction modulating effect is exerted.

TEER reversibility with chitosan nanoparticles has been reported previously, including in a study with chitosan nanoparticles based on a chitosan oligosaccharide formed via ionic gelation (Ye *et al*. 2013 and Vllasaliu *et al*. 2010).

A clear ability to decrease TEER has been previously reported with chitosan nanoparticles. For example, in a similar study chitosan nanoparticles were prepared using ionotropic gelation through the method of spinning disc processing technology. Test samples were also formed in HBSS and applied to Caco-2 cells. HBSS was used as a control and baseline as within this research. Chitosan in solution was compared against chitosan nanoparticles. As the chitosan nanoparticles increased in concentration, cells decreased in TEER over a course of 3 hours to 86%, 32% and 24% above the original baseline value (Loh *et* al. 2012). A similar effect is shown in another study using chitosan chloride nanoparticles prepared by ionic gelation, with nanoparticles at 0.0125 mg/ml being able to cause a dramatic reduction in TEER in Caco-2 cells, to <20% of the baseline value (Vllasaliu *et al.* 2010).

It could be hypothesised that the reason why the chitosan:OVA nanoparticles in this work did not induce a dramatic reduction in Caco-2 monolayer TEER relates to the surface charge reduction of the systems, similarly to the toxicity effect. It was hypothesised in a similar study the reduced charge density at the surface of the nanoparticles, compared to the soluble form of chitosan, was responsible for a much lower effect on chitosan nanoparticles compared to solution, decreasing the TEER (Sadeghi *et al.* 2008). Similarly, in our chitosan:OVA nanosystems the reduction of positive surface charge and shielding of amine chitosan groups by OVA may be responsible for the decreased effect on tight junctions, hence cell monolayer TEER, compared to previous observations with chitosan only nanoparticles.

Permeability studies were performed to determine OVA as a model antigen complexed within chitosan nanoparticles moved across the Caco-2 monolayers. This was studied over a 3-hour period. Data demonstrates OVA permeability (apparent permeability coefficient, P_{app}) is higher when applied in chitosan:OVA form compared to equivalent dose of OVA in solution. It must be noted that due to the nature of the experimental procedure, whereby fluorescently labelled OVA was quantified, it is not possible to establish whether chitosan:OVA nanoparticles permeated the cell monolayers or if OVA dissociated from the nanoparticles, before or during the transit process. However, confocal microscopy data (Figures 4.10 and 4.11) shows chitosan:OVA nanoparticles are taken up by Caco-2 cells (within polarised monolayer culture).

The polymer chitosan enhanced nanoparticle uptake from electrostatic interactions occuring when the positive amine groups on chitosan bound to the negatively charged intergrins on the epithelial cell surface. As stated above it is not known whether FITC-OVA was released after dissociation from nanoparticles or whether the chitosan:FITC-OVA nanoparticles passed through the cells. Throughout the permeability studies in different concentrations tested, the concentration of FITC-OVA was kept the same. Chitosan concentration varied it was this variable which showed the relationship between permeability and the concentration used. The higher the concentration (0.1 mg/ml) the increase in permability of FITC-OVA in Caco-2 cells. A way to test and improve the permability studies would be to fluorescently label chitosan. This would

measure the permeability of chitosan and demonstrate if FITC-OVA dissociated with chitosan before passing through the Caco-2 cells.

In similar research chitosan nanoparticles were prepared via ionic gelation method using tripolyphosphate. Permeability studies using a Caco-2 cell line took place using FD4 as a model macromolecule. The transwell was tested in different conditions: FD4 alone, chitosan nanoparticles and hydrocaffeic acid chitosan nanoparticles with FD4. This study found that the FD4 permeability was increased with the addition of nanoparticles compared to when applied alone in solution (Soliman *et al.* 2014). Prior to this, a study also used FD4 and FD10 as model drugs and clearly demonstrated that chitosan nanoparticles markedly enhanced the permeability of FD4 and FD10, by 7.6 fold and 6.5 fold, respectively. However, this study also showed that chitosan nanoparticles dramatically reduced cell monolayer TEER, suggesting a tight junction modulating effect (Vllasaliu *et al.* 2010). Interestingly, work in this thesis also shows an increase in payload (OVA) permeability across Caco-2 monolayers, which is notable considering the higher molecular weight of OVA compared to FD4 or FD10, but without a clear demonstration of a tight junction effect (TEER).

Permeability data in this work showed FITC-OVA within chitosan:FITC-OVA nanoparticles crossed Caco-2 monolayers more efficiently than FITC-OVA alone in solution, with a 5-fold enhancement in permeability. The mechanism responsible for this increased apical-to-basolateral permeability of FITC-OVA is more likely to relate to nanoparticle trancellular uptake by Caco-2 cells rather than the effect on the paracellular route. Chitosan:OVA's potential to open up Caco-2 tight junctions and allowing the OVA to diffuse through the paracellular route is not clear due to the effect of the nanoparticle system on cell monolayer TEER not being notably lower than OVA solution.A transcellular rather than paracellular effect is more likely, and is also confirmed by confocal microscopy, which shows fluorescence presence in cells (FITC-OVA in chitosan:FITC-OVA nanoparticles). The relatively small size of chitosan:OVA nanoparticles prepared in this work (compared to previous studies reporting chitosan nanoparticle preparation with the ionic gelation method) is likely to facilitate the cell uptake of nanoparticles.

4.6 Conclusion

Overall, the research within this chapter tested various biological effects of chitosan:OVA nanoparticles, including cytotoxicity (MTS and LDH assay), effect on tight junctions (TEER) and FITC:OVA permeability in Caco-2 monolayers. It was found that all chitosan:OVA nanoparticle concentrations testedwere not toxic to the Caco-2 cells in MTS assay or LDH assay and were over the cell viability threshold (60%). It was also found that TEER decrease with chitosan:OVA nanoparticles is not clear as the effect does not go beyond that of OVA solution alone. Permeability studies showed FITC-OVA permeability is notably facilitated following nanoparticle application compared to OVA solution. Lastly confocal imaging showed fluorescence presence, assumed to be due to chitosan:FITC-OVA nanoparticles in the interior of Caco-2 cells. Together, the data suggests that chitosan:OVA nanoparticles are not toxic towards Caco-2 cells and are able to improve antigen delivery, most likely through the transcellular route.

4.7 References

1. Chan, F., K., M., Moriwaki, K. and Rosa, M., J., D. (2013). *Detection of Necrosis by Release of Lactate Dehydrogenase (LDH) Activity*, Methods in Molecular Biology, 979: 65-70.
2. Chen, C., M., Chen, S., M., Chien, P., J. and Yu, H., Y. (2015). *Development of an Enzymatic Assay Systemof D-Lactate using D-Lactate Dehydrogenase and a UV-LED Fluorescent Spectrometer,* Journal of Pharmaceutical and Biomedical Analysis, 116: 150-155.
3. Loh, J., W., Saunders, M. and Lim, L., Y. (2012). *Cytotoxicity of the Monodispersed Chitosan Nanoparticles Against the Caco-2 Cells*, Toxicology and Applied Pharmacology, 262(3): 273-282.
4. Sadeghi, A., M., M., Dorkoosh, F.A., Avadi, M., R., Weinhold, M., Bayat, A., Delie, F., Gurny, R., Larijani, B., Rafiee- Tehrani, M. and Junginger, H., E. (2008). *Permeation enhancer effect of chitosan and chitosan derivatives: comparison of formulations as*

soluble polymers and nanoparticulate systems on insulin absorption in Caco-2 cells, European Journal of Pharmaceutics and Biopharmaceutics, 70(1): 270–278.

5. Soliman, G., M., Zhang, Y., L., Merle, G., Cerruti, M. and Barralet, J. (2014). *Hydrocaffeic Acid Chitosan Nanoparticles with Enhanced Stability, Mucoadhesion and Permeation Properties*, European Journal of Pharmaceutics and Biopharmaceutics, 88(3): 1026-1037.
6. Vllasaliu, D., Harris- Exposito, R., Heras, A., Casettari, L., Garnett, M., Illum, L. and Stolnik, S. (2010). *Tight Junction Modulation by Chitosan Nanoparticles: Comparison with Chitosan Solution*, International Journal of Pharmaceutics, 400(1-2): 183-193.
7. Yang, M., H., Chung, T., W., Lu, Y., S., Chen, Y., L., Tsai, W., C., Jong, S., B., Yuan, S., S., Liao, P., C., Lin, P., C. and Tyan, Y., C. (2015). *Activation of the Ubiquitin Proteasome Pathway by Silk Fibroin Modified Chitosan Nanoparticles in Hepatic Cancer Cells*, International Journal of Molecular Sciences, 16: 1657-1676.
8. Ye, Y., Xu, Y., Liang, W., Leung, G., P., H., Cheung, K., H., Zheng, C., Chen, F. and Lam, J., K., W. (2013). *DNA-Loaded Chitosan Oligosaccharide Nanoparticles with Enhanced Permeability across Calu-3 Cells*, Journal of Drug Targeting, 21(5): 474-486.

Chapter 5

In Vivo Study of Chitosan:OVA Nanoparticles for Immune Response

5.1 Introduction

This chapter details an investigation of whether chitosan:OVA nanoparticles are able to induce a positive immune response in mice following gastrointestinal administration (to stimulate oral delivery). To measure the immune response, IgG and IgA were measured and IgG1 and IgG2A subclasses were analysed, as well as total IgG using an indirect ELISA. This was carried out at the National Institute for Biological Standards and Control (NIBSC) by myself. The IgG subclasses provide evidence in antibody responses of CD4 positive T cell functions in acquiring immunity. IgG1 is the most abundant Ig in the IgG subclass (50%). Th1 and Th2 response reflects the IgG1 response (Nakayama *et al*. 2012). IgG2a is a marker for Th1 and Th2 lymphocytes and is the second most abundant antibody in the human immune system. IgG2a responses are usually not as high as IgG1. However, as it is a marker for Th1 and Th2 activation it is still important to measure (Mountford *et al*. 1996). IgA measurement in this study was important as this immunoglobulin inhabits the mucosa and can give an indication of mucosal response. IgA response has been shown to play an important role in immunity; it activates the alternative pathway in the complement system which in turn helps to prevent serious infections (Roos *et al*. 2001).

Although a number of nanosystems have been tested previously for mucosal vaccine delivery, one of the most extensively researched nanoparticle systems are those formulated from chitosan. For example, chitosan nanoparticles have shown to produce a response when cholera toxin and OVA (used as an adjuvant) have been used (Huang *et al*. 2008), as well as hepatitis B surface antigen and meningococcal C oligosaccharides (Slütter and Jiskoot. 2010). However, due to the great diversity in chitosan systems, including the type of chitosan molecule used (e.g. specific salt form and molecular weight), as well as formulation method, this study focused on a specific chitosan

(ultrapure chitosan chloride) and formulation method (ionic gelation) which had previously shown significant potential for enhancing mucosal drug absorption (Casettari *et al*. 2012, Vllasaliu *et al*. 2012 and Casettari *et al*. 2012).

Chapters 3 and 4 showed that chitosan nanoparticles fabricated in this work capable of complexing with OVA, display a good overall toxicity profile and enhance OVA permeability across Caco-2 monolayers. Following this demonstration, this chapter tested the performance of the system *in vivo*. This is important as the *in vitro* outcome of many drug formulation systems is often not reproduced *in vivo*. In this case transwell systems designed to deliver the therapeutic payload across the mucosal surfaces, the epithelial models may not faithfully represent the more complex mucosal surfaces, which consists of multiple cell types and have mucus presence. The immune response to chitosan:OVA nanoparticles in animal studies was measured by performing indirect ELISAs on mouse sera, looking at individual immunoglobulins; IgG, IgG1, IgG2A and IgA carried out at NIBSC by myself. This was to establish which part of the immune system was involved in any positive response that may take place.

5.2 Methods

5.2.1 Preparation of chitosan:OVA nanoparticles for *in vivo* studies

Only one concentration of nanoparticles was prepared, namely 1 mg/ml (1:1 chitosan:OVA mass ratio). This concentration has shown the opitmal size, charge, toxicity and permeation following previous *in vitro* studies. 4 mg chitosan was dissolved in 2 ml of MES/HBSS solution (pH 6.0). In a separate scintillation vial, 4 mg endotoxin-free OVA was dissolved in 2 ml MES/HBSS solution. 1.5 ml of chitosan solution and 1.5 ml of OVA solution (both at 2 mg/ml) were then mixed in a scintillation vial (a total volume of 3 ml of nanoparticles was needed overall), with the overall final concentration of both chitosan and OVA at 1 mg/ml. TPP was added to this solution in a dropwise manner using a needle (with stirring) to produce the nanoparticles. These were then sent to the National Institute for Biological Standards and Control (NIBSC) for use in *in vivo* studies.

5.2.2 Oral immunisation of BALB/c mice

This was performed by Dr Donna Bryan at NIBSC. (Ethical approval was obtained, 2015). At no point were the nanoparticles sterilised before immunisation. 25 BALB/c mice were immunised with chitosan:OVA nanoparticles with or without 15 µg cholera toxin (*Vibrio cholerae*), as well as OVA alone with or without 15 µg cholera toxin (added as a second adjuvant to further enhance the mucosal response). This was done by oral gavage. A subcutaneous group was used as a positive control with a lower dose of OVA. Mice were pre-bled at day -1 and immunised at days 0, 7, 14 and 28. Each group of mice were assigned a sample. A tail bleed was taken at day 20 and terminal bleed was performed at day 28. Serum was prepared and stored at -80 °C. Faecal samples were collected and placed into an Eppendorf containing a protein degradation inhibition solution at day 28. Intestinal washes were carried out at day 28. This was performed by removing the small intestine and washing it with a protein degradation inhibition solution, the supernatant was stored at -80 °C.

5.2.3. Quantitation of IgG, IgG1, IgG2a and IgA by indirect ELISA following oral immunisation of mice

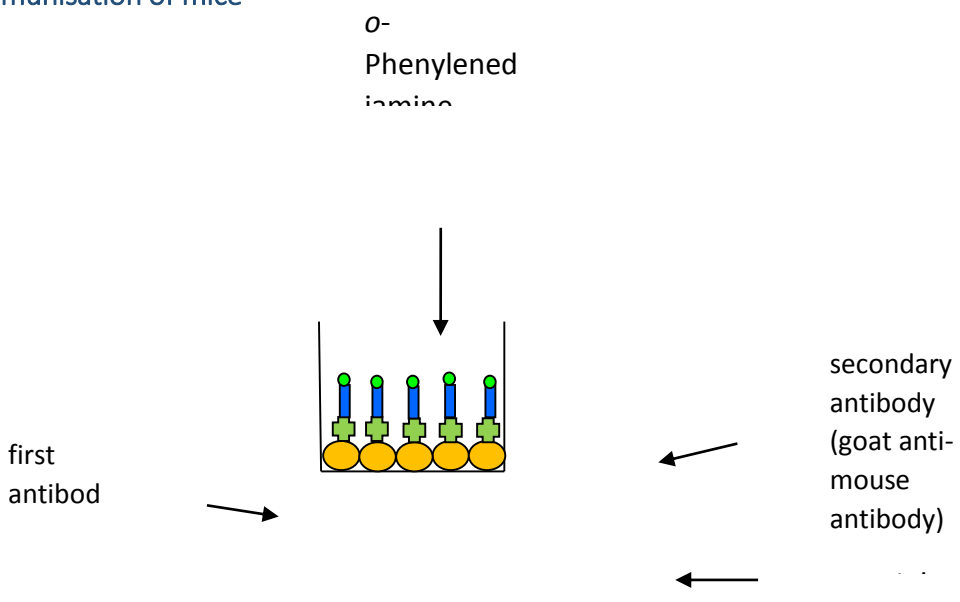

Figure 5.1 A diagram of an indirect ELISA.

95 ml of carbonate buffer was prepared (see section 2.2.3.5) and then placed in a duran bottle to which 950 µl of endograde OVA (endotoxin free) was added and mixed. This particular type of OVA was chosen based on previous research that it does not cause any immune response due to toxins. Using a multi pipette, 100 µl of the mixture was placed into 9 96 well plates. The plates were then incubated at 37 °C for 90 minutes and then at 4 °C overnight.

After the plates were taken out of the fridge, the ovalbumin mixture was aspirated out. The plates were placed in the plate washer. The 9 plates were washed with the prepared wash buffer (see section 2.2.3.3.). The plates were blocked with the prepared assay diluent (Section 2.2.3.4.); 100 µl was applied per well to all plates and placed in the incubator for 30 minutes at 37 °C. This is an important step in the ELISA protocol. Blocking the wells with assay diluent ensures a reduction in background noise, the prevention of non-specific binding and stabilisation of proteins absorbed to the plate already (OVA). Meanwhile the samples were prepared. 490 µl of assay diluent was placed in an Eppendorf, followed by 10 µl of collected mouse sera. 5 sample groups with 5 mice in each group were used, as depicted in table 5.1.

Group	Sample
1	200µl Ovalbumin mixed with sodium bicarbonate.
2	200µl Ovalbumin mixed with cholera toxin and sodium bicarbonate.
3	200µl Chitosan:OVA nanoparticles in PBS.
4	200µl Chitosan:OVA nanoparticles with cholera toxin.
5	200µl Ovalbumin alone mixed with PBS administered subcutaneously (control).

Table 5.1 Mouse sera samples used in indirect ELISA's

The positive control was reference sera (dilution 1:50) placed in row 1 and 2, a blank of assay diluent was also used in column 12.

Samples were applied to the plates and incubated for 90 minutes at room temperature (approximately 22 °C). The plates were washed using the same process as before (see above). The secondary antibody was prepared. 95 ml of assay diluent mixed with 31.5

µl of goat anti-mouse antibody in a duran bottle. 100 µl was applied to every well in all 9 plates and left at room temperature for 90 minutes. The *o*-Phenylenediamine dihydrochloride (OPD) peroxidase substrate (horseradish peroxidase enzyme) was prepared. 50 ml of dH_2O was applied to two plastic containers; 5 gold wrapped tablets were added to one container and 5 silver wrapped tablets were added to another container. The containers were wrapped in foil and the tablets dissolved by continuous stirring. Once dissolved, the tablets wrapped in silver solution was poured into the container containing the gold wrapped tablets. Once the plates were ready, they were washed using the plate washer. 100 µl of the OPD substrate was applied to all the wells in the plates to label the second antibody (goat anti-mouse antibody). These were placed in a dark cupboard for 20 minutes. The reaction was stopped with hydrochloric acid and 50 µl applied to all the wells in all 9 plates. The plates were read with the plate reader at 492 nm.

The role of each component of an indirect ELISA:

- Endograde free OVA- antigen used.
- Mouse sera samples- used to bind to the chosen antigen
- Goat anti- mouse antibody- used to bind to primary antibody
- OPD peroxidase substrate- used to label the secondary antibody to read optical density.

5.3 Results

Total IgG, IgG1, IgG2A and IgA were tested throughout the *in vivo* studies. This was in order to determine the mechanisms of the immune response. There were 5 groups with 5 mice in each group for repeats.

Figure 5.2 shows the response elicited with ovalbumin mixed with bicarbonate. This was non-existent to minimal. This sample was not expected to show a response, but was used as a baseline. It does not match the same pattern as the positive control. The standard deviation was 0.024 and geomean 0.237 indicating a poor response. The value of the SD is to define the distribution of the blank samples of different mice, the

geometric mean determines the central tendancy of the product of the blank samples of different mice. This determines the 'cut off' for antibody titres on the ELISA and figure 5.2

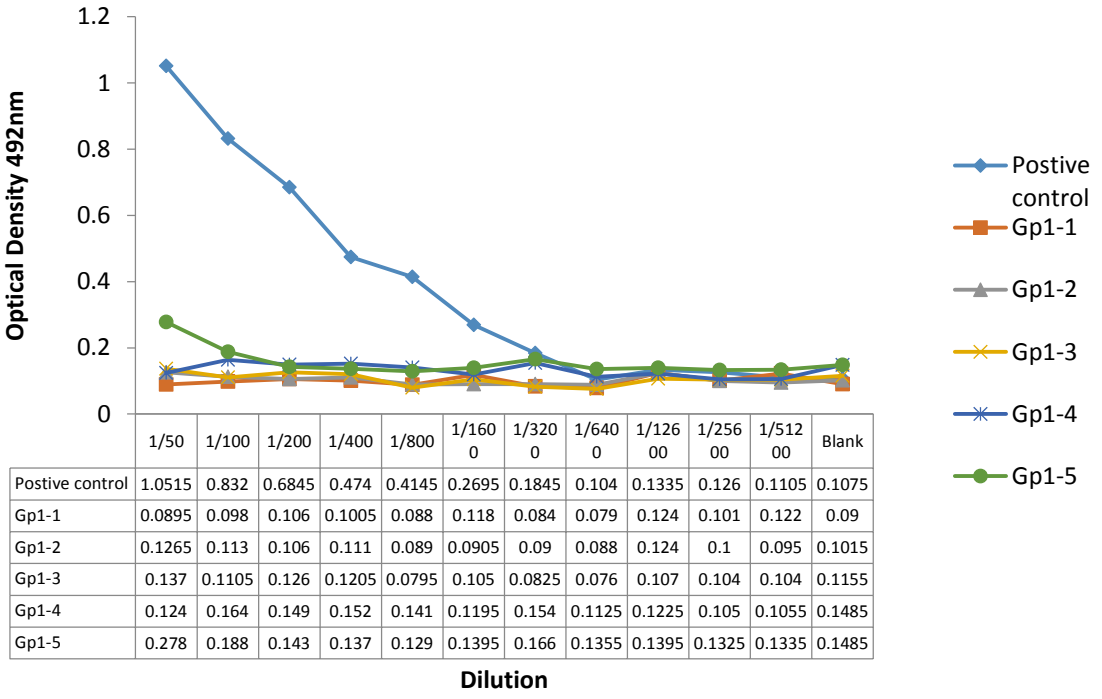

	1/50	1/100	1/200	1/400	1/800	1/1600	1/3200	1/6400	1/12600	1/25600	1/51200	Blank
Postive control	1.0515	0.832	0.6845	0.474	0.4145	0.2695	0.1845	0.104	0.1335	0.126	0.1105	0.1075
Gp1-1	0.0895	0.098	0.106	0.1005	0.088	0.118	0.084	0.079	0.124	0.101	0.122	0.09
Gp1-2	0.1265	0.113	0.106	0.111	0.089	0.0905	0.09	0.088	0.124	0.1	0.095	0.1015
Gp1-3	0.137	0.1105	0.126	0.1205	0.0795	0.105	0.0825	0.076	0.107	0.104	0.104	0.1155
Gp1-4	0.124	0.164	0.149	0.152	0.141	0.1195	0.154	0.1125	0.1225	0.105	0.1055	0.1485
Gp1-5	0.278	0.188	0.143	0.137	0.129	0.1395	0.166	0.1355	0.1395	0.1325	0.1335	0.1485

Figure 5.2 IgG1 response of group 1: ovalbumin mixed with bicarbonate. Positive control is standard reference sera.

Figure 5.3 shows the immune response to the combination of ovalbumin and cholera toxin. A clear response is apparent with two mice, with the highest response from mouse 2-2 at 0.824. These show a similar pattern to the positive control but with a lower response. This sample was another baseline and could be compared with chitosan:OVA nanoparticles to determine whether the system showed an increased response compared to the combination of ovalbumin with cholera toxin. The standard deviation was 0.138 and geomean 0.277 (slightly higher than for ovalbumin mixed with bicarbonate, figure 5.2).

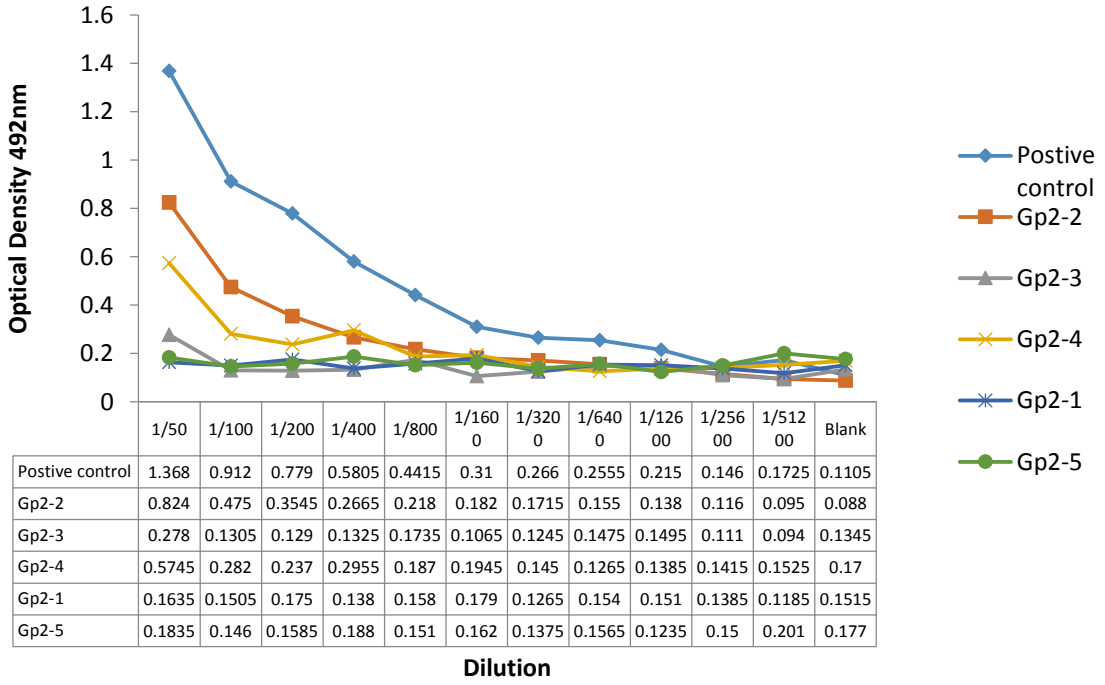

	1/50	1/100	1/200	1/400	1/800	1/1600	1/3200	1/6400	1/12600	1/25600	1/51200	Blank
Postive control	1.368	0.912	0.779	0.5805	0.4415	0.31	0.266	0.2555	0.215	0.146	0.1725	0.1105
Gp2-2	0.824	0.475	0.3545	0.2665	0.218	0.182	0.1715	0.155	0.138	0.116	0.095	0.088
Gp2-3	0.278	0.1305	0.129	0.1325	0.1735	0.1065	0.1245	0.1475	0.1495	0.111	0.094	0.1345
Gp2-4	0.5745	0.282	0.237	0.2955	0.187	0.1945	0.145	0.1265	0.1385	0.1415	0.1525	0.17
Gp2-1	0.1635	0.1505	0.175	0.138	0.158	0.179	0.1265	0.154	0.151	0.1385	0.1185	0.1515
Gp2-5	0.1835	0.146	0.1585	0.188	0.151	0.162	0.1375	0.1565	0.1235	0.15	0.201	0.177

Figure 5.3 IgG1 response for group 2: ovalbumin with cholera toxin. Positive control is standard reference sera.

Figure 5.4 shows IgG1 response to chitosan:OVA nanoparticles (group 3). The graph suggests the absence of an IgG1 response in mice following oral immunisation with chitosan:OVA nanoparticles.

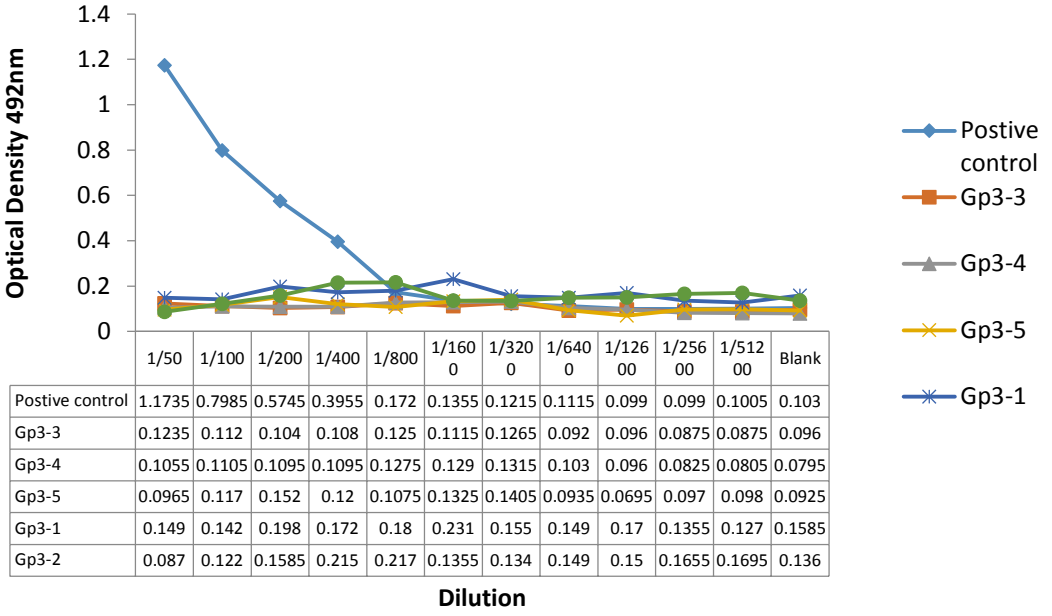

	1/50	1/100	1/200	1/400	1/800	1/1600	1/3200	1/6400	1/12600	1/25600	1/51200	Blank
Postive control	1.1735	0.7985	0.5745	0.3955	0.172	0.1355	0.1215	0.1115	0.099	0.099	0.1005	0.103
Gp3-3	0.1235	0.112	0.104	0.108	0.125	0.1115	0.1265	0.092	0.096	0.0875	0.0875	0.096
Gp3-4	0.1055	0.1105	0.1095	0.1095	0.1275	0.129	0.1315	0.103	0.096	0.0825	0.0805	0.0795
Gp3-5	0.0965	0.117	0.152	0.12	0.1075	0.1325	0.1405	0.0935	0.0695	0.097	0.098	0.0925
Gp3-1	0.149	0.142	0.198	0.172	0.18	0.231	0.155	0.149	0.17	0.1355	0.127	0.1585
Gp3-2	0.087	0.122	0.1585	0.215	0.217	0.1355	0.134	0.149	0.15	0.1655	0.1695	0.136

Figure 5.4 IgG1 response to chitosan:OVA nanoparticles. Positive control is standard reference sera.

IgG1 response to chitosan:OVA nanoparticles with cholera toxin is shown in figure 5.5. Cholera toxin was added to nanoparticles as an extra adjuvant. The data does not follow a clear pattern. None of the samples follow the positive control pattern. Standard deviation was 0.02 and the graph had a geomean of 0.275. This was similar to figure 5.3.

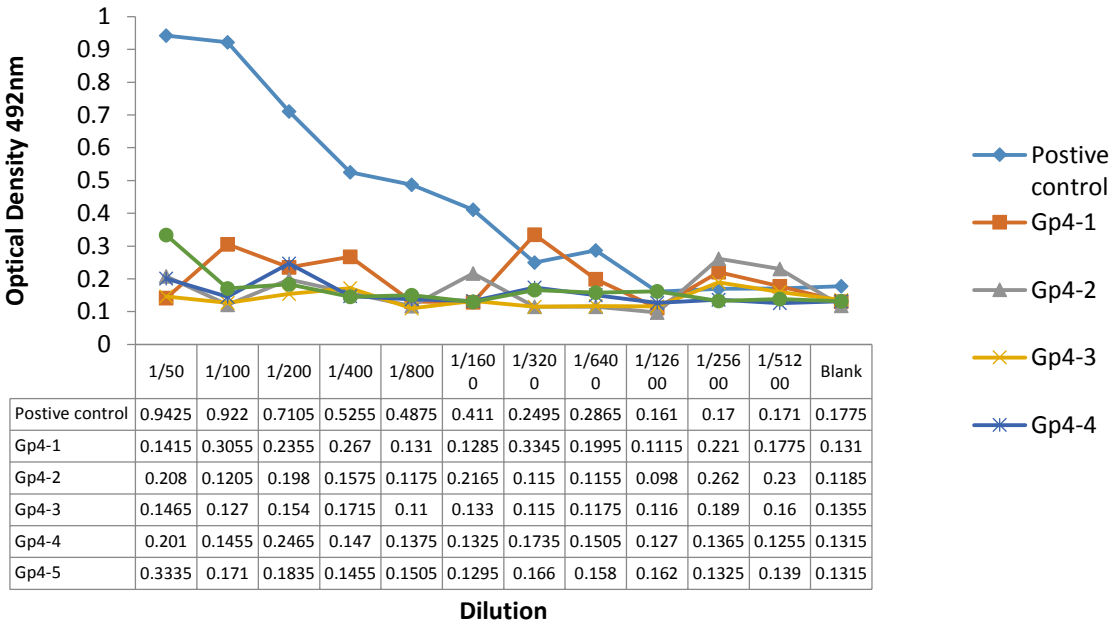

	1/50	1/100	1/200	1/400	1/800	1/1600	1/3200	1/6400	1/12600	1/25600	1/51200	Blank
Postive control	0.9425	0.922	0.7105	0.5255	0.4875	0.411	0.2495	0.2865	0.161	0.17	0.171	0.1775
Gp4-1	0.1415	0.3055	0.2355	0.267	0.131	0.1285	0.3345	0.1995	0.1115	0.221	0.1775	0.131
Gp4-2	0.208	0.1205	0.198	0.1575	0.1175	0.2165	0.115	0.1155	0.098	0.262	0.23	0.1185
Gp4-3	0.1465	0.127	0.154	0.1715	0.11	0.133	0.115	0.1175	0.116	0.189	0.16	0.1355
Gp4-4	0.201	0.1455	0.2465	0.147	0.1375	0.1325	0.1735	0.1505	0.127	0.1365	0.1255	0.1315
Gp4-5	0.3335	0.171	0.1835	0.1455	0.1505	0.1295	0.166	0.158	0.162	0.1325	0.139	0.1315

Figure 5.5 IgG1 response in group 4: chitosan:OVA nanoparticles with cholera toxin. Positive control is standard reference sera.

Figure 5.6 shows subcutaneous administration control group. The samples gave rise to a mixed IgG1 response, with 4 mice showing a higher response than the positive control. The standard deviation was 0.023. A geomean of 0.302 indicates an increase compared to figures 5.2- 5.5above.

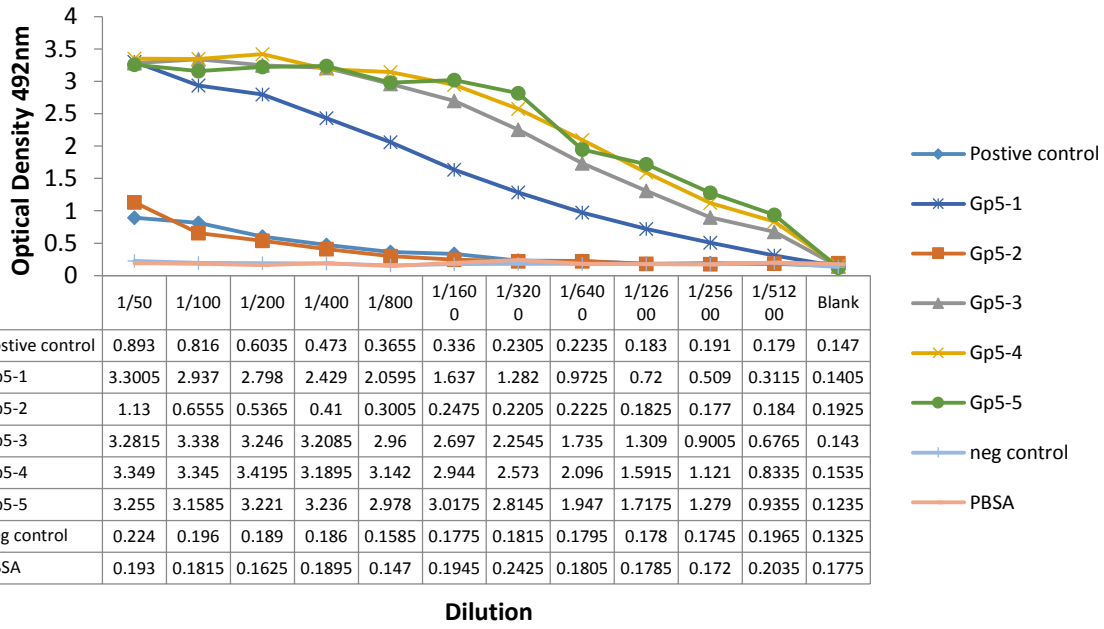

	1/50	1/100	1/200	1/400	1/800	1/1600	1/3200	1/6400	1/12600	1/25600	1/51200	Blank
Postive control	0.893	0.816	0.6035	0.473	0.3655	0.336	0.2305	0.2235	0.183	0.191	0.179	0.147
Gp5-1	3.3005	2.937	2.798	2.429	2.0595	1.637	1.282	0.9725	0.72	0.509	0.3115	0.1405
Gp5-2	1.13	0.6555	0.5365	0.41	0.3005	0.2475	0.2205	0.2225	0.1825	0.177	0.184	0.1925
Gp5-3	3.2815	3.338	3.246	3.2085	2.96	2.697	2.2545	1.735	1.309	0.9005	0.6765	0.143
Gp5-4	3.349	3.345	3.4195	3.1895	3.142	2.944	2.573	2.096	1.5915	1.121	0.8335	0.1535
Gp5-5	3.255	3.1585	3.221	3.236	2.978	3.0175	2.8145	1.947	1.7175	1.279	0.9355	0.1235
neg control	0.224	0.196	0.189	0.186	0.1585	0.1775	0.1815	0.1795	0.178	0.1745	0.1965	0.1325
PBSA	0.193	0.1815	0.1625	0.1895	0.147	0.1945	0.2425	0.1805	0.1785	0.172	0.2035	0.1775

Figure 5.6 IgG1 response of group 5: ovalbumin mixed with PBS, administered subcutaneously. Positive control is standard reference sera. Negative control is a blank.

Figure 5.7 shows IgG2a response with chitosan:OVA nanoparticles. There appears to be no particular pattern in this instance, however most samples are above the positive control line. The standard deviation is 0.026 and geomean 0.468, the latter being notably higher than any previous figures.

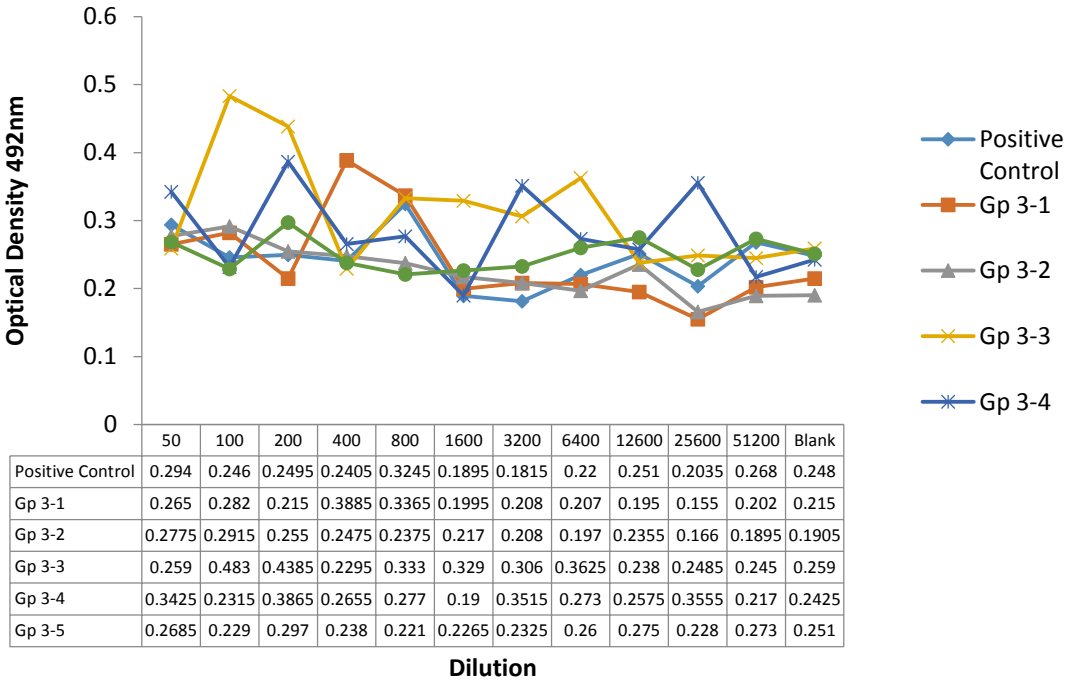

	50	100	200	400	800	1600	3200	6400	12600	25600	51200	Blank
Positive Control	0.294	0.246	0.2495	0.2405	0.3245	0.1895	0.1815	0.22	0.251	0.2035	0.268	0.248
Gp 3-1	0.265	0.282	0.215	0.3885	0.3365	0.1995	0.208	0.207	0.195	0.155	0.202	0.215
Gp 3-2	0.2775	0.2915	0.255	0.2475	0.2375	0.217	0.208	0.197	0.2355	0.166	0.1895	0.1905
Gp 3-3	0.259	0.483	0.4385	0.2295	0.333	0.329	0.306	0.3625	0.238	0.2485	0.245	0.259
Gp 3-4	0.3425	0.2315	0.3865	0.2655	0.277	0.19	0.3515	0.273	0.2575	0.3555	0.217	0.2425
Gp 3-5	0.2685	0.229	0.297	0.238	0.221	0.2265	0.2325	0.26	0.275	0.228	0.273	0.251

Figure 5.7 shows IgG2a response in group 3: chitosan:OVA nanoparticles. Positive control is standard reference sera.

Figure 5.8 shows an IgG2a response to chitosan/OVA nanoparticles with the addition of cholera toxin at a 1:50 dilution. There is no trend, with sample values above the positive control and constant decrease and increase in response value. There is no clear indication were the antibody titres end. The standard deviation is higher at 0.063 and geomean is 0.473. There is one anomaly where sample 3 peaks at 1:3200 dilution at 1.091. This could be down to background noise or the plate washer needles being blocked with a previous sample causing contamination in this particular study.

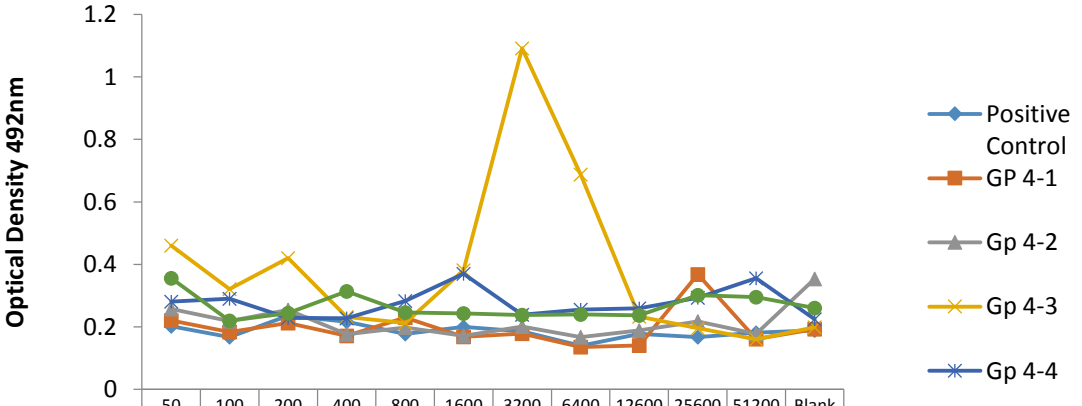

	50	100	200	400	800	1600	3200	6400	12600	25600	51200	Blank
Positive Control	0.202	0.1675	0.236	0.2165	0.178	0.2005	0.1855	0.1395	0.177	0.167	0.1815	0.189
GP 4-1	0.221	0.184	0.2125	0.171	0.23	0.1685	0.179	0.1355	0.141	0.3685	0.1615	0.193
Gp 4-2	0.257	0.2185	0.2545	0.1765	0.198	0.1715	0.2015	0.167	0.1885	0.217	0.1775	0.354
Gp 4-3	0.46	0.321	0.4205	0.232	0.2125	0.381	1.091	0.688	0.2325	0.196	0.1605	0.1995
Gp 4-4	0.2805	0.2905	0.229	0.228	0.2835	0.37	0.239	0.2555	0.259	0.2935	0.356	0.225
Gp 4-5	0.356	0.219	0.2445	0.3135	0.246	0.243	0.238	0.24	0.237	0.301	0.2955	0.261

Figure 5.8 shows IgG2a response in group 4: chitosan:OVA nanoparticles with cholera toxin. Positive control is standard reference sera.

Figure 5.9 shows total IgG response to chitosan:OVA nanoparticles at a 1:50 dilution. The figure shows a slight increase in response to the chitosan:OVA nanoparticles. The highest value at 1:50 is 0.278, although the positive control was 2.106. The standard deviation was 0.013 and geomean 0.221.

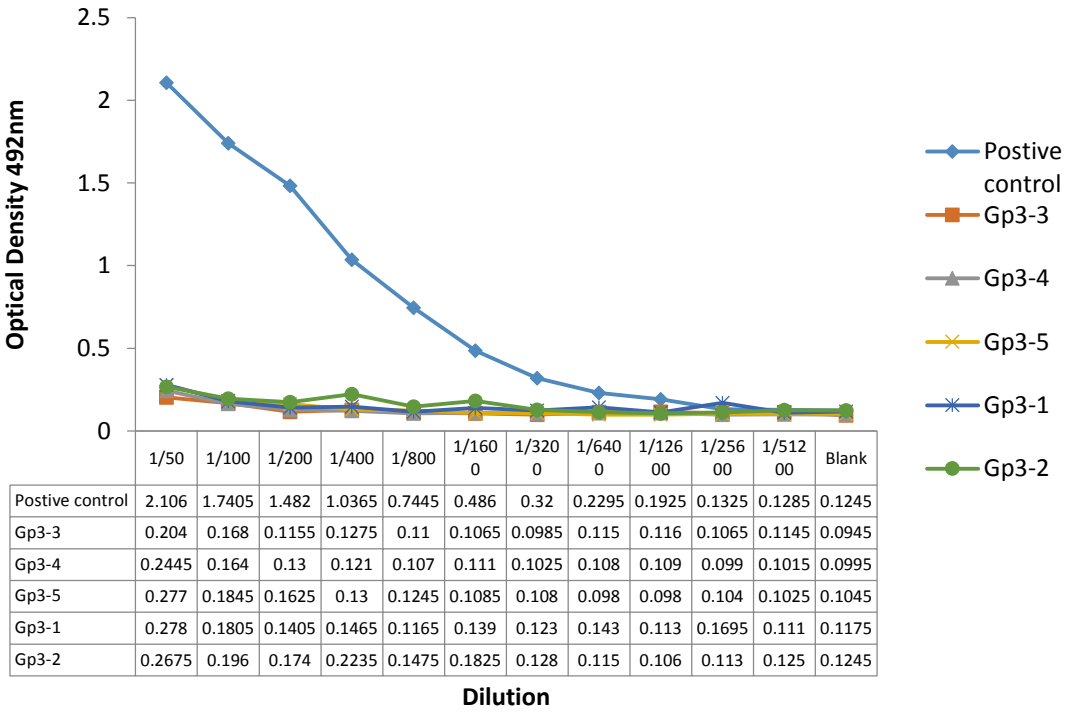

	1/50	1/100	1/200	1/400	1/800	1/1600	1/3200	1/6400	1/12600	1/25600	1/51200	Blank
Postive control	2.106	1.7405	1.482	1.0365	0.7445	0.486	0.32	0.2295	0.1925	0.1325	0.1285	0.1245
Gp3-3	0.204	0.168	0.1155	0.1275	0.11	0.1065	0.0985	0.115	0.116	0.1065	0.1145	0.0945
Gp3-4	0.2445	0.164	0.13	0.121	0.107	0.111	0.1025	0.108	0.109	0.099	0.1015	0.0995
Gp3-5	0.277	0.1845	0.1625	0.13	0.1245	0.1085	0.108	0.098	0.098	0.104	0.1025	0.1045
Gp3-1	0.278	0.1805	0.1405	0.1465	0.1165	0.139	0.123	0.143	0.113	0.1695	0.111	0.1175
Gp3-2	0.2675	0.196	0.174	0.2235	0.1475	0.1825	0.128	0.115	0.106	0.113	0.125	0.1245

Figure 5.9 total IgG response to 1:50 dilution group 3: chitosan:OVA nanoparticles. Positive control is standard reference sera.

Figure 5.10 reveals total IgG response in chitosan:OVA nanoparticles with cholera toxin at a 1:50 dilution. A similar trend to figure 5.9 is apparent. There is a positive trend on the graph, the highest value is 0.593 showing the addition of cholera toxin increases the immune response. The standard deviation was 0.006 and geomean is 0.230.

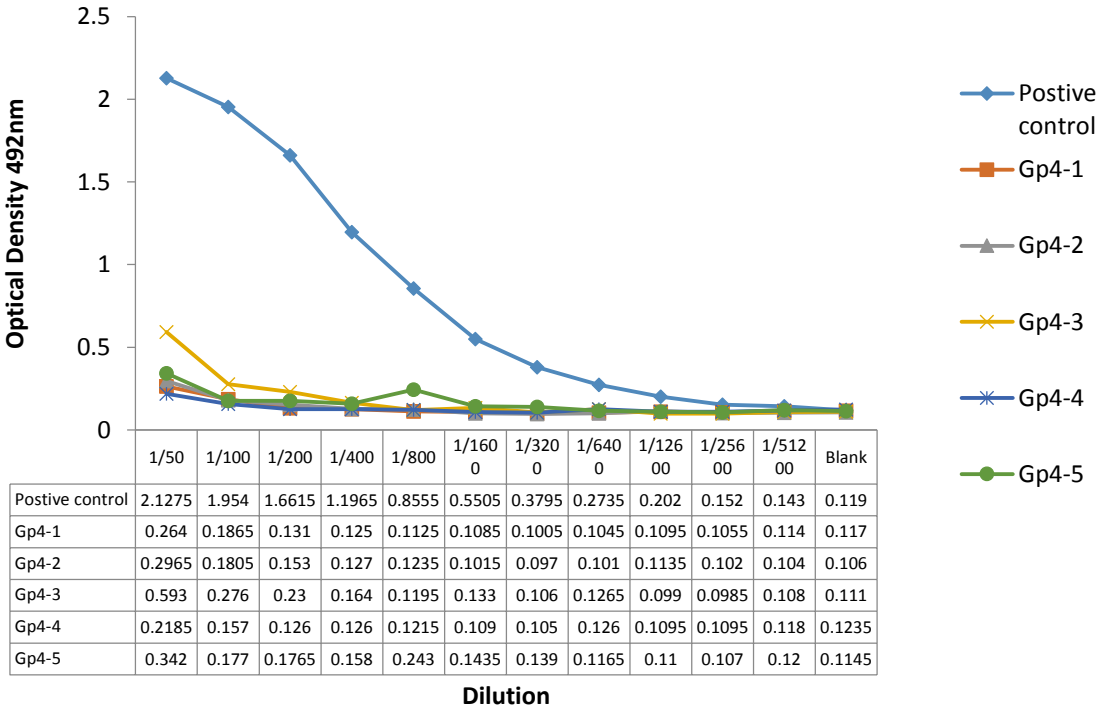

	1/50	1/100	1/200	1/400	1/800	1/1600	1/3200	1/6400	1/12600	1/25600	1/51200	Blank
Postive control	2.1275	1.954	1.6615	1.1965	0.8555	0.5505	0.3795	0.2735	0.202	0.152	0.143	0.119
Gp4-1	0.264	0.1865	0.131	0.125	0.1125	0.1085	0.1005	0.1045	0.1095	0.1055	0.114	0.117
Gp4-2	0.2965	0.1805	0.153	0.127	0.1235	0.1015	0.097	0.101	0.1135	0.102	0.104	0.106
Gp4-3	0.593	0.276	0.23	0.164	0.1195	0.133	0.106	0.1265	0.099	0.0985	0.108	0.111
Gp4-4	0.2185	0.157	0.126	0.126	0.1215	0.109	0.105	0.126	0.1095	0.1095	0.118	0.1235
Gp4-5	0.342	0.177	0.1765	0.158	0.243	0.1435	0.139	0.1165	0.11	0.107	0.12	0.1145

Figure 5.10 total IgG response in group 4: chitosan:OVA nanoparticles with cholera toxin. Positive control is standard reference sera.

As total IgG response with chitosan:OVA nanoparticles with cholera toxin was apparent starting with a 1:50 dilution, a 1:10 dilution was tested as well. Figure 5.11 shows a higher response compared to previous scenarios. The highest total IgG response value is 1.222, there is a trend to this graph with all the samples following the same pattern as the positive control. The standard deviation is 0.003 which shows a very narrow distribution of data and the geomean is 0.168.

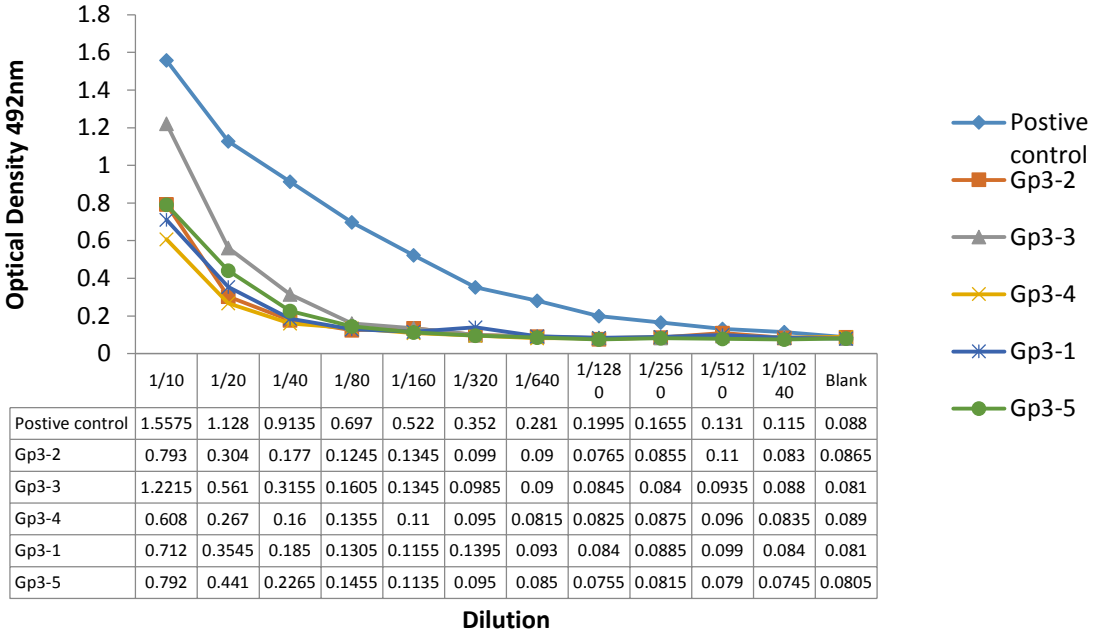

	1/10	1/20	1/40	1/80	1/160	1/320	1/640	1/1280	1/2560	1/5120	1/10240	Blank
Postive control	1.5575	1.128	0.9135	0.697	0.522	0.352	0.281	0.1995	0.1655	0.131	0.115	0.088
Gp3-2	0.793	0.304	0.177	0.1245	0.1345	0.099	0.09	0.0765	0.0855	0.11	0.083	0.0865
Gp3-3	1.2215	0.561	0.3155	0.1605	0.1345	0.0985	0.09	0.0845	0.084	0.0935	0.088	0.081
Gp3-4	0.608	0.267	0.16	0.1355	0.11	0.095	0.0815	0.0825	0.0875	0.096	0.0835	0.089
Gp3-1	0.712	0.3545	0.185	0.1305	0.1155	0.1395	0.093	0.084	0.0885	0.099	0.084	0.081
Gp3-5	0.792	0.441	0.2265	0.1455	0.1135	0.095	0.085	0.0755	0.0815	0.079	0.0745	0.0805

Figure 5.11 total IgG response in chitosan:OVA nanoparticles (group 3), starting at 1:10 dilution. Positive control is standard reference sera.

Figure 5.12 shows immune response to the chitosan:OVA nanoparticles with cholera toxin and demonstrates a trend similar to control. However, figure 5.11 shows a higher response than figure 5.12. Figure 5.12 shows a mean of 0.077 whilst figure 5.11 shows a mean of 0.084. The geomean is 0.154 which is again lower than figure 5.11. We can conclude from these two figures that the samples with the addition of cholera toxin produces a lower immune response than the samples without, which is not what was observed in previous experiments.

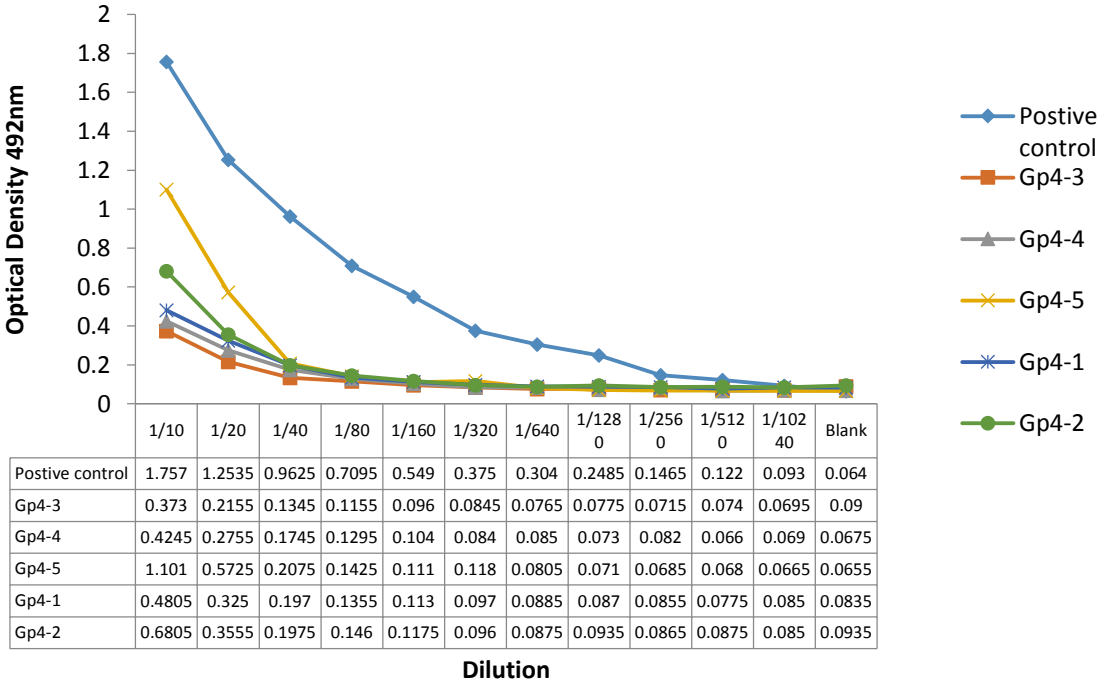

	1/10	1/20	1/40	1/80	1/160	1/320	1/640	1/1280	1/2560	1/5120	1/10240	Blank
Postive control	1.757	1.2535	0.9625	0.7095	0.549	0.375	0.304	0.2485	0.1465	0.122	0.093	0.064
Gp4-3	0.373	0.2155	0.1345	0.1155	0.096	0.0845	0.0765	0.0775	0.0715	0.074	0.0695	0.09
Gp4-4	0.4245	0.2755	0.1745	0.1295	0.104	0.084	0.085	0.073	0.082	0.066	0.069	0.0675
Gp4-5	1.101	0.5725	0.2075	0.1425	0.111	0.118	0.0805	0.071	0.0685	0.068	0.0665	0.0655
Gp4-1	0.4805	0.325	0.197	0.1355	0.113	0.097	0.0885	0.087	0.0855	0.0775	0.085	0.0835
Gp4-2	0.6805	0.3555	0.1975	0.146	0.1175	0.096	0.0875	0.0935	0.0865	0.0875	0.085	0.0935

Figure 5.12 total IgG response to group 4: chitosan:OVA nanoparticles with cholera toxin, starting at 1:10 dilution. Positive control is standard reference sera.

Figure 5.13 shows IgA response to intestinal washes of BALB/c mice treated with chitosan:OVA nanoparticles. Response is apparent at higher dilutions. All of the samples are above the positive control. The standard deviation is 0.038 and geomean is high at 0.675. The reading for the blank was high and could have been background noise. As it was also a higher dilution (1:2) this could have contributed to it.

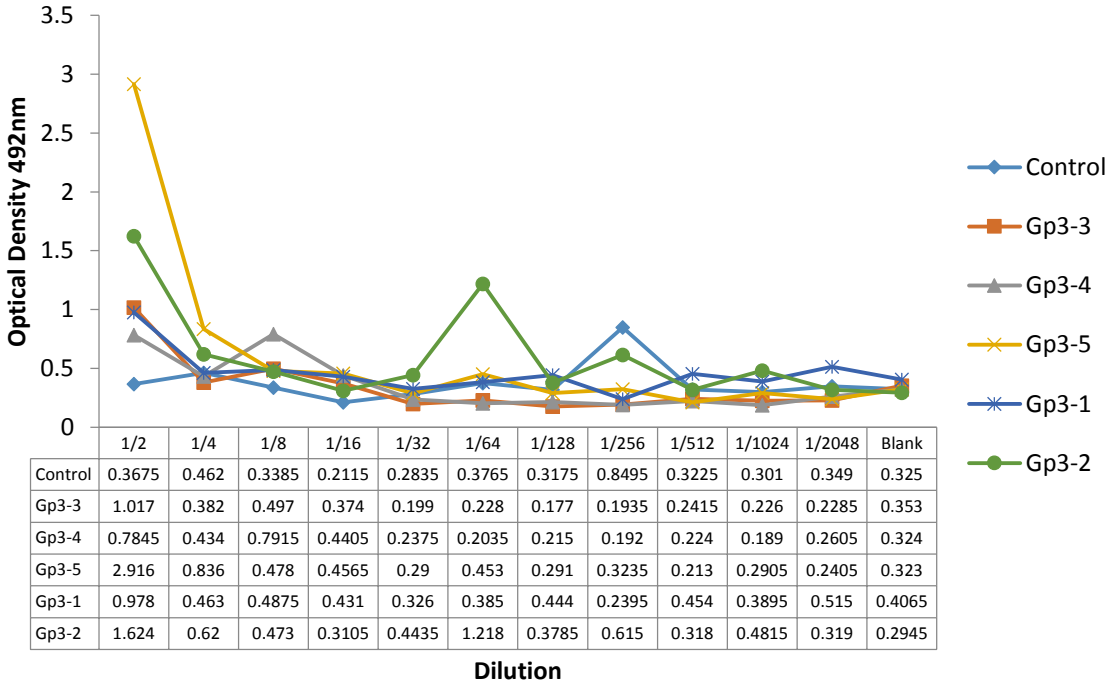

	1/2	1/4	1/8	1/16	1/32	1/64	1/128	1/256	1/512	1/1024	1/2048	Blank
Control	0.3675	0.462	0.3385	0.2115	0.2835	0.3765	0.3175	0.8495	0.3225	0.301	0.349	0.325
Gp3-3	1.017	0.382	0.497	0.374	0.199	0.228	0.177	0.1935	0.2415	0.226	0.2285	0.353
Gp3-4	0.7845	0.434	0.7915	0.4405	0.2375	0.2035	0.215	0.192	0.224	0.189	0.2605	0.324
Gp3-5	2.916	0.836	0.478	0.4565	0.29	0.453	0.291	0.3235	0.213	0.2905	0.2405	0.323
Gp3-1	0.978	0.463	0.4875	0.431	0.326	0.385	0.444	0.2395	0.454	0.3895	0.515	0.4065
Gp3-2	1.624	0.62	0.473	0.3105	0.4435	1.218	0.3785	0.615	0.318	0.4815	0.319	0.2945

Figure 5.13 IgA response in intestinal washes (1:2 dilution) of group 3: chitosan:OVA nanoparticles. Positive control is standard reference sera.

Figure 5.14 shows IgA intestinal washes response to chitosan:OVA nanoparticles with cholera toxin. A greater immune response at dilution 1:2 is seen but steeply decreases. The values remain low throughout the rest of the graph. The standard deviation is 0.049 and geomean 0.496 is relatively high. This again could be down to the stronger dilution used.

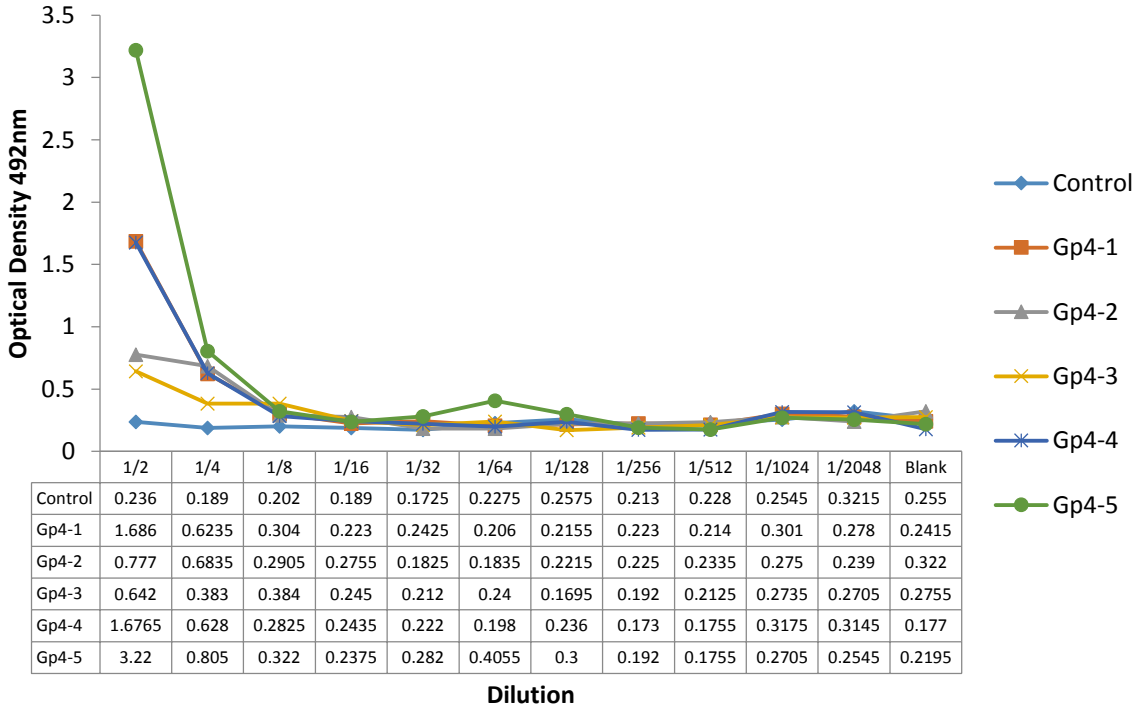

	1/2	1/4	1/8	1/16	1/32	1/64	1/128	1/256	1/512	1/1024	1/2048	Blank
Control	0.236	0.189	0.202	0.189	0.1725	0.2275	0.2575	0.213	0.228	0.2545	0.3215	0.255
Gp4-1	1.686	0.6235	0.304	0.223	0.2425	0.206	0.2155	0.223	0.214	0.301	0.278	0.2415
Gp4-2	0.777	0.6835	0.2905	0.2755	0.1825	0.1835	0.2215	0.225	0.2335	0.275	0.239	0.322
Gp4-3	0.642	0.383	0.384	0.245	0.212	0.24	0.1695	0.192	0.2125	0.2735	0.2705	0.2755
Gp4-4	1.6765	0.628	0.2825	0.2435	0.222	0.198	0.236	0.173	0.1755	0.3175	0.3145	0.177
Gp4-5	3.22	0.805	0.322	0.2375	0.282	0.4055	0.3	0.192	0.1755	0.2705	0.2545	0.2195

Figure 5.14 response to IgA intestinal washes 1:2 dilution group 4: chitosan:OVA nanoparticles with cholera toxin. Positive control is standard reference sera.

Figure and condition tested	Ig response
5.2 IgG1-ovalbumin mixed with bicarbonate.	No IgG1 response was detected.
5.3 IgG1-ovalbumin mixed with cholera toxin and sodium bicarbonate	A limited IgG1 response (0.82) was detected.
5.4 IgG1-chitosan:OVA nanoparticles in PBS.	No IgG1 response was detected

5.5 IgG1-chitosan:OVA nanoparticles with cholera toxin.	No clear IgG1 response shown.
5.6 IgG1-ovalbumin alone mixed with PBS administered subcutaneously.	A clear IgG1 response was shown by 4 mice for the positive control.
5.7 IgG2a-chitosan:OVA nanoparticles in PBS.	There was no clear IgG2a response shown.
5.8 IgG2a-chitosan:OVA nanoparticles with cholera toxin.	There was no response or trend to IgG2a.
5.9 total IgG-chitosan:OVA nanoparticles in PBS.	There was a limited response shown.
5.10 total IgG-chitosan:OVA nanoparticles with cholera toxin.	There was a small response shown (0.59).
5.11 total IgG (1:10 dilution) chitosan:OVA nanoparticles in PBS.	There was a large response demonstrated (1.22)
5.12 total IgG (1:10 dilution) chitosan:OVA nanoparticles with cholera toxin.	There was a large response (1.10).
5.13 IgA-chitosan:OVA nanoparticles in PBS.	There was no clear response.
5.14 IgA-chitosan:OVA nanoparticles with cholera toxin.	There was no response.

Table 5.2 Summary of Ig responses via different conditions tested.

In summary there were unexpected and surprising results. IgG1 produced no results, there were also no clear IgG2a results. Total IgG (1:50 dilution) produced a small response, so a stronger dilution was produced. Total Ig (1:10) produced a strong and robust response to the chitosan nanoparticles clearly matching the pattern of the positive control sera used. The response was stronger without the cholera toxin which was unexpected. IgA did not produce any valid response.

5.4 Discussion

Looking at the data in this chapter, it is apparent that chitosan:OVA nanoparticles, which successfully enhanced transepithelial permeability of OVA in the Caco-2 intestinal model (chapter 4). The chitosan:OVA nanoparticles did not produce an IgG1 or IgG2a response following oral immunisation.

A study used BALB/b mice during immunisation studies with alginate coated chitosan nanoparticles encapsulating measles antigen, prepared via ionotropic gelation using tripolyphosphate. The alginate protects the chitosan:measle nanoparticles from degradation during the immunisation studies. The mice were immunised via the oral route; a subcutaneous vaccination group was also carried out to serve as a positive control. The mice sera were tested using ELISA for IgG antibody. Intestinal washes were also carried out - this was to extract immunoglobulins from mucin in the small intestine. The study found the presence of measles specific IgG and IgA in the serum tested, the subsequent antibody titres through a DBS (dried blood spot) assay concluded as the immunisations increased, the antibody titres increased. It was also found that the IgG levels were higher for low molecular weight chitosan than higher molecular weight chitosan. These responses increased over a period of 14 days after plateauing. However, the subcutaneous group demonstrated the highest antibody titre (used as a positive control). From the intestinal lavages there was an increase in IgA secretion in low molecular weight alginate coated chitosan nanoparticles. There was a significant correlation with the amount of IgA induced and the molecular weight of the chitosan. The lower the molecular weight the more IgA was produced. The subcutaneous group did not produce any IgA response, even with the addition of booster immunisations (Biswas *et al.* 2015).

The above study employed alginate:chitosan nanoparticles and measles as an antigen and mice used were immunised via the oral route, similarly to our work. The difference in observations between the above study and our work is probably related to the antigen. OVA used in our work may not elicit as strong an immune response as the measles antigen. However, the discrepancy in observations could also be related to the different formulation (chitosan:OVA versus alginate:chitosan).

Chitosan:OVA:diphtheria toxoid nanoparticles were prepared in a similar study. The chitosan:OVA:diphtheria loaded nanoparticles were subsequently up taken by Peyers patches (which are the target for oral vaccinations) after the chitosan:OVA:diphtheria nanoparticles were intragastrically fed to mice (Lubben *et al*. 2001). For chitosan microparticles to be up taken by Peyers patches the size needs to be <10 µm in diameter (Islam *et al*. 2012). The uptake was demonstrated via confocal laser scanning microscopy. The chitosan:OVA:diphtheria nanoparticles easily associated with the negatively charged DNA. It has shown promising results via nasal delivery producing mucosal responses, which is why it is a promising candidate for oral vaccine delivery (Lubben *et al*. 2001).

Similar research used chitosan:OVA nanoparticles administered nasally, producing significant mucosal responses. Following administration of chitosan:OVA nanoparticles, mice exhibited a significant increase in IgG antibodies and a long lasting immune response, similarly to intramuscular administration (Li *et al*. 2001). IgA antibody response was also significantly increased compared to that of a soluble antigen. Diphtheria toxoid was used as well as OVA in the chitosan nanoparticles in the previous study. This produced an increased uptake in Peyers patches in the ileum (Lubben *et al.* 2001). The difference between our work and the above study is related to the antigen. The OVA used did not produce a strong immune response compared to diphtheria toxoid used (Lubben *et al*. 2001). The rest of the study was conducted in a similar method to our research. Different results were exhibited however the chitosan:OVA nanoparticles were administered nasally, not orally (Li *et al*. 2001).

Comparable research studied the immune response from synthesised chitosan derivatives delivered orally using OVA as an antigen (Suksamran *et al*. 2012). Quaternisation of chitosan can increase and preserve its solubility and positive charge within a neutral pH (Chen *et al*. 2013). One of chitosans qualities is its ability to cause an immune response without any off target immunogenicity (Islam *et al*. 2012). Six groups of six female BALB/c mice were immunised on days 0 and 14, each group with a different sample. A positive subcutaneous group of 100 µg OVA with 200 ml of $Al(OH)_3$ was used, and a negative control of 500 µg OVA in PBS administered orally. The rest of the samples used in the groups were chitosan derivatives with different aromatic moieties. Tail

bleeds were performed on day 0 and after anaesthetising the mice on day 21 a cardiac puncture was performed to collect blood samples. Serum samples obtained from the tail bleeds were kept separate (Suksamran *et al*. 2012). ELISAs were performed to determine the IgG OVA specific antibody response (Slütter *et al*. 2009). As expected the IgG titres for day 0 were very low, after the second immunisation the IgG levels significantly increased. The samples using OVA in chitosan derivative solutions induced a higher immune response than OVA in PBS (negative control); although the immune response was lower than OVA with $Al(OH)_3$ (positive control). The differences between the immune responses of the chitosan derivatives varied. The derivative sample with the highest immune response was $TM_{65}CM_{50}$, compared to TM_{65}, $TM_{56}Bz_{42}$ and $TM_{53}Py_{40}$. All concentrations used were 0.1 mg/ml (Suksamran *et al*. 2012).

Compared to the above study, our research employed a similar method. BALB/c mice were used, although more immunisations were applied (Suksamran *et al*. 2012). Serum samples were collected, there were no faecal samples collected or intestinal gavages performed. The difference between the above study and our research is different derivatives of chitosan were tested (Suksamran *et al*. 2012). In comparison, our work used one chitosan formulation (chitosan:OVA nanoparticles). An improvement to our research would be comparison of different chitosan derivatives, but our study was based on previously demonstrated potential (clear absorption enhancing effects) of ultrapure chitosan chloride.

Another study demonstrated, chitosan microparticles were prepared and three vaccination studies were carried out. The first vaccination study consisted of three groups of five mice vaccinated intragastrically with the following solutions: chitosan:diphtheria toxin microparticles, diphtheria toxin in PBS and chitosan microparticles alone. A second study was carried out to determine a dose dependant relationship. The last vaccination study to take place used two groups of six mice, one group received 40 fl diphtheria toxin associated chitosan microparticles and the second group received 40 fl diphtheria toxin alone. The results showed that for the first vaccination study, the group with chitosan alone demonstrated no IgG response as expected. The group vaccinated with diphtheria toxin in PBS also showed no IgG response until week 6 when a small titre of 20 was detected. The mice vaccinated with

diphtheria toxin mixed with chitosan microparticles showed no immune response until week 4 but IgG antibody response then increased until week 6 (Lubben *et al*. 2003). After the first study it was concluded association to chitosan microparticles greatly increased an immune response (Lubben *et al*. 2003 and Li *et al*. 2001). The second study showed groups vaccinated with diphtheria toxin alone produce a small immune response. The groups vaccinated with diphtheria toxin and chitosan microparticles induced a high immune response and dose dependency. The third study concludes the group vaccinated with diphtheria toxin in PBS produced a low IgA response, while chitosan:diphtheria microparticles produced a significantly higher IgA response. However, the antigen utilised in this study (diphtheria toxin) has a stronger affinity to produce an immune response than OVA, which may explain the lack of IgA mucosal response (Lubben *et al*. 2003).

Chitosan nanoparticles were prepared via ionotropic gelation, this consisted of chitosan concentrations (0.1- 0.5 %) mixed with acetic acid. rHBsAg (Hepatitis B antigen) (4-8 µg/ml) was dissolved in sodium sulphate (2.5 %) and applied to chitosan/acetic acid dropwise whilst stirring. In addition 5 % of PVA (anti-digestive agent) and a few drops of pure glycerol was added to increase bond formation between PVA and chitosan. Immunisation took place with 4 month old Wister rats. Five groups with six rats in each group were immunised orally with the following samples; control (300 µl saline), blank PVA- coated chitosan nanoparticles (300 µl of PBS saline), rHBsAg (300 µl with 6 µg rHBsAg), PVA coated rHBsAg (300 µl with 6 µg rHBsAg) and rHBsAg (300 µl with 6 µg of rHBsAg injected intramuscularly). The results showed PVA-coated rHBsAg chitosan nanoparticles produced a significant response almost matching that of the intramuscular formulation. This study concluded that this amount of IgG produced was protective against hepatitis B (Shrestha and Rath, 2014).

Overall, this chapter shows the chitosan:OVA nanoparticles, which were previously shown to have the ability to enhance OVA permeability across Caco-2 intestinal epithelial monolayers, do not show a clear ability to induce an immune response *in vivo* (in mice). Therefore, further formulation manipulation is required. For example an enteric coating for protection against enzymatic degration and a stronger antigen used,

in order to fulfil the potential of chitosan as a suitable material to enhance mucosal vaccine delivery.

There were several limitations associated with this part of the study. The vaccination of the BALB/c mice was carried out at NIBSC (London) however the chitosan:OVA nanoparticles were formulated at the university laboratorys (Lincoln). The chitosan:OVA nanoparticles therefore were transported via first class tracking post to NIBSC. This created a disadvantage, there was a time lapse of approximately 1-3 days where nanoparticle temperature was not regulated, this could have caused aggregation of the nanoparticles. This would have had a significant effect upon the nanoparticles and in turn the study.

During the *in vitro* studies the nanoparticles were formulated first before a variety of cell studies took place. There was no time lapse between formulation and study. However with the *in vivo* studies there was a time lase of 1-3 days. This would have caused aggregation. The packaging was protective but ambient temperature, unlike the storage conditions of the nanoparticles which was refrigerator temperature. During this time lapse the nanoparticles would have become unstable and possibly aggregated.

Another limitation is the weight of each mouse was not taken into account, meaning the larger the mouse the increase in the dosage. The oral polio vaccine dosage is 2 drops (0.1ml) in comparison to our nanoparticle dosage of 0.2ml (World Health Organisation, 2010). This is double the dosage, however this is dependant on the potency of the antigen used. The less potent the antigen the higher the dosage would need to be. There are three types of polio, the potency of each strain is as follows; type 1 is 800,000, type 2 is 100,000 and type 3 is 500,000. It is expressed as the amount of virus contained in the recommended dose as tissue culture ineffective doses (World Health Organisation, 2010). The potency of the chitosan:OVA nanoparticles is unknown. OVA, used as the antigen, is not as potent as a virus, due to limitations within the lab this was not allowed. Although still creates a small immune response seen in figures 5.11 and 5.12.

5.5. Conclusion

Overall the research within this chapter tested the oral vaccine delivery potential of chitosan:OVA nanoparticles in mice and tested different immunoglobulins to establish mechanistic information. Overall, induction of immune response by chitosan:OVA nanoparticles was not convincing. IgG1 response was somewhat higher with the cholera toxin added as a second adjuvant which was used to enhance the immune response of the vaccine. IgG2a response was low although both groups 3 and 4 displayed no trend. Total IgG (dilution 1:10) response was apparent in both groups 3 and 4, interestingly the immune response was higher when chitosan:OVA nanoparticles were given without the addition of cholera toxin (figure 5.10). IgA response was not obvious. This may be attributed to model antigen selection (OVA). Overall, this chapter demonstrates the importance of performing *in vivo* studies for drug delivery formulations by showing that the promising *in vitro* performance of systems does not necessarily reproduce *in vivo*.

5.6 References

1. Biswas, S., Chattopadhyay, M., Sen, K., K. and Saha, M., K. (2015). *Development and Characterisation of Alginate Coated Low Molecular Weight Chitosan Nanoparticles as new Carriers for Oral Vaccine Delivery in Mice*, Carbohydrate Polymers, 121: 403-410.
2. Casettari, L., Vllasaliu, D., Castagnino, E., Stolnik, S., Howdle, S. and Illum, L. (2012). *Review: PEGylated Chitosan Derivatives: Synthesis, Characterisations and Pharmaceutical Applications*, Topical Issue on Biorelated Polymers, Progress in Polymer Science, 37(5): 659- 685.
3. Casettari, L., Vllasaliu, D., Lam, J., K., W., Soliman, M. and Illum, L. (2012). *Review: Biomedical Applications of Amino Acid- Modified Chitosans: A Review*, Biomaterials, 33(30): 7565- 7583.
4. Chen, M., C., Mi, F., L., Liao, Z., X., Hsiao, C., W., Sonaje, K., Chung, M., F., Hsu, L., W. and Sung, H., W. (2013). *Recent Advances in Chitosan- Based Nanoparticles for Oral Delivery of Macromolecules*, Advanced Drug Delivery Reviews, 65(6): 865-879.
5. Harde, H., Agrawal, A., K. and Jain, S. (2015). *Tetanus Toxoids Loaded Glucomannosylated Chitosan Based Nanohoming Vaccine Adjuvant with Improved*

Oral Stability and Immunostimulatory Response, Pharmaceutical Research, 32(1): 122-134.

6. Huang, C., F., Wu, T., C., Chu, Y., H., Hwang, K., S., Wang, C., C. and Peng, H., J. (2008). *Effect of Neonatal Sublingual Vaccination with Native or Denatured Ovalbumin and Adjuvant CpG or Cholera Toxin on Systemic and Mucosal Immunity in Mice,* Scandinavian Journal of Immunology, 68(5): 502-510.
7. Islam, M., A., Firdous, J., Choi, Y., J., Yun, C., H. and Cho, C., S. (2012). *Design and Application of Chitosan Microspheres as Oral and Nasal Vaccine Carriers: an Updated Review*, International Journal of Nanomedicine, 7: 6077-6093.
8. Li, C., Li, Z. and Cuizhen, C. (2001). *Studies on Protein Antigen/ Chitosan Nanoparticles for Nasal Vaccine Delivery*, Europe Pubmed Central, [accessed: 11/10/2015].
9. Lubben, I., M., v.d, Kersten, G., Fretz, M., M., Beuvery, C., Verhoef, J., C. and Junginger, H., E. (2003). *Chitosan Microparticles for Mucosal Vaccination against Diphtheria: Oral and Nasal Efficacy Studies in Mice*, Vaccine, 21(13-14): 1400-1408.
10. Lubben, I., M., v.d, Verhoef, J., C., Borchard, G. and Junginger, H., E. (2001). *Chitosan for Mucosal Vaccination*, Advanced Drug Delivery Reviews 52: 139–144.
11. Mountford, A., P., Fisher, A. and Wilson, R., A. (1996). *The Profile of IgG1 and IgG2a Antibody Responses in Mice Exposed to Schistosoma Mansoni*, Parasite Immunology, 16(10): 521-527.
12. Nakayama, T., Kumagai, T., Ishii, K., J, and Ihara, T. (2012). *Alum- Adjuvanted H5N1 Whole Virion Inactivated Vaccine (WIV) Induced IgG1 and IgG4 Antibody Responses in Young Children*, Vaccine, 30(52): 7662-7666.
13. Roos, A., Bouwman, L., H., Gijlswijk-Janssen, D., J., V., Faber-Krol, M., C., Stahl, G., L. and Daha, M., R. (2001). *Human IgA Activates the Complement System via the Mannan- Binding Lectin Pathway*, The Journal of Immunology, 167(5): 2861-2868.
14. Shrestha, B. and Rath, J., P. (2014). *Poly (Vinyl Alcohol)- Coated Chitosan Microparticles act as an Effective Oral Vaccine Delivery System for Hepatitis B Vaccine in Rat Model*, IET Nanobiotechnology, 8(4): 201-207.
15. Slütter, B. and Jiskoot, W. (2010). *Dual Role of CpG as Immune Modulator and Physical Crosslinker in Ovalbumin Loaded N-Trimethyl Chitosan (TMC) Nanoparticles for Nasal Vaccination,* Journal of Controlled Release, 148(1): 117-121.

16. Slütter, B., Soema, P., C., Ding, Z., Verheul, R., Hennink, W. and Jiskoot, W. (2010). *Conjugation of Ovalbumin to Trimethyl Chitosan Improves Immunogenicity of the Antigen*, Journal of Controlled Release, 143(2): 207-214.
17. Slütter, B., Plapied, L., Fievez, V., Sande, M., A., Rieux, A., D., Schneider, Y., J., Riet, E., V., Jiskoot, W. and Préat, V. (2009). *Mechanistic Study of the Adjuvant Effect of Biodegradable Nanoparticles in Mucosal Vaccination*, Journal of Controlled Release, 138(2): 113-121.
18. Suksamran, T., Kowapradit, J., Ngawhirunpat, T., Rojanarata, T., Sajomsang, W., Pitaksuteepong, T. and Opanasopit, P. (2012). *Oral methylated N-aryl chitosan derivatives for inducing immune responses to ovalbumin*, Tropical Journal of Pharmaceutical Research, 11(6): 899-908.
19. Walke, S., Srivastava, G., Nikalje, M., Doshi, J., Kumar, R., Ravetkar, S. and Doshi, P. (2015). *Fabrication of Chitosan Microspheres using Vanillin/ TPP Dual Crosslinkers for Proteins Antigen Encapsulation*, Carbohydrate Polymers, 128: 188-198.
20. World Health Organisation. (2010). *Polio Vaccines and the Polio Immunisation in the Pre-Eradication Era: WHO Position Paper*, Weekly Epidemiological Record, 23(85): 213- 228.
21. Vllasaliu, D., Casettari, L., Fowler, R., Exposito- Harris, R., Garnett, M., Illum, L. and Stolnik, S. (2012). *Absorption- Promoting Effects of Chitosan in Airway and Intestinal Cell Lines: A Comparative Study*, International Journal of Pharmaceutics, 430(1-2): 151- 160.

Chapter 6

Summary and Future Directions

6.1 Overall Summary

The oral route offers potential for vaccine delivery, achieving mucosal response. The mucosal surface of the gastrointestinal tract however presents several barriers to achieving mucosal response through oral administration of vaccines. An ideal orally administered vaccine delivery system needs to protect the vaccine from physiological barriers of the gastrointestinal system, including the harsh biochemical environments and ensure that the payload reaches M cells where it induces an immune response.

This work examined a chitosan molecule (chloride salt) for its potential to act as a system facilitating vaccine delivery (chapter 3). Work initially assessed the ability of this chitosan to complex OVA as a model antigen into nanoparticles. Characterisation studies showed chitosan:OVA nanoparticles at 1:1 mass ratio displayed optimal characteristics, such as a diameter below 200nm and a positive zeta potential. Chitosan could clearly complex with OVA and release it when coming into contact with heparin (negatively charged). OVA stability within the chitosan nanoparticles was not compromised due to complexation. Some protection from trypsin was evident by chitosan nanoparticles however not from exposure to HCl.

The formulation prepared in this work was tested *in vitro* using Caco-2 monolayers as a model of the intestinal epithelium (chapter 4). This is usually a standard approach before *in vivo* studies. Caco-2 studies examined the effect of chitosan:OVA nanoparticles on TEER and OVA permeability rather than induction of immune response, (absence of relevant immune cells in the Caco-2 intestinal model does not allow that assessment). It was found that chitosan:OVA nanoparticles were not toxic to Caco-2 cells, as confirmed via MTS and LDH assays and as a result further studies were carried out. During TEER studies, reversible decrease in TEER was apparent, which further indicated that the chitosan:OVA nanoparticles were not toxic or damaging to the cells or their tight

junctions. However a clear effect of TEER is uncertain due to a significant decrease when OVA control solution was applied to the cells. Permeability studies showed chitosan:OVA nanoparticles produced a higher OVA permeability compared to, equivalent concentration of OVA in solution.

The experiments detailed in chapter 5 investigated whether an immune response occurred after oral administration of nanoparticles in BALB/s mice. The data revealed there was no response, as determined by measuring IgG1, IgG2a or IgA response. However, there was some response in total IgG which was in fact higher when no cholera toxin was added as an extra adjuvant. More studies are needed to confirm this response, including the use of stronger model antigens in order to increase the mucosal immune response.

Overall, this work showed that although chitosan is able to complex with protein-based therapeutics such as vaccines into nano size entities, which show interesting effects *in vitro*, the desired biological response *in vivo* may not be adequate and requires optimisation. Based on this work, it is not possible to confirm or rule out the potential of chitosan for oral vaccine delivery. However, an important conclusion from this study is that macromolecular absorption enhancement seen in *in vitro* intestinal models do not reliably predict an *in vivo* immune response from vaccine delivery systems.

6.2 Future Directions

Oral vaccine delivery is an actively researched area. Types and derivatives of chitosan, such as ultra pure chitosan chloride, CMC, TMC and PEGylated chitosan, as well as other materials will continue to be investigated for their potential in this field. These systems will need to be optimised, via the use of a stronger antigen and a protective enteric coating, in order to provide adequate response. This optimisation will have to be specific for each antigen. The role of *in vitro* intestinal models in their current form, including Caco-2, in predicting *in vivo* immune response following vaccine delivery is not clear. However, in *vitro* intestinal models of increased complexity, such as those based on co-culture of multiple cell types, including immune cells, have been proposed. These

models may be more applicable and more useful in predicting the *in vivo* performance of vaccine delivery systems.